The Pennsylvania State University

The Graduate School

Department of Mechanical and Nuclear Engineering

USING TOPOLOGY OPTIMIZATION TO IMPROVE DESIGN

FOR ADDITIVE MANUFACTURE

A Thesis in

Mechanical Engineering

by

Ian Ferguson

Submitted in Partial Fulfillment
of the Requirements
for the Degree of

Master of Science

August 2015

The thesis of Ian Ferguson was reviewed and approved* by the following:

Mary Frecker
Professor of Mechanical & Biomedical Engineering
Thesis Co-Advisor

Timothy W. Simpson
Professor of Mechanical & Industrial Engineering
Thesis Co-Advisor

Pan Michaleris
Professor of Mechanical Engineering

Karen Thole
Professor of Mechanical Engineering
Head of the Department of Mechanical and Nuclear Engineering

*Signatures are on file in the Graduate School

ABSTRACT

Additive manufacturing (AM) offers new design freedom to create topologies with complex surfaces and internal structures that could not be produced by traditional manufacturing processes. Due to this design flexibility, parts designed for AM have the potential to withstand the same structural loads as traditionally manufactured parts at lower masses. In an attempt to reduce the mass of structural parts to a minimum, optimization techniques such as topology optimization can be employed to achieve geometries that may be unintuitive to designers. While in many cases AM is the only means to realize such an optimized design, the constraints of the particular AM process may require a design to be modified before it can be produced.

This thesis examines the current state of topology optimization technology and investigates how topology optimization software fits into the workflow of design for AM. This is achieved by exploring the problem of minimizing the mass of a mounting plate for an aerospace vehicle. Optimization is performed with varying boundary conditions and materials to observe their effect on resulting topologies and design performance. The results are then manually interpreted to conform to AM constraints. A 60% weight savings was achieved over the current mounting plate design, but the optimization software did not take AM constraints into account. Manual design modifications were required to ensure that the design was one continuous part and that a suitable prototype of the optimized design could be produced.

In the context of this problem, the benefits and limitations of incorporating topology optimization into design for AM are presented. It was found that manual design workflow for AM requires the designer to iterate design around performance, while incorporating topology optimization into the workflow requires the designer to iterate design around manufacturability.

TABLE OF CONTENTS

LIST OF FIGURES

LIST OF TABLES

ACKNOWLEDGEMENTS

Chapter 1

Introduction and Literature Review

1.1 Motivation

Additive manufacturing processes offer a higher degree of design freedom compared to traditional manufacturing methods. These processes are able to produce complex surfaces, topologies, and internal structures that can translate into parts that can withstand greater structural loads at lower masses. This new capability is of particular interest to the aerospace industry, where even modest weight reductions can yield significant fuel cost savings over the lifetime of a vehicle [1].

While current computer-aided design (CAD) tools allow for the design of organic geometries with complex features, the problem of optimizing the mechanical properties of a part (mass, compliance, etc.) manually can prove time consuming. An engineer would propose a design, analyze its performance using finite element analysis (FEA), and then make revisions based on the results to improve the performance of the design. Performing numerous trial-and-error iterations of this process can still lead to suboptimal designs, as the surfaces and topologies that can be produced with additive manufacturing are nearly infinitely variable.

Topology optimization offers engineers a way to bypass much of this manual iteration. A topology optimization algorithm is able to take the design envelope, boundary conditions, loading, performance targets, and objectives as inputs, and output an optimal structure for whichever objective is chosen. In many cases, mass is the objective to be minimized; so, the algorithm will output a lightweight design. While this may not always be a global optimum in terms of structural efficiency, it offers the designer a feasible, lightweight design that identifies

the critical load paths necessary for function. The results of three-dimensional topology optimization often cannot be directly manufactured in any way other than additive manufacturing [2]. However, as discussed in Section 1.4, additive manufacturing processes have numerous limitations that may require the revision of optimized designs for production.

1.2 Topology Optimization Theory

The goal of topology optimization is to determine the optimal allocation of material within a specified region [3]. This is achieved by minimizing (or maximizing) a property of the structure, subject to constraints and boundary conditions. The design domain is discretized into finite elements, and one of a number of optimization techniques are used to determine which elements should contain material and which should be voids [4]. This is in contrast to shape optimization, in which the goal is to determine the optimum shape of a domain with a prescribed topology; so, the boundary of the design domain is the design variable. Ideally, the results of a topology optimization would return elements consisting of only material or only voids. This is referred to as a "black-and-white" or "0-1" problem; however, taking this approach leads to 2^N (where N is the number of elements) possible combinations of solid and empty elements, making the problem impractical to solve for most models. Instead, the integer variable (0 or 1) is replaced by a continuous variable, and a penalty function is introduced to drive the solution as closely as possible to discrete 0-1 values [5]. This process is referred to as relaxation of the design domain.

For the purposes of designing structural parts from an isotropic material, the Solid Isotropic Material with Penalization method (SIMP) [6] is commonly used in both research efforts and commercial software. In this method, the continuous variables introduced are the element densities. Each element carries with it an associated density ranging from 0-1, which is analogous to the amount of material in the element. This allows for gradient-based optimization

techniques to be applied to the problem, which are significantly more computationally effective than solving the integer problem. The introduction of a penalty function drives element densities towards either 0 or 1. The SIMP method achieves this by expressing the elastic modulus $\mathbf{E}$ as [5]:

$$E(x) = \rho(x)^p E^0, \quad p > 1$$

$$\int_{\Omega} \rho(x)\, d\Omega \leq V; \quad 0 \leq \rho(x) \leq 1, \quad x \in \Omega$$

(1.1)

where ρ is the element density, p is the penalization factor, Ω is the design domain, and V is the total structure volume. While interpolating material properties based on a non-physical model may seem arbitrary, Bendsøe and Sigmund [6] developed a method of selecting the penalization factor such that the interpolated properties would be representative of a composite microstructure consisting of void and material. The densities are assumed constant over each element, and the element stiffness matrices can be scaled before being assembled into the global stiffness matrix:

$$K_e = \rho_e^p K_e^0$$

(1.2)

Gradient-based optimization methods can then be employed, but once convergence is achieved, there may remain some elements with intermediate densities. The designer then sets a density threshold to determine which elements will be considered fully dense and which will be considered void. This threshold should be low enough that the connectivity and structural integrity of the domain are preserved.
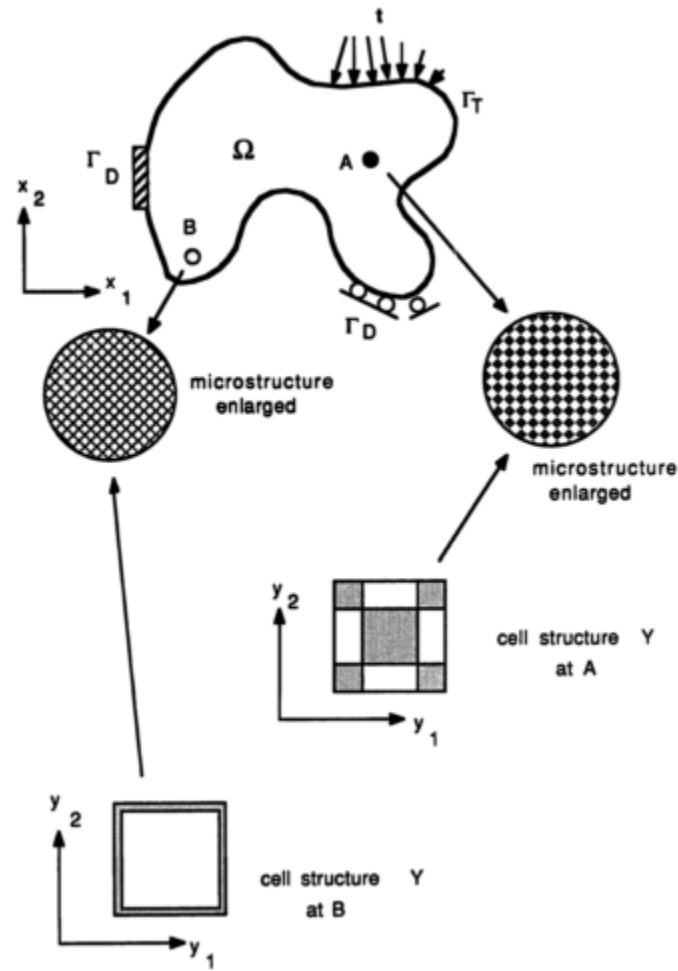
Figure 1-1. A structure with composite microstructure [4]

A different way to relax the 0-1 problem is through the homogenization method [4]. As shown in Figure 1-1, with this technique, the element density is introduced through microstructure. The material is represented as a composite of material and void, normally some solid with holes of a prescribed geometry (rectangular, circular, etc.). Since the microstructure assigned may be anisotropic, an orientation angle must also accompany each element [4]. This can make the homogenization approach advantageous for working with anisotropic materials. The microstructure itself offers some measure of penalization, but normally additional penalization must be introduced. A disadvantage of the homogenization method is that more design variables

are required per element than the SIMP method. In spite of this, it is often convenient to use homogenization with compliance as the cost function or constraint [7].

Another method for parameterizing the topology optimization problem is through the level set method (LSM). Though not yet incorporated into commercial software, the level set method offers the possibility for discrete representation of the boundaries between solid and void, which is advantageous for moving from optimized results to a manufacturable part. LSM achieves this by describing the material interface as the iso-contours of a level set function [8]. This function can be discretized by the same mesh used for the design domain, and it can be updated during the optimization process by the solution of the Hamilton-Jacobi equations [9].

1.3 Introduction to Additive Manufacturing

The various topology optimization methods often suggest design topologies consisting of complex surfaces and internal structures. In many cases the only way to produce them is through additive manufacturing (AM). ASTM F2792-12a [10] defines additive manufacturing as "a process of joining materials to make objects from 3D model data, usually layer upon layer, as opposed to subtractive manufacturing methodologies." Since no access to internal features is needed for subtractive operations, the complex topologies generated by optimization can be produced. This can be completed with only basic dimensional details of the design and a knowledge of how the AM process functions, in contrast to traditional manufacturing processes, which require analysis of the geometry to determine the order in which part features should be created.

There are seven general processes for AM: (1) binder jetting, (2) directed energy deposition, (3) material extrusion, (4) material jetting, (5) powder bed fusion, (6) sheet lamination, and (7) vat photopolymerization [10]. As a goal of this research is to design a

mounting plate to be produced by AM, the focus in this thesis is on processes available to

produce prototypes or functional parts. Direct metal laser sintering (DMLS) is a powder bed

fusion process capable of producing parts from metal powders, and so it would be well suited to

producing a functional part [10]. Fused deposition modeling (FDM) is a material extrusion

process that produces thermoplastic parts well suited to form prototypes of the mounting plate

example used in this thesis [10].

Fused deposition modeling (FDM) is one of the most developed and widely researched

AM processes [11]. In this process, heat is used to liquefy a polymer that is fed into the system in

the form of a filament as shown in Figure 1-2. This liquid polymer is pushed into the build

chamber by a tractor wheel arrangement that generates the extrusion pressure. The extrusion head

follows a computer-controlled tool path to deposit the liquid polymer onto the current layer. This

process is then repeated until all layers of the part are completed [11].
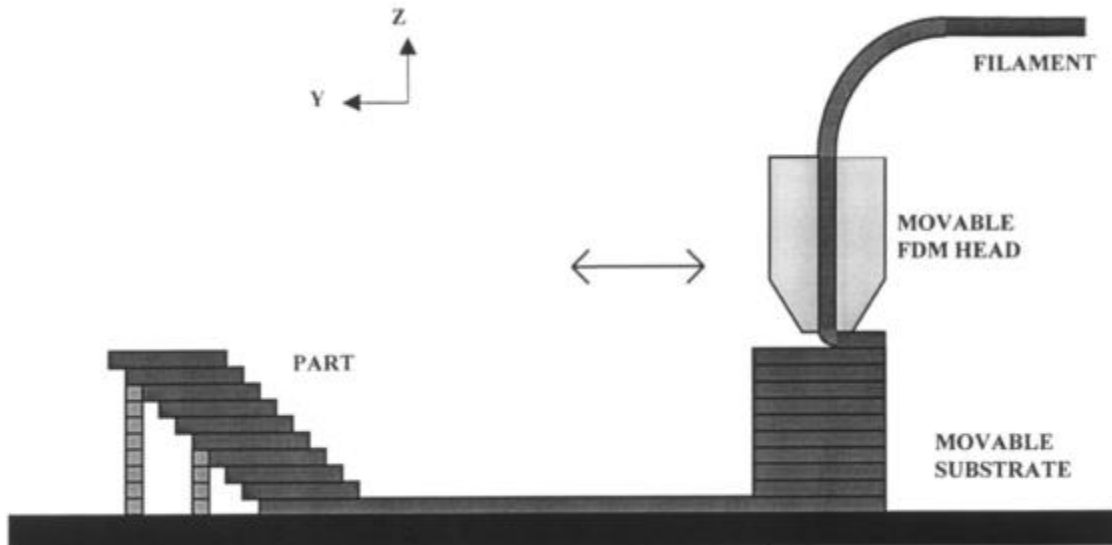
Figure 1-2. Fused deposition modeling [12]

FDM machines with the ability to print multiple materials have the advantage of printing dissolvable support structures with some polymers. Any supports that need to be printed can be dissolved using water; so, even internal support structures can be removed easily. FDM does have difficulty meeting demands of build speed, accuracy, and material density [11]. Processes with particularly fine filaments have long build times because they are limited by low feed rates and travel speeds. Since all nozzles in current FDM processes are circular, it is impossible to draw sharp corners, leading to a lack of accuracy in small parts. The circular filament cross-section also makes it impossible to produce fully dense parts, as there is no way to arrange circular sections in a plane without voids [11].

Direct metal laser sintering (DMLS) is a powder bed fusion process that differs significantly from FDM in several ways. The first, and most apparent, is that DMLS can be used to manufacture metallic parts. More importantly, for design considerations, the material is deposited and then heated, rather than the other way around. In DMLS, a layer of powdered material (in this case metal) is drawn across the surface of the build platform by a recoater blade, the material is melted by a laser, and the process is repeated layer by layer until the part is completed [11,13]. This process is shown in Figure 1-3.
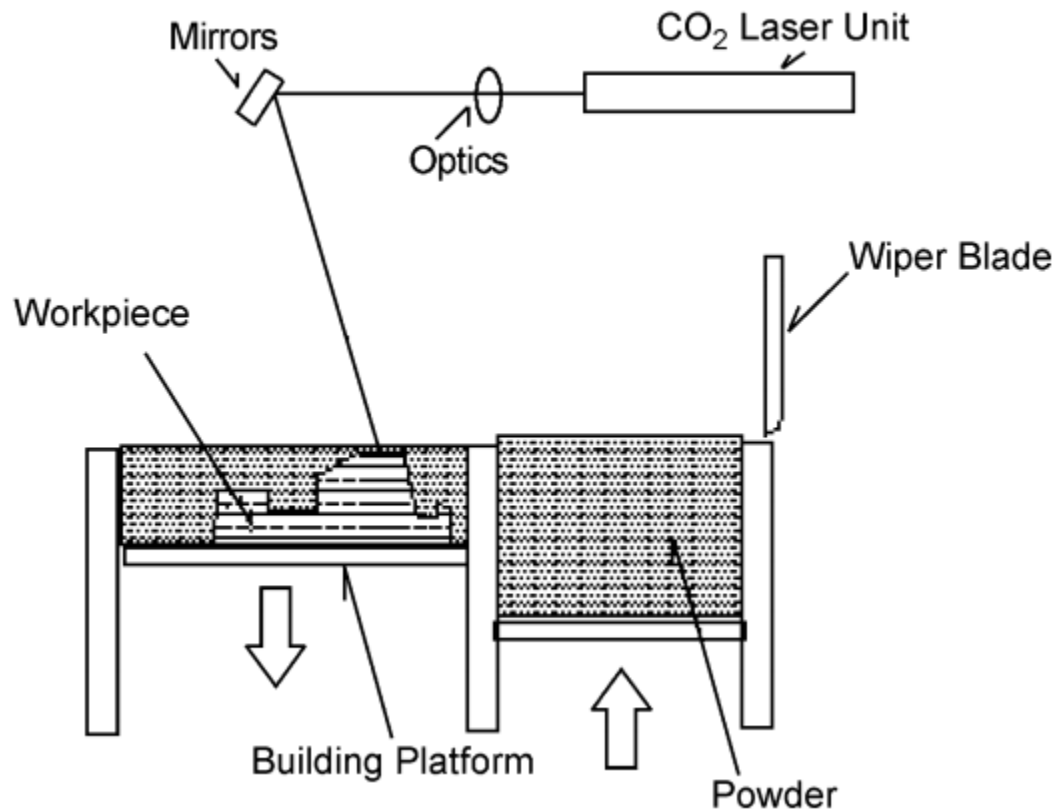
Figure 1-3. Direct metal laser sintering [13]

An advantage of the powder bed is that the powder left in the build chamber from previous layers can offer a small measure of support to subsequent layers. However, due to the fact that the fusion is essentially a continuous weld, distortion is a common problem; so, supports must be included to anchor the structure to the build plate and prevent warping to avoid a collision between the recoater blade and the part as it is being fabricated [11]. These supports are nearly always a necessity and can prove difficult to remove, often requiring hand tools to access areas where machining is not possible [1].

Though there are many types of additive manufacturing processes, most share a basic set of manufacturing constraints. As the part is built up vertically, the previous layer must support the next for successful manufacture. Due to this fact, all processes come with a minimum build angle

from the horizontal. If a feature must be printed with an overhang that exceeds the build angle,

then it must be supported to prevent deformation due to gravity (see Figure 1-4).
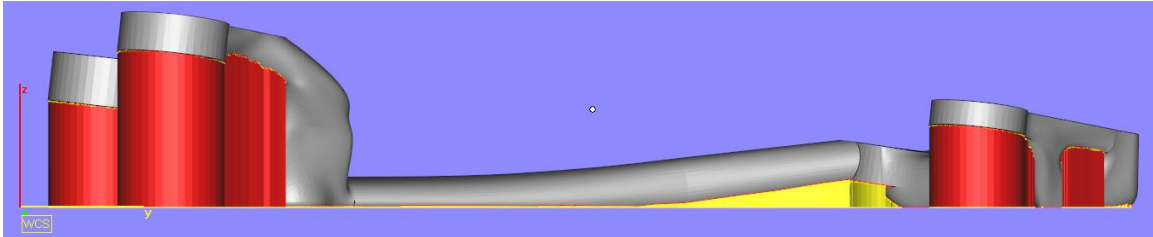
Figure 1-4. Example of support material (red and yellow) for a part (gray) (credit Corey Dickman)

Another process-specific manufacturing constraint is the minimum member size. Each

AM process has different constraints on layer thickness, as well as resolution in the build plane,

which dictate how thin a feature can be printed without failure. For processes that involve powder

beds or liquid vats, the geometry of the part must not contain any sealed voids that would trap

non-structural material from being removed during post-processing.

1.4 Integration of Topology Optimization into Design for Additive Manufacture

Though the basic methods of topology optimization have been established for several

decades [14], it has only been relatively recently that the potential of combining topology

optimization with AM has begun to be realized. Much of the early work involved with coupling

topology optimization and additive manufacturing has been in the medical and aerospace fields.

Tissue engineering requires scaffolding that allows for the diffusion of cells, nutrients, and

oxygen while structurally supporting the tissue [15]. Dias et al. [15] and Almeida et al. [16] show

that topology optimization problems can be solved to design a structurally efficient cubic, porous

unit cell for use in creating tissue scaffolding. Chahine et al. [17] shows that similar methods can

be employed to design both isotropic and anisotropic lattices that, by their porosity, aid in the osteointegration and function of bone implants. Both the porosity and the small scale of these applications make it infeasible to produce these structures in any method other than AM.

In the aerospace industry, topology optimization coupled with AM has shown itself to be useful as a weight reduction tool. Sepp et al. [18] documents the redesign of a low pressure turbine guide vane using topology optimization. The end result can be manufactured only through AM due to its complex interior structures. Their work illustrates that even critical parts can benefit from redesign for AM.

A more popular example of design for AM from the aerospace industry is the GrabCAD GE Bracket Challenge [1]. In this contest, members of the online GrabCAD community were given the current design for a titanium engine bracket and the loading it needed to support, and were tasked with reducing the weight as much as possible (see Figure 1-5). The new designs were required to stay within the spatial envelope of the current part and had to be manufacturable using AM. Many successful entries started by using some form of topology optimization, which was then manually interpreted by the designer to arrive at a suitable design.

Figure 1-5. GE Bracket Challenge original part (left) and winner (right) [1]

Current commercial topology optimization software is tailored to traditional manufacturing processes, and so includes manufacturing constraints for machining, casting, and extrusion. While a constraint for casting or extrusion could be applied to a design for AM to ensure that the structure would have no unsupported overhangs, the resulting structure would be overdesigned and may lose the advantages that AM offers. The only manufacturing constraint currently offered by most commercial optimization software that directly applies to AM is that of a minimum member size.

Brackett, et al. [2] assessed the needs in topology optimization tools for AM. To achieve a true global optimum on minimizing the mass of a structural component, the mesh of the optimization problem must be sufficiently fine to take advantage of the smallest members producible by a particular AM process. As topology optimization methods were previously used primarily as a load path visualization tool to assist in the design of traditionally manufactured parts, mesh size was able to remain relatively coarse. Finer meshes greatly increase the computations necessary to arrive at a converged result. Brackett et al. [2] posed two possible solutions: The first solution would be a "hard-kill" method: elements that remain at extremely low density over many iterations would be removed from the model entirely for subsequent iterations. The second solution would involve remeshing between optimization iterations, adding refinement to structurally important areas. As a side effect of mesh refinement, optimization interpretation could be eliminated from the design process or minimized; at a sufficiently fine mesh size, the boundary of the structure could be directly exported as an STL file and manufactured without the need for fitting surfaces.

Current commercially available optimization packages also fail to take advantage of AM's capability of creating variable density and multi-material parts. Rezaie and Badrossamay [19] suggest the possibility of removing the penalty functions from the SIMP method and to instead interpret the varying element densities with cell structures of varying thicknesses in the

hopes of creating more structurally efficient designs. Gaynor et al. [20] modified the SIMP method to accommodate multiple materials for use in the design of compliant mechanisms to be printed using a polyjet three-dimensional printing process, but this methodology has not yet been adopted in commercial topology optimization software.

Leary et al. [21] proposed a method to reduce the necessity of support structure when printing 3D structures designed with topology optimization. After a SIMP optimization is run, the print orientation of the resulting structure is decided by the user. An algorithm then identifies the regions prone to failure due to overhangs and inserts structural supports that conform to the minimum build angle constraint of the process. With minimal structural material added, this method is able to reduce the time of manufacture when compared with traditional support structure, though the end result is a higher mass.

1.5 Objective for the Thesis

The objective in this thesis is to investigate the effect of incorporating topology optimization into the designer's workflow when using additive manufacture. To achieve this objective, an example problem involving a metallic mounting plate used to connect a rectangular box to a conical section of an aerospace vehicle is investigated. The current mounting plate used by our collaborators is machined from a solid block of 7050-T7451 aluminum alloy and weighs 7.99lbs. Given a design domain, loading, and connectivity requirements prescribed by our collaborators, topology optimization is performed to achieve a lightweight design that takes advantage of the capabilities of additive manufacturing.

Ideally, a functional prototype would be realized using DMLS with a comparable aluminum alloy. Unfortunately, the build size of the mounting plate exceeds the dimensions of the EOS M280 system available for this research, and it is not an effective use of powder, given

the large build volume. Instead, a suitable prototype is fabricated out of Ultem 9085, a thermoplastic on the Fortus 400mc FDM machine that is available for this research. This allows the optimized design to be fabricated at full-scale and placed alongside the current part for comparison.

1.6 Overview of the Thesis

Chapter 2 investigates and compares currently available topology optimization software. This comparison includes a description of the software that is reviewed and evaluated, the results of three test problems, and a software recommendation. Chapter 3 details the formulation of the mounting plate example problem. This includes the properties of the current part and available design space, the modeling setup, the topology optimization setup, and the results extraction methodology. Chapter 4 presents the results of the topology optimization cases described in Chapter 3. This includes the optimized topologies and mechanical properties of cases run, the addition of a connecting geometry to join the optimized results, the prototyping of interpreted designs, and the workflow ramifications revealed by this example problem. Chapter 5 summarizes the contributions of the research and discusses possible areas for future research.

Chapter 2

Software Review

There are numerous free, educational, and commercial topology optimization software packages available to engineers and designers. These optimization solvers have different capabilities that make them better suited to different problems and uses. Some of the software packages investigated in this research are better suited to load path visualization for educational purposes, while others offer the capability to output fully functional designs. To determine the best software for the mounting plate example problem, twenty different topology optimization software tools are investigated, and their capabilities are compared to make a recommendation for software to use for this application. Ultimately, Altair Engineering's OptiStruct was selected for use with the mounting plate example problem as discussed in this chapter.

2.1 Method and Results of Comparison

Information on the twenty topology optimization software tools investigated was gathered through a combination of searching through online documentation, contacting the software companies directly, and in two cases, downloading trail versions. The topology optimization software tools were investigated for the following capabilities:

- Shape optimization

- Compatibility with other finite element analysis (FEA) platforms

- Eigenvalue/vibration analysis and/or optimization

- Symmetry constraints

- Draw constraints

- Extrusion constraints

- Minimum and maximum member dimension constraints

- Lattice structure geometry support

- Results smoothing

- Training availability and accessibility

- Computing requirements

- Price

The results of the investigation (detailed results in Appendix A) showed that based on their capabilities, the various pieces of software could be divided into two groups: (1) commercial software and (2) educational tools. Table 2-1 shows the categorization of the software reviewed.

Table 2-1. Classification of Investigated Software

Commercial Software	Educational Tools
• Altair OptiStruct	• BESO3D
• Vanderplaats Genesis	• ParetoWorks
• Simulia Tosca	• CATOPTO*
• Abaqus ATOM	• Topostruct
• MSC Nastran	• ProTOp
• SolidThinking Inspire	• SmartDO*
• Within Enhance	• META4ABQ
• PERMAS-TOPO	• ToPy
• FEMtools Optimization	• TRINITAS
• OPTISHAPE-TS	• TopOpt

*outdated software

Those that fell into the commercial software group could solve numerous types of problems with various manufacturing constraints, and they had well-documented capabilities and points of contact. The educational tools investigated were generally suited to problems with

simple loading, and they did not support vibration analysis, shape optimization, or results
extraction and smoothing. A subset of the investigation results is shown in Figure 2-1 to illustrate
these differences.

Software	Company	FEA platform(s)	Shape Optimization	Eigenvalue analysis/optimization	Integrated result post processing/ smoothing
Optistruct	Altair Engineering	Hyperworks, NASTRAN	Yes	Yes	Yes
Genesis	Vanderplaats R&D	Genesis, ANSYS	Yes	Yes	Yes
SIMULIA TOSCA STRUCTURE 8.0	FE-Design (Dassault Systems)	Ansys, Abaqus, NASTRAN	Yes	Yes	Yes
ATOM (Abaqus Unified FEA)	Dassault Systems	Abaqus	Yes	Yes	Yes
MSC.Nastran	MSC Software	NASTRAN	Yes	Yes	Yes
Inspire	Solidthinking (Altair Engineering)	Hyperworks (uses OptiStruct Solver)	No	Yes	Yes
Enhance	Within	integrated	Yes	Yes	Yes
PERMAS-TOPO	Intes	Permas	Yes (separate module)	Yes	Yes
FEMtools optimization	Dynamic Design Solutions	NASTRAN, ABAQUS, ANSYS	Yes	Yes	No
OPTISHAPE-TS	Quint	Ansys	Yes	Yes	Yes
Educational Tools					
BESO3D	RMIT University	Abaqus	No	No	No
ParetoWorks	SciArt, LLC.	Integrated (Solidworks)	No	No	No
CATOPTO*	Creative Engineering Services	ABAQUS, ANSYS, NASTRAN, OPTISTRUCT, PERMAS and TOSCA	No	Yes	No
topostruct	Sawpan Design	n/a	No	No	Yes
ProTOp	Center for Advanced Engineering Software and Simulations	standalone	No	No	No
SmartDO*	FEA-Opt Technology	ansys (available workbench add-in)	No	No	No
META4ABQ		Abaqus	No	No	No
ToPy	n/a	standalone (Python)	No	No	No
TRINITAS	Linkoping University	standalone	No	No	No
TopOpt	TopOpt	standalone	No	No	No

*outdated software

Figure 2-1. Primary differences between commercial software and Educational tools

None of the tools investigated supported manufacturing constraints specifically for AM. Minimum and maximum member sizes do play a part in design for AM, but constraints on build orientation, overhangs, and supports were missing from all tools investigated.

All of the commercial software investigated utilizes the SIMP method for topology optimization and includes vibration analysis and optimization, as well as manufacturing constraints for symmetry, draw direction, extrusion, and member thickness. With the exception of SolidThinking's Inspire [22], every piece of software also included a means to perform shape optimization. On the other hand, with the exception of Within's Enhance [23], every commercial software lacked support for using lattice structures in optimization. This shows that the current state of topology optimization technology is not adapted to AM. With the growing popularity of AM, it is likely that software companies will look to incorporate similar features into future versions of their products.

2.2 Software Trials

Of those topology optimization tools that fit into the commercial software category, trial versions of two products were obtained to compare ease of use and optimization results. Altair Engineering's OptiStruct [24] and SolidThinking's Inspire [22] were chosen for comparison as both tools have similar capabilities (see Appendix A), but while OptiStruct uses an FEA-type interface comparable to most of the other commercial tools, Inspire offers a streamlined interface.

When working with OptiStruct, a user has access to every part of the optimization problem but at the cost of user-friendliness. The problem must be defined in Altair's FEA preprocessor: HyperMesh. The model is then exported and sent to the OptiStruct Solver. The finite element mesh must be defined manually, and while OptiStruct offers more loading and response types than Inspire, they must be applied either through direct manipulation of the solver

input file or by navigating the HyperMesh interface, which is a mix of text and graphics that may not be intuitive to new users. Figure 2-2 illustrates these steps, and Figure 2-3 shows the HyperMesh interface.
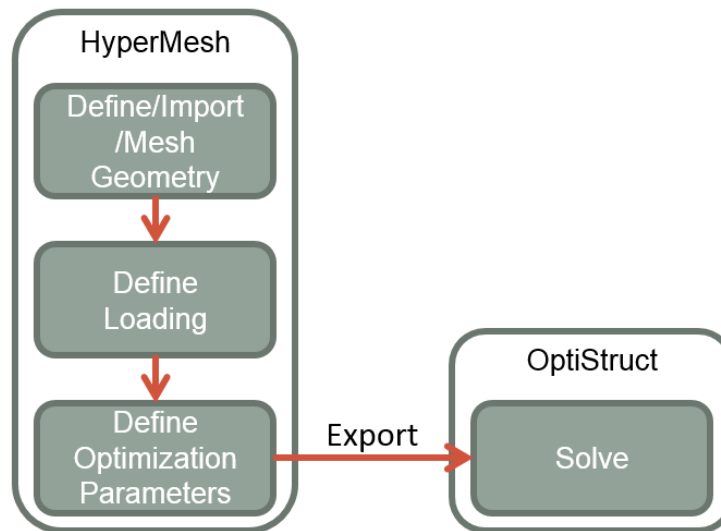
Figure 2-2. HyperMesh to OptiStruct workflow
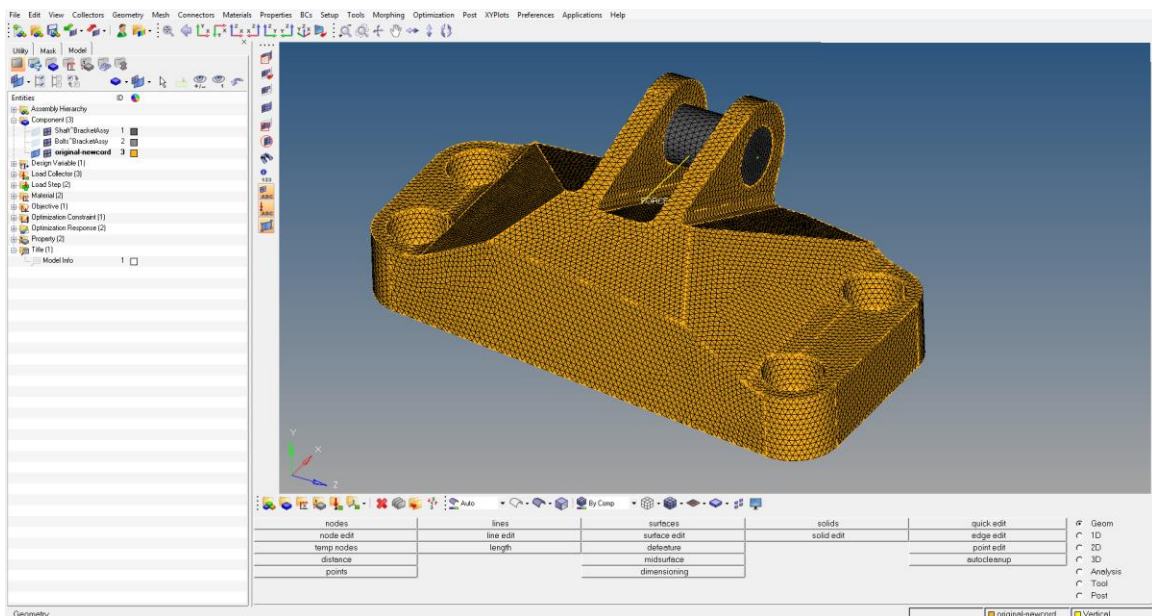
Figure 2-3. HyperMesh interface

Inspire, on the other hand, offers users a simplified graphical interface (see Figure 2-4). Modeling as well as geometry editing tools are placed directly on the home screen and represented by images that reflect their function as opposed to text options in a drop-down menu. The finite element mesh is created and refined automatically, saving time on preprocessing. While this time saved is valuable, the loading tools do not allow for load cases of the same complexity offered by OptiStruct. SolidThinking is now owned by Altair Engineering, and so the topology optimization solver used by Inspire is OptiStruct, but the simplified interface coupled with automatic meshing reduces Inspire to essentially black box functionality.
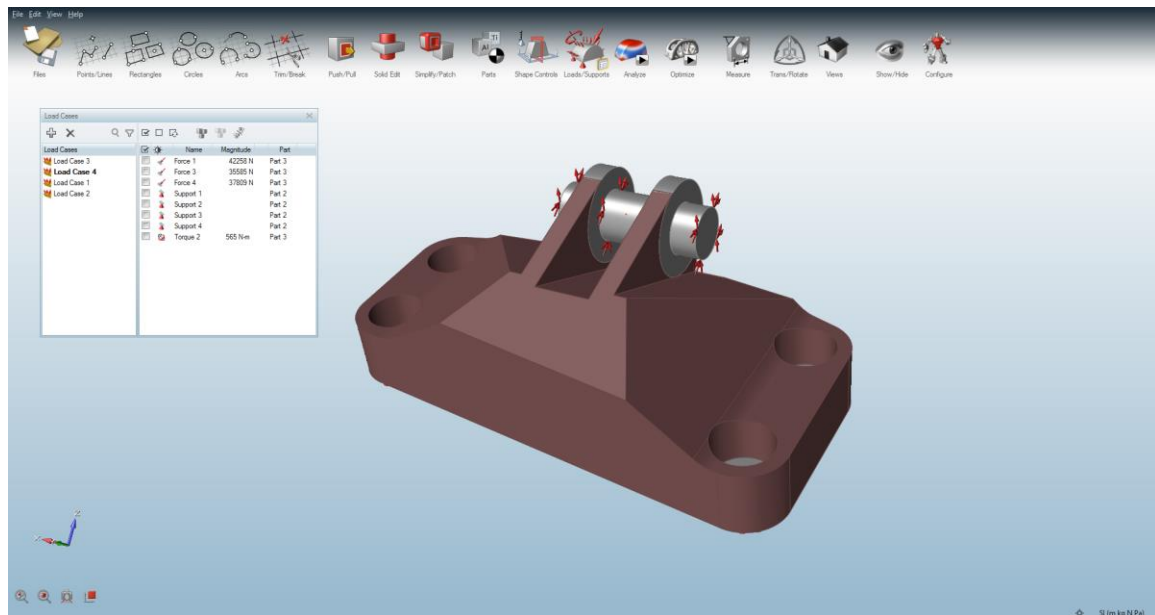
Figure 2-4. Inspire Interface

2.3 Topology Optimization Software Test Problems

To compare performance between Inspire and OptiStruct, three test problems were modeled and optimized with each program. These test problems were compared qualitatively for resulting geometry and optimization time. The first test problem was that of a structure spanning a gap. A rectangular design space was defined with the bottom corners constrained to zero displacement, and a vertical point load was applied to the midpoint of the top of the design space (see Figure 2-5).

Figure 2-5. Test problem 1

The optimization objective was to minimize compliance with the constraint of using only 20% of the original design space volume. The results from OptiStruct and Inspire are shown in Figures 2-6 and 2-7, respectively.
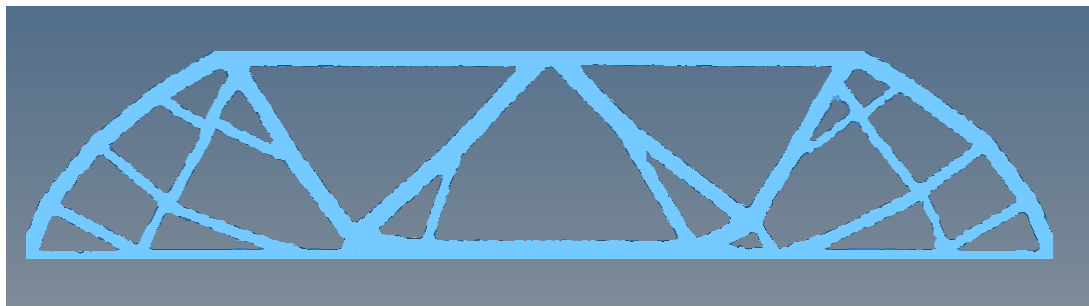
Figure 2-6. Test problem 1 - OptiStruct results
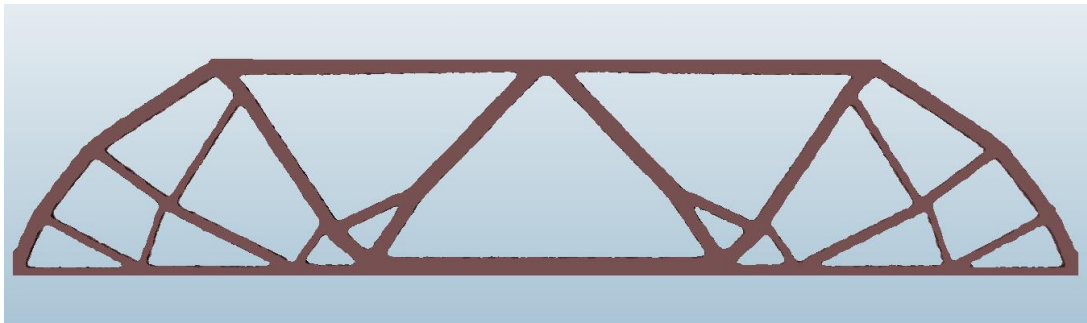
Figure 2-7. Test problem 1 - Inspire results

These results show similar topologies and similar member sizing. The most noticeable difference between the two optimizations was the solver run time. The OptiStruct optimization took about two minutes, while Inspire took about ten minutes, both running on a Windows 8.1 64-bit computer with an Intel® Core™ i5-4200 CPU @ 2.80GHz (4 CPUs) and 8GB RAM. This could be due to Inspire's automatic meshing functionality performing several iterations of refinement.

The second test problem was a cantilever beam. A rectangular design space was constrained to zero displacement on its left side, and a downward point force was applied to the midpoint of its right side (see Figure 2-8).
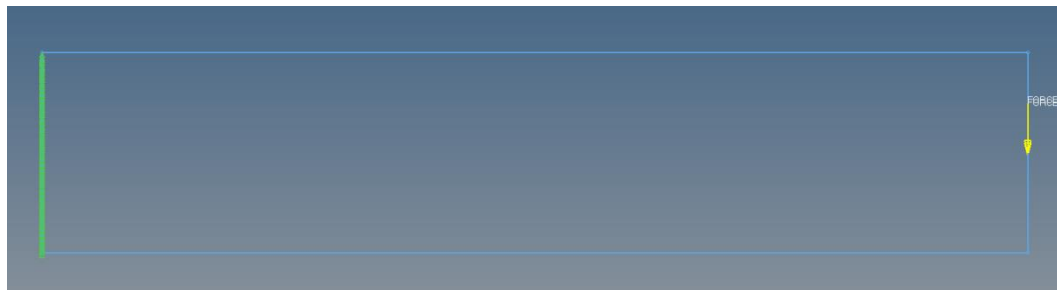
Figure 2-8. Test problem model 2

Again, the objective was to minimize compliance with the constraint of using only 20% of the design space volume. The results from OptiStruct and Inspire are shown in Figures 2-9 and 2-10, respectively.
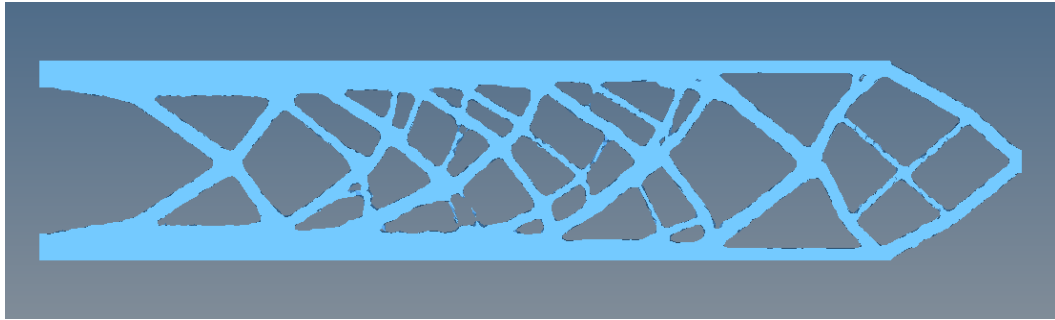
Figure 2-9. Test problem 2 - OptiStruct Results
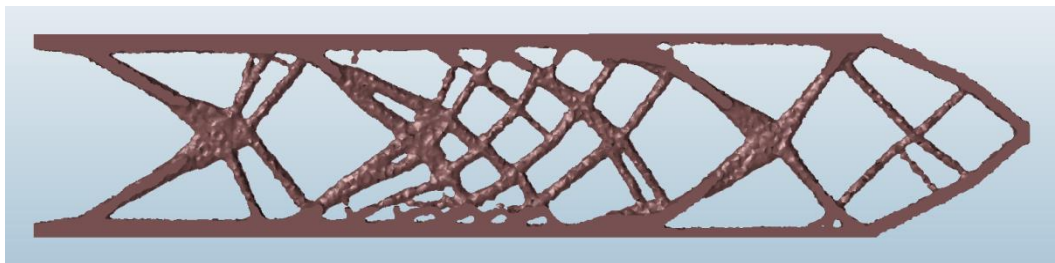
Figure 2-10. Test problem 2 - Inspire Results

These results again show qualitatively similar topologies but with slightly different member thicknesses. Again, the OptiStruct solution took about two minutes, and the Inspire solution took ten minutes, both running on a Windows 8.1 64-bit computer with an Intel® Core™ i5-4200 CPU @ 2.80GHz (4 CPUs) and 8GB RAM.

The final test problem for comparison was the GE Bracket Challenge [1]. This test problem was an airline engine bracket subject to four loading conditions. Figure 2-11 shows the loading conditions, and Figure 2-12 shows the design space.
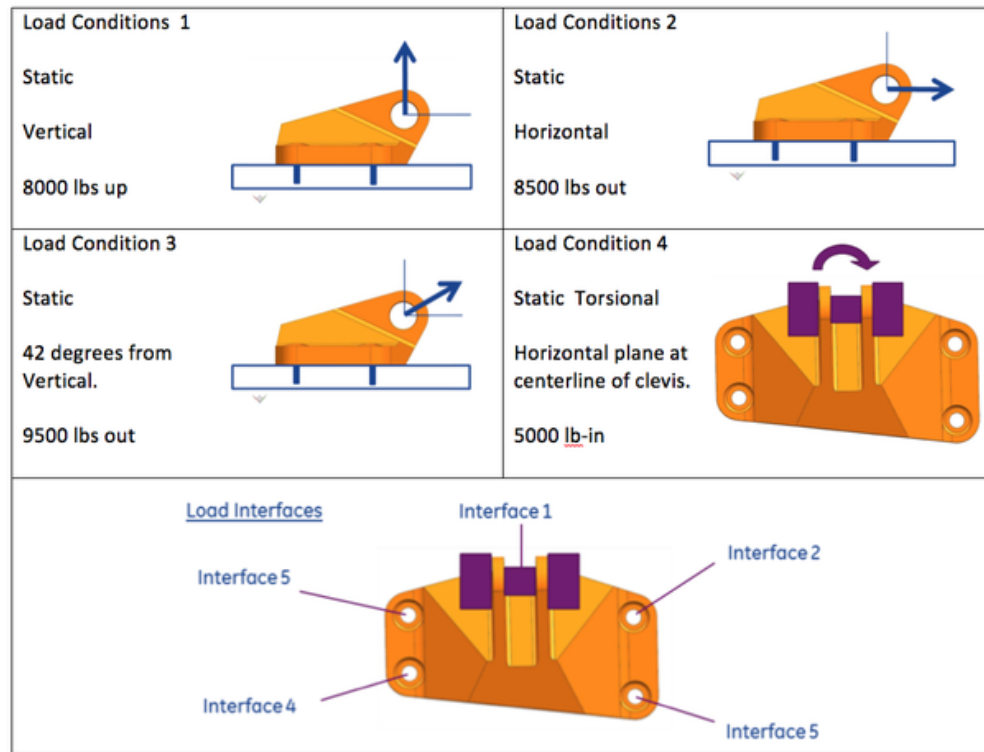
Figure 2-11. GE Bracket Challenge loading conditions [1]
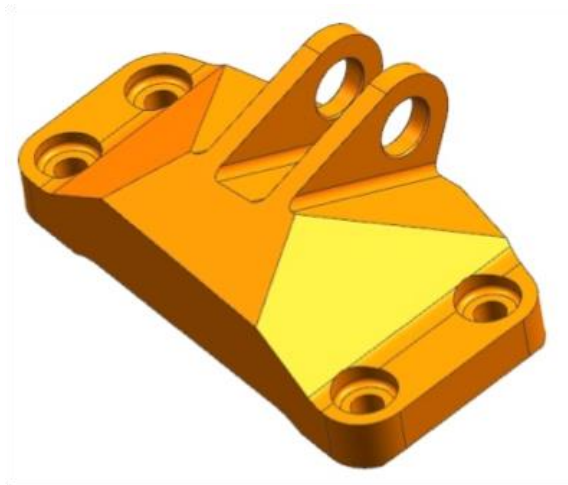
Figure 2-12. GE Bracket Challenge design space [1]

This test problem again used a minimum compliance objective with a 20% volume

constraint, but it also included a yield stress constraint. This test problem also used non-design

space at the bolts and clevis for application of loads and constraints. The results from OptiStruct

and Inspire are shown in Figures 2-13 and 2-14, respectively.
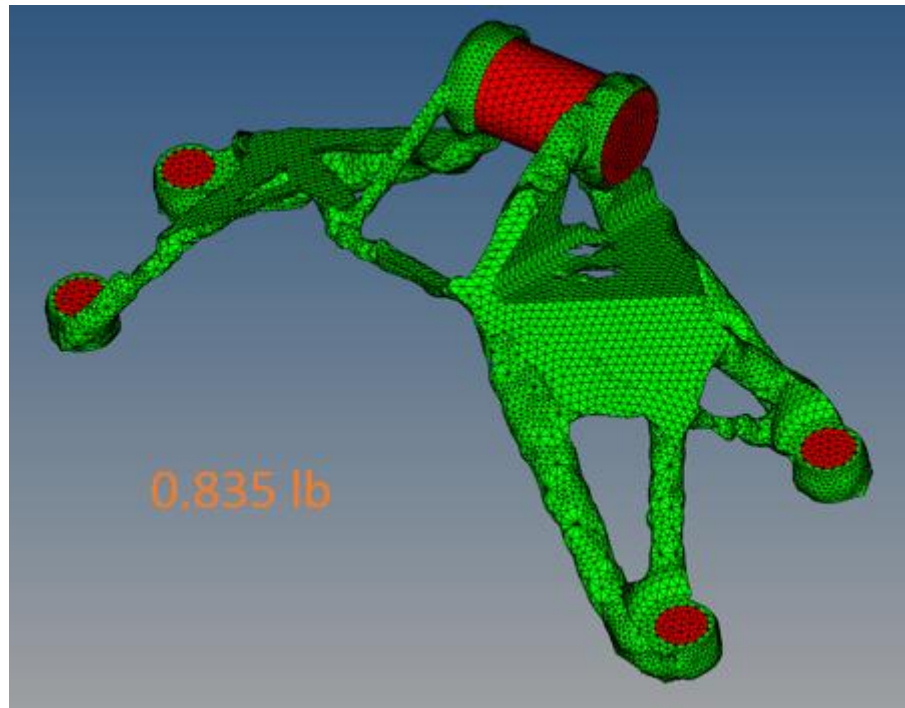
Figure 2-13. GE Bracket Challenge OptiStruct results: green design space, red non-design bolts
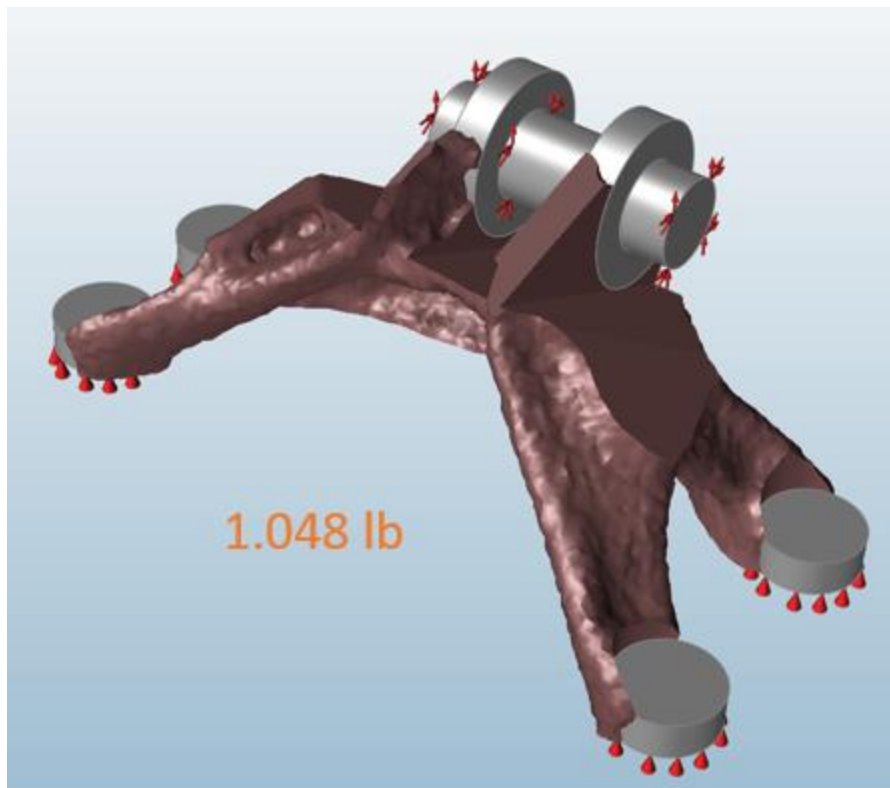
Figure 2-14. GE Bracket Challenge Inspire Results

These results differ more noticeably than the previous test problems. The OptiStruct result contains 0.213 lbm less material than the Inspire result with a different topology. Both programs have removed the most amount of material from the same areas; so, the differences in topology may be due to Inspire's black box functions (i.e., meshing, refinement). As with the previous test problems, solution time was noticeably different. Whereas OptiStruct took about 20 minutes to optimize, Inspire required three hours to converge on a Windows 8.1 64-bit computer with an Intel® Core™ i5-4200 CPU @ 2.80GHz (4 CPUs) and 8GB RAM.

2.4 Software Recommendation

The objectives and constraints of the mounting plate example problem shaped the requirements for topology optimization software recommendation. Suitable software would need to be able to optimize with respect to part mass or volume, while offering constraints on stress, force, and first natural frequency. The software would also need to include some easily accessible form of training so that the goals of the project could be achieved by its deadline. Additionally, the software used for the project would ideally serve an array of functions as opposed to only performing topology optimization. This way, our collaborators could be recommended a software package that they could use for size and shape optimization as well as general FEA.

After performing the comparison between Inspire and OptiStruct, OptiStruct is recommended as the best-fit software to the mounting plate example problem. Though the user interface is more complicated than Inspire, it allows the user to control every aspect of the optimization. The longer pre-processing time is offset by its comparably faster solving time, which is crucial for testing the effects of numerous boundary conditions and design parameters. Experience from the trial version coupled with Altair's online training would allow for this research to be completed in a timely fashion.

For this work, OptiStruct 12.0 was used for static, modal, and buckling analyses and optimization, but the solver is also capable of performing thermal analyses and optimization. In addition to topology optimization of 2D and 3D domains, OptiStruct can perform size, free size, topography, shape and free shape optimization. OptiStruct also supports multi-model optimization; that is, one part can be divided into multiple separate design domains with different properties to be optimized for various objectives. This allows for different manufacturing constraints and materials to be impressed upon discrete regions of the part.

OptiStruct is able to perform topology optimization using objective and constraint functions for elements that may or may not form part of the design space. For the purposes of this example problem, OptiStruct responses for stress, volume, natural frequency, and static force were used, but there are many more responses available for more complex analyses and optimizations. A full description of each of these responses can be found in Appendix B. The detailed problem formulation for the mounting plate example are given the next chapter.

Chapter 3

Problem Formulation for Mounting Plate Example

3.1 Current Part and Design Space

The current mounting plate design is constructed from 7050-T7451 aluminum alloy and weighs 7.99 pounds. The design is the intellectual property of our collaborators and cannot be shown, but it may be noted that the design is roughly rectangular in shape with a tapered shape that has been designed to be manufactured by machining. The current design has four bolt and washer interfaces to a rectangular box that sits on top of the plate, and eight bolt and washer interfaces to connect to swivel mounts that attach it to the conic surface of the aerospace structure. The current design also includes slots for wire harnessing with the assistance of zip ties.

To illustrate how topology optimization can be used to redesign the plate, the available design envelope is defined as the maximum dimensions of the current part (see Figure 3-1), including the curved surface conforming to the conic and the current interface locations. This design envelope would allow any optimized design to be produced and immediately used in place of the current part.
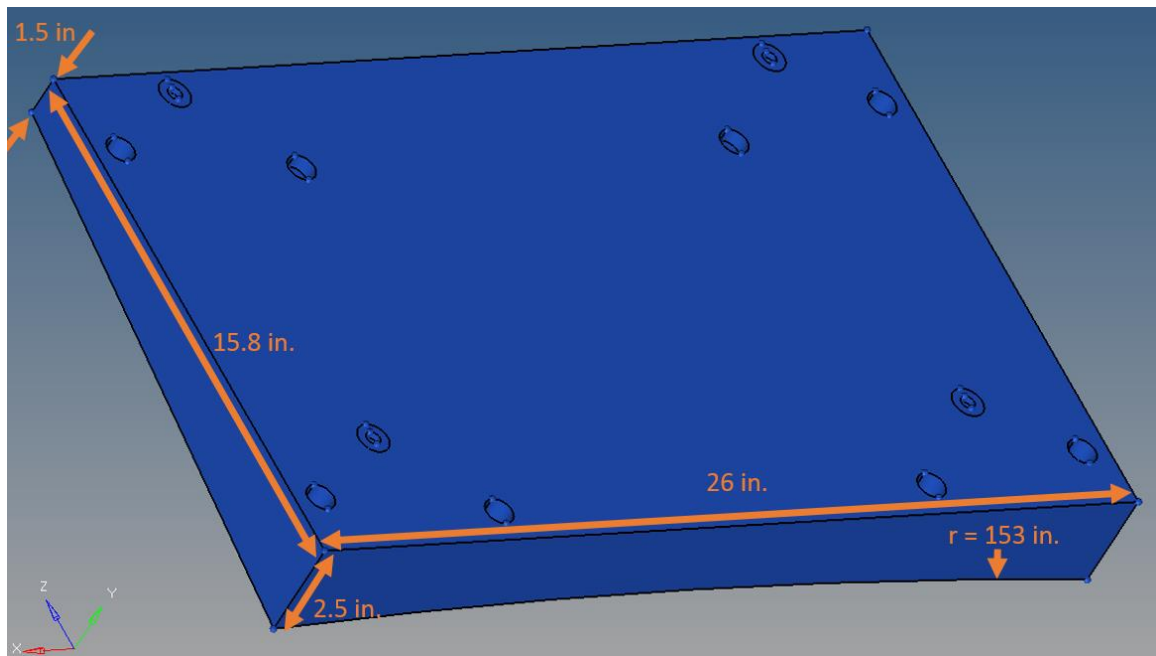
Figure 3-1. Mounting plate design envelope

3.2 Modeling Setup

Two coordinate systems were used to define boundary conditions and loading. The global coordinate system, in which all loading data was given, was defined as the center of the conic, a set distance away from the forward and aft ends of the mounting plate, with the axial direction in the direction of the taper of the conic (see Figure 3-2). The local coordinate system was defined as a Cartesian system with the origin at the midpoint of the forward edge of the box-side of the mounting plate.
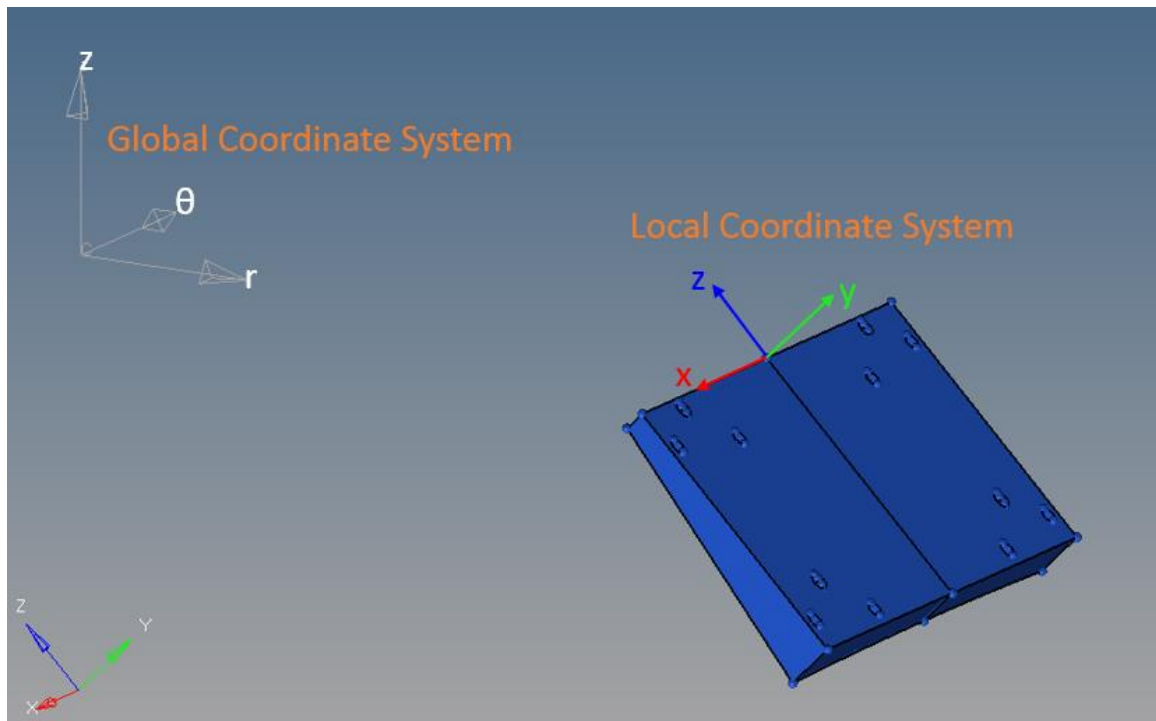
Figure 3-2. Mounting plate cylindrical coordinate systems

The mounting plate design envelope was divided into finite elements. As the design

envelope was symmetrical about the y-z axis, only half of the envelope was meshed, and then the

resulting elements were mirrored to complete the mesh. This was achieved by using HyperMesh's

automatic 3D meshing tool, Tetramesh [25]. Tetramesh allows the user to fill an enclosed volume

with first- or second-order tetrahedral elements by first generating a shell mesh around the

volume, and then using user-defined parameters to fill the volume with solid elements. The

parameters used for the mounting plate mesh were minimum element size, maximum element

size, proximity, and curvature. For this mesh, the maximum element size was 0.3in, and the

minimum element size was 0.08in. The proximity and curvature parameters then automatically

refined the mesh to the minimum size limit in small features and areas of high curvature. The

result was a mesh with fine elements around the interfaces, and larger elements throughout the

rest of the envelope as shown in Figure 3-3. Further refinement in the optimization stage was not

possible because the solver would have required more memory than was available on the
computer used.
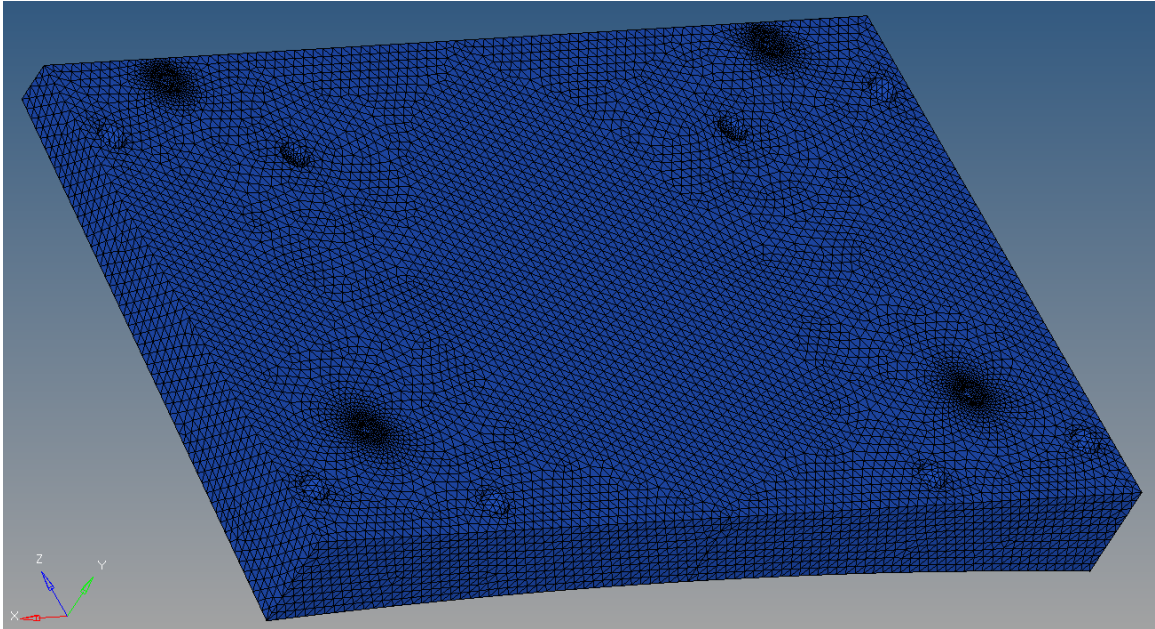
Figure 3-3. Meshed design envelope

The mechanical effects of the conic and box were accounted for through appropriate
boundary conditions. The loading data and interface types drove the selection of boundary
conditions and methods of applying loads. A number of different boundary conditions and
methods of applying loads may be appropriate for analyzing a part with defined geometry.
However, the topology optimization algorithm will allocate material specifically to support the
loads applied with the boundary conditions defined; so, several different boundary conditions and
load types were used for optimization to observe the degree to which they influence the results.

The bolt and washer interfaces between the mounting plate and the conic were modeled
in two ways: (1) the bolt was connected to the inside surface of the interface, and (2) the washers
were connected to the areas of the interface that they contact. This was achieved by applying one
of two boundary conditions on the nodes on the surface of interest. The first boundary condition

took the conic to be completely rigid. In this model, zero-displacement single-point constraints (SPCs) were placed on the aforementioned interfaces. The second boundary condition modeled the conic as rigid in all directions except along the axes of the bolted interfaces. Stiff spring elements were placed along these axes, with a zero-displacement SPC on the conic end, and the other attached to the interface surface of interest by way of rigid connectors (RBE2 elements). This spring boundary condition was run with spring constants of 10^5 lbf/in and 10^4 lbf/in. These values were chosen to observe the effect of slight elasticity in the nearly rigid conic on the optimized results. Figure 3-4 shows the different interface boundary conditions explored:
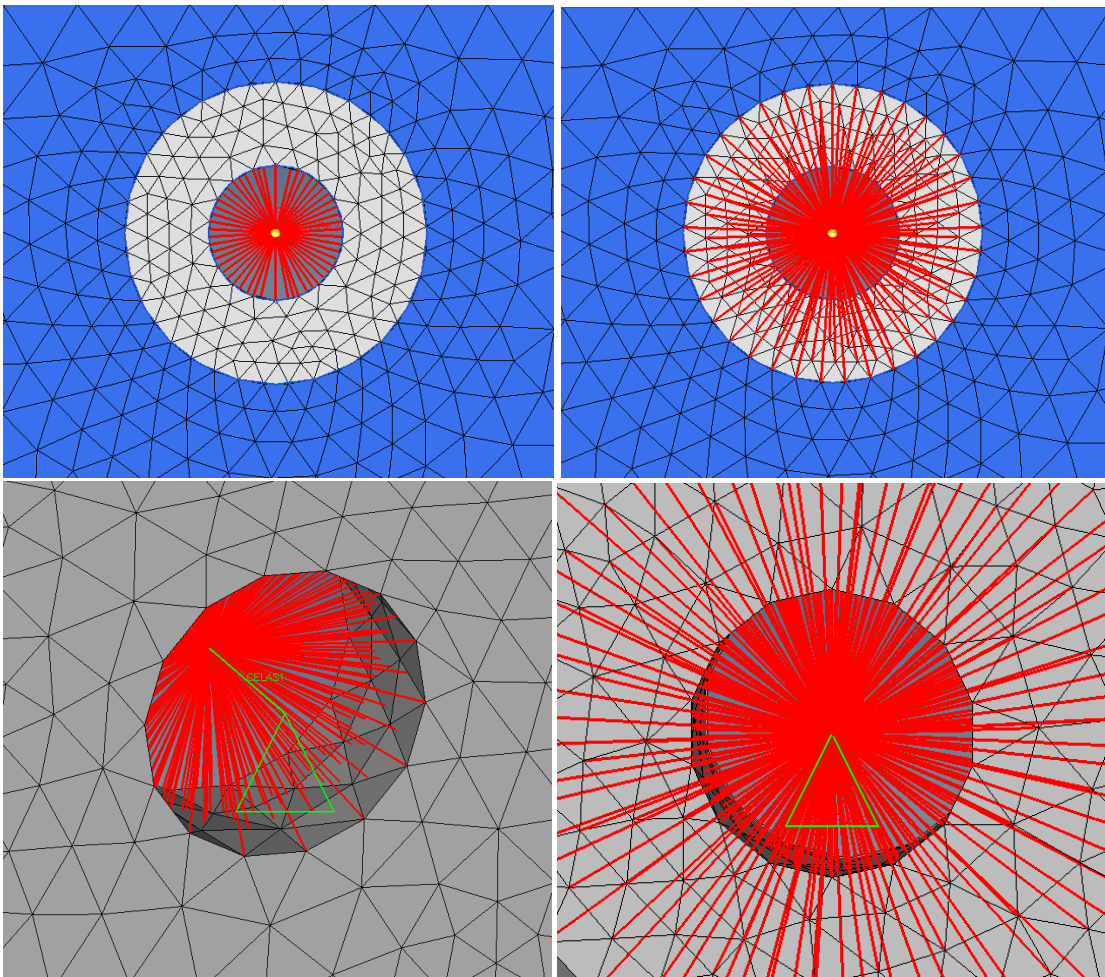
Figure 3-4. Bolted connections connected to bolt surface (top left), washer surface (top right), supported by a spring (green, bottom left), supported rigidly (bottom right)

The four interfaces between the mounting plate and the box were modeled similarly to the conic/plate interfaces, with one set of boundary conditions reflecting attachment along the bolt contact surface, and one set connecting via the washer contact surfaces. The box itself was then modeled as perfectly rigid, or perfectly elastic, as the box compliance was unknown. The rigid case placed a point mass at the center of gravity of the box and attached it to the interface surfaces by rigid connectors (RBE2 elements). The elastic case involved computing the resultant loads created by the box on each interface for each load case, applying those loads to the center points of each interface, and then connecting these center points to the interface surfaces with rigid elements.

In all cases other than the elastic case, loading was applied completely through gravitational loads in the global cylindrical coordinate system defined earlier in this section (see Figure 3-2). In the elastic case, the same gravitational loads were applied, but since the box was modeled as resultant forces, each load case was defined as the combination of the resultant forces and a gravitational force. A summary of the boundary loading conditions used is shown in Table 3-1.

Table 3-1. Boundary and loading condition cases for optimization

		Interface Boundary Conditions			
		Bolt Surface Interfaces		Washer Surface Interfaces	
		Fully Constrained	Springs	Fully Constrained	Springs
Box model	Rigid Box (gravitational loading only)	✓	✓	✓	✓
	Elastic Box (gravitational and resultant loading)	✓	✓	✓	✓

3.3 Optimization Setup

The first step in setting up the optimization parameters was dividing the given mounting plate design envelope into the design space to be optimized and the non-design space to be kept regardless of its structural contribution. The necessity of maintaining the existing interfaces led to taking the volumes at the bolted connections between the upper and lower washers as non-design space. The rest of the given design envelope was set as design space for optimization as shown in Figure 3-5.
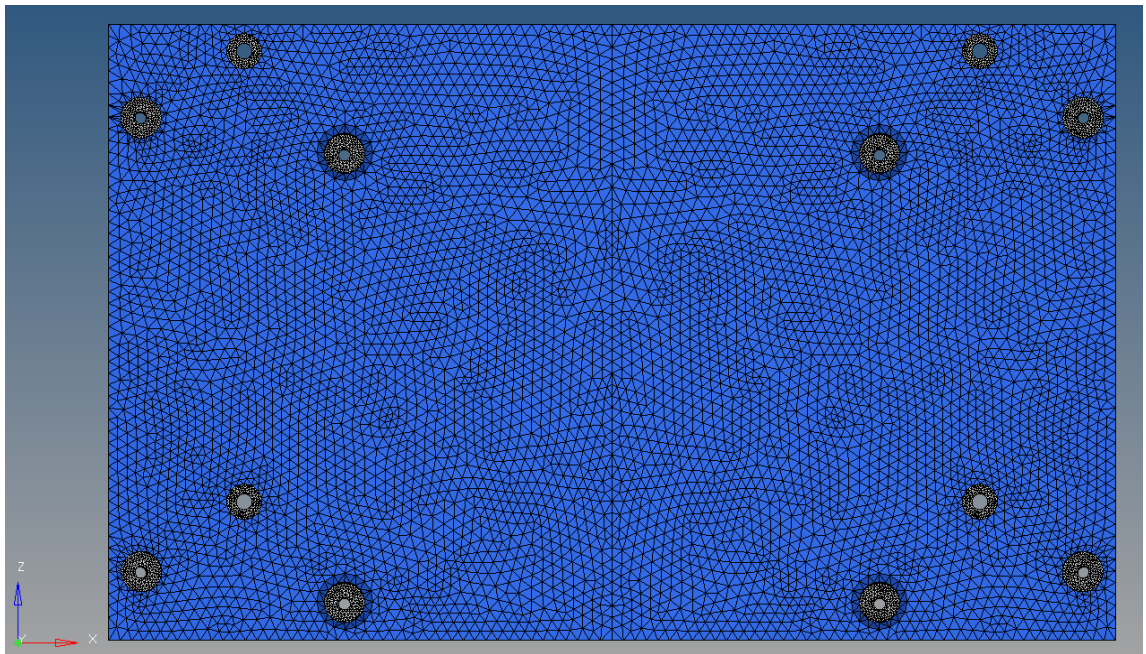
Figure 3-5. Design space (blue) and non-design space (gray)

The responses of interest were then defined, including all quantities to be constrained or optimized. For all optimizations, OptiStruct predicted the values of punch loads at each of the eight plate-to-conic interfaces as well as the first and second natural frequencies of the part. OptiStruct also returned the value of volume fraction (the ratio of current iteration volume to initial volume) at each iteration.

Constraints on the optimization were dictated by the problem statement. An upper bound of 480lbf was set on the punch loads at each of the eight plate to conic interfaces, a 1.6 factor of safety was set against yield failure, a 2.0 factor of safety was set against ultimate failure, and a 100 Hz minimum first natural frequency constraint was defined. The objective function was to minimize volume fraction, which is equivalent to minimizing mass or volume.

This optimization setup was run first with the 7050-T7451 aluminum alloy of the current part to determine which of the boundary conditions described in Section 3.2 were most physically meaningful (see the results in Section 4.1.2). After the boundary conditions were investigated, the optimization was then run again with the most physically meaningful boundary conditions using titanium alloy Ti-6Al-4V, a titanium alloy used in many aerospace applications and the same alloy used in the GrabCAD GE Bracket Challenge [1].

3.4 Results Extraction

The results of each optimization were viewed in Altair HyperView [25], which displayed a contour or iso-map of element densities at each iteration of optimization. For each optimization, the element density threshold for display was lowered to the point at which connectivity was preserved between the plate/box and plate/conic interfaces. This threshold was recorded and used for OptiStruct's geometry extraction tool, OSSmooth [25].

OSSmooth was used to extract the geometry of the optimized results at or below the entered element density threshold and exported in a .STEP (STandard for the Exchange of Product model data) or .STL (STereoLithogrophy) file format. While the .STL simply used the faces of the tetrahedral mesh, OSSmooth fits NURBS surfaces to the surface nodes of the optimized result to generate a .STEP file. The element size used was too large to allow the

topology to reduce to smooth surfaces during optimization; so, the outputs of OSSmooth required manual interpretation.

The surface-fit STEP files were imported into SolidWorks and traced manually to fit continuous surfaces. This was achieved by defining reference planes at different cross-sections of the part, tracing each cross-section to create 2D sketches, and then using surfacing tools to connect the cross-sections while conforming to the rest of the extracted geometry. The results were interpreted conservatively; every element of the optimized results was included inside the boundaries of the traced surfaces. An example of this process is shown in Figure 3-6. Details of the results obtained from this process are described in the next chapter.
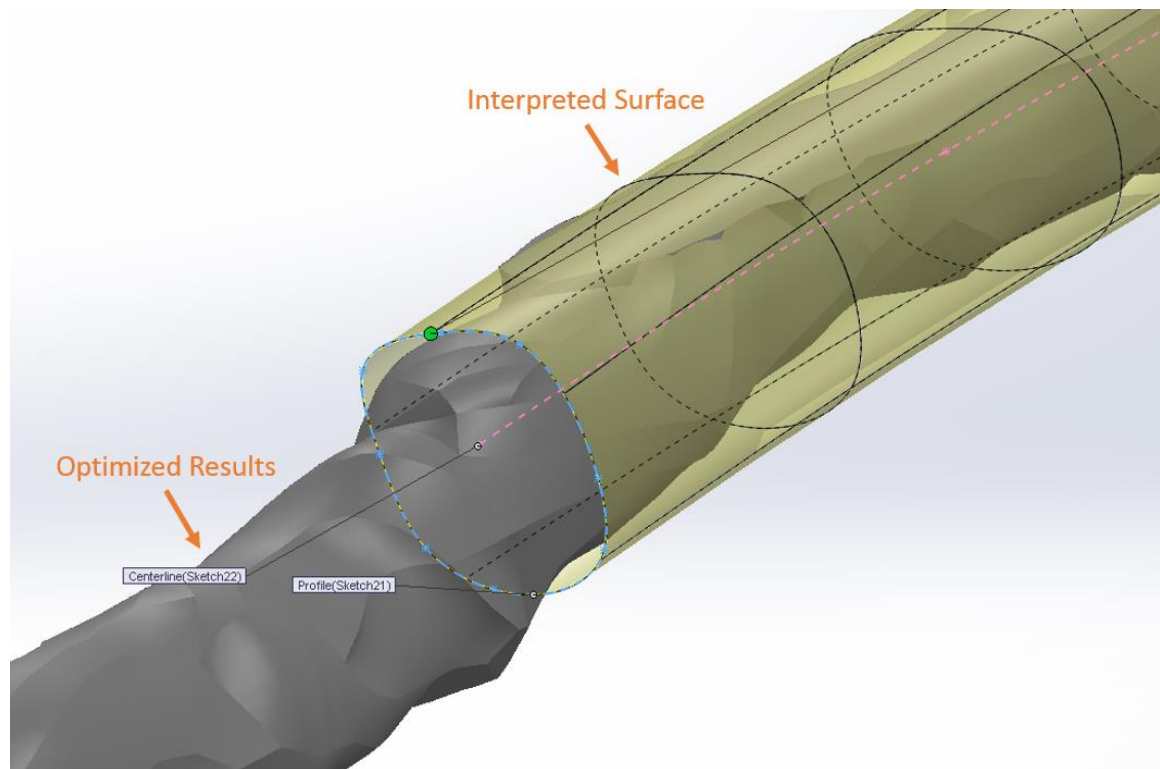
Figure 3-6. SolidWorks surfacing tools

Chapter 4

Results and Discussion

4.1 Mounting Plate Topology Optimization Results

4.1.1 Selecting a Density Threshold

The first step in interpreting the topology optimization results for the mounting plate example problem was selecting an element density threshold for extraction. As OptiStruct utilizes the SIMP method of topology optimization, the optimized results included all elements in the design space as well as each element's associated density. The same threshold was to be used for each optimization performed so that the results would be commensurate, allowing comparisons between different results. The threshold also had to ensure that domain connectivity was preserved, which was the driving factor behind threshold choice in this problem. Various thresholds were evaluated until the results represented a continuous structure. Figures 4-1 and 4-2 show the optimized results of the case with an elastic box and washer interfaces at 0.5 and 0.3 density thresholds, respectively. These thresholds did not represent a continuous structure; so, the threshold was reduced further to 0.1, yielding the resulting geometry shown in Figure 4-3.
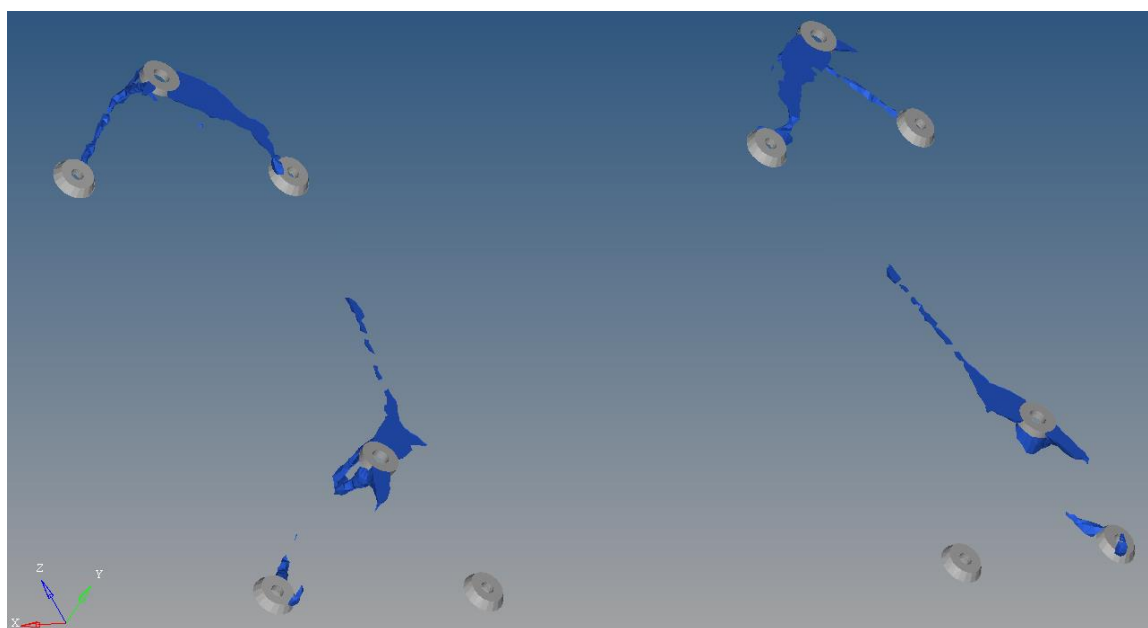
Figure 4-1. Optimized results at 0.5 density threshold
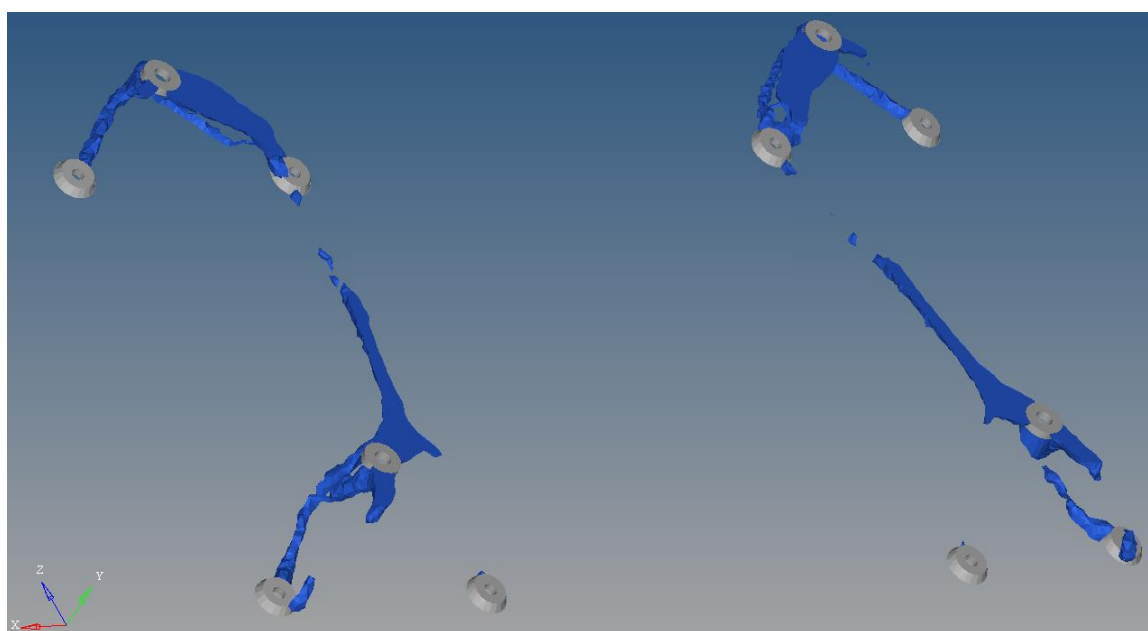
Figure 4-2. Optimized results at 0.3 threshold
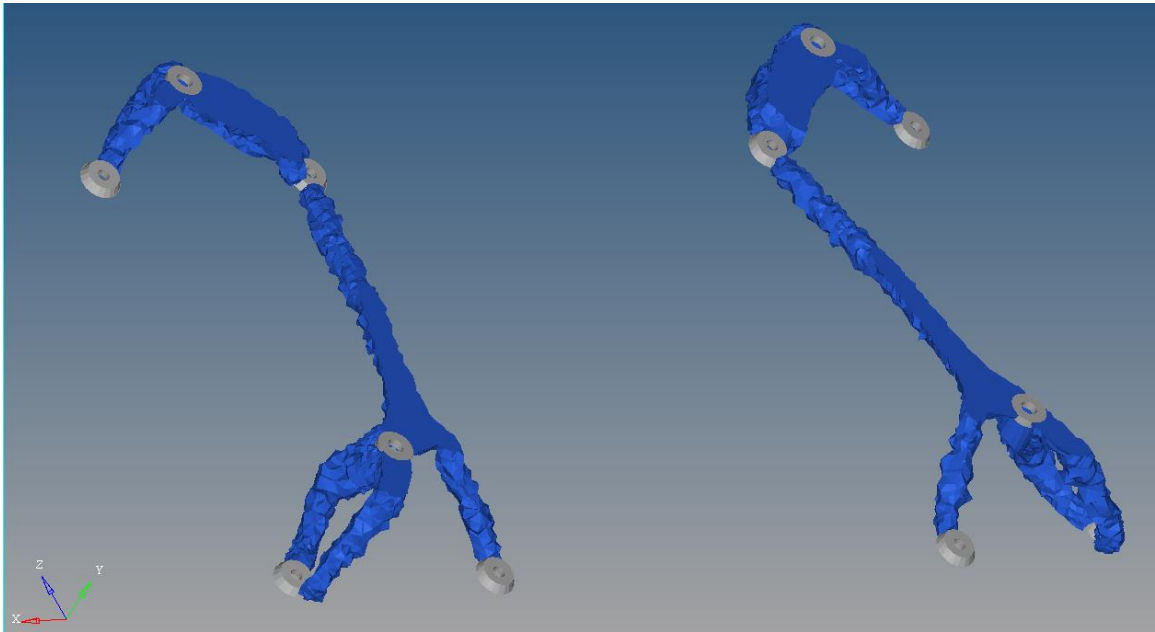
Figure 4-3. Optimized results at 0.1 threshold

To prevent sharp corners in the extracted geometry, the "thin layer" option was selected

when extracting the geometry with OSSmooth. This option forces the extracted geometry to

include one layer of elements around all non-design space. This step was performed to minimize

stress concentrations and ensure that the interfaces were well supported. The result of this

operation is shown in Figure 4-4.
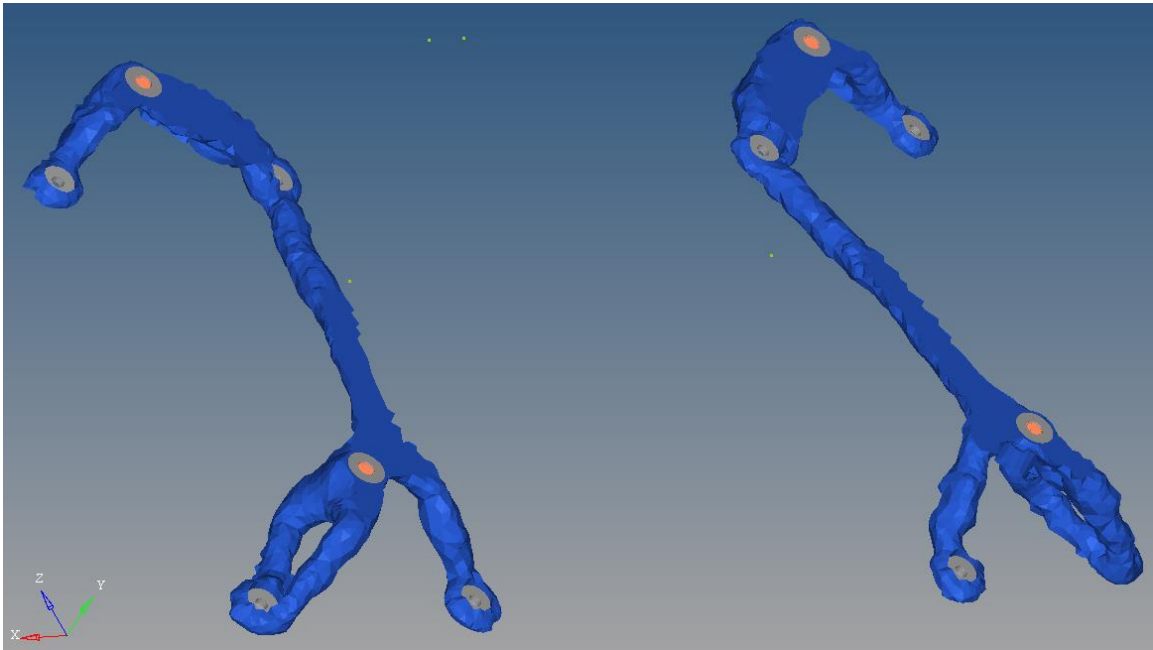
Figure 4-4. Optimized results at 0.1 threshold

One possible explanation for the necessity of selecting a low threshold is the mesh size. If the optimization could be performed with a finer mesh, then the optimization algorithm may be able to converge on a result that is continuous at a higher element density threshold. A load path may only require a thin member for support with a given material, but with a coarse mesh, thin members cannot be realized. Instead, thicker members appear at lower element densities because the material is less structurally crucial.

4.1.2 Mechanical Properties of Optimized Results

The results of the optimization runs outlined in Section 3.3 show the importance of modeling choices and boundary condition selection. The four results of the mounting plate optimization runs with fully constrained plate/conic interfaces are shown in Figures 4-5 to 4-8. Results of the elastic box, washer interfaces case using stiff springs at the plate/conic interfaces

with degrees of stiffness k=10^5 lbf/in and k=10^4 lbf/in are shown in Figures 4-9 and 4-10

respectively. Optimized results are shown in blue, non-design material in gray, and boundary

conditions/rigid connections modeling the box are shown in orange.
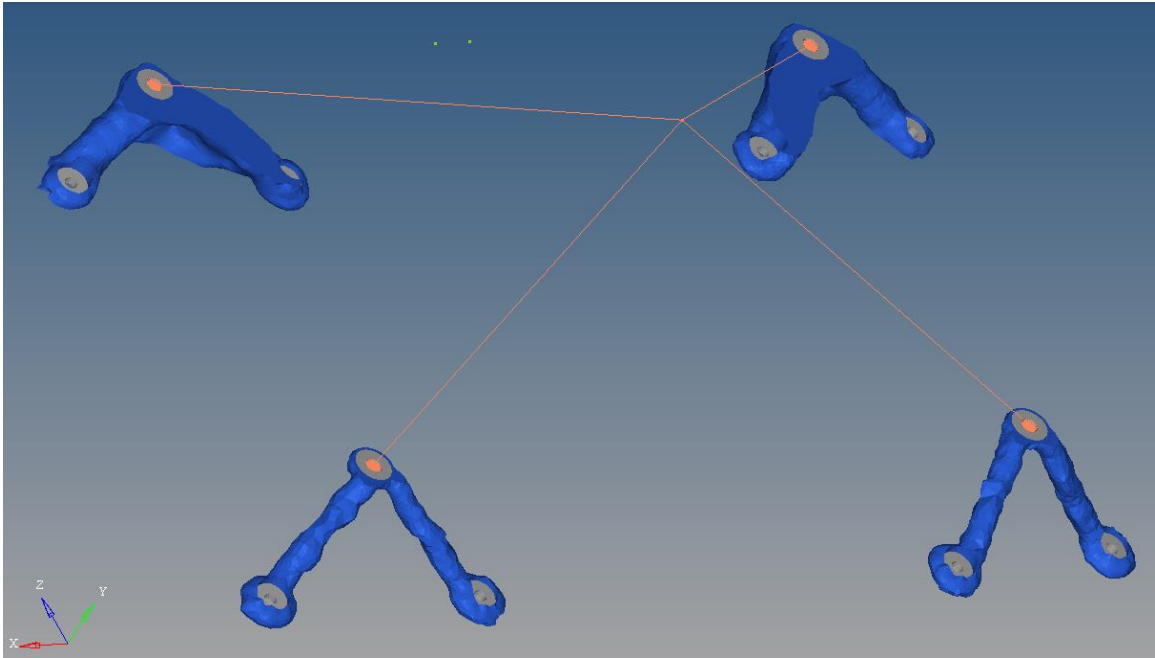
Figure 4-5. Optimized results of rigid box with connections at bolt surfaces
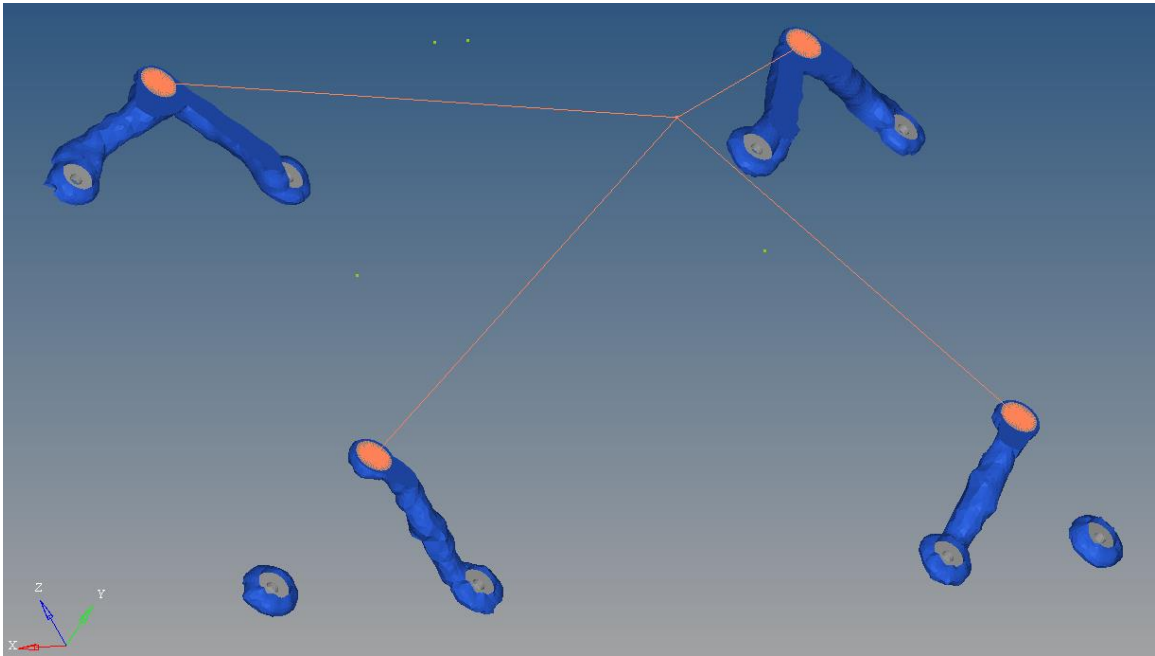
Figure 4-6. Optimized results of rigid box with connections at washer surfaces
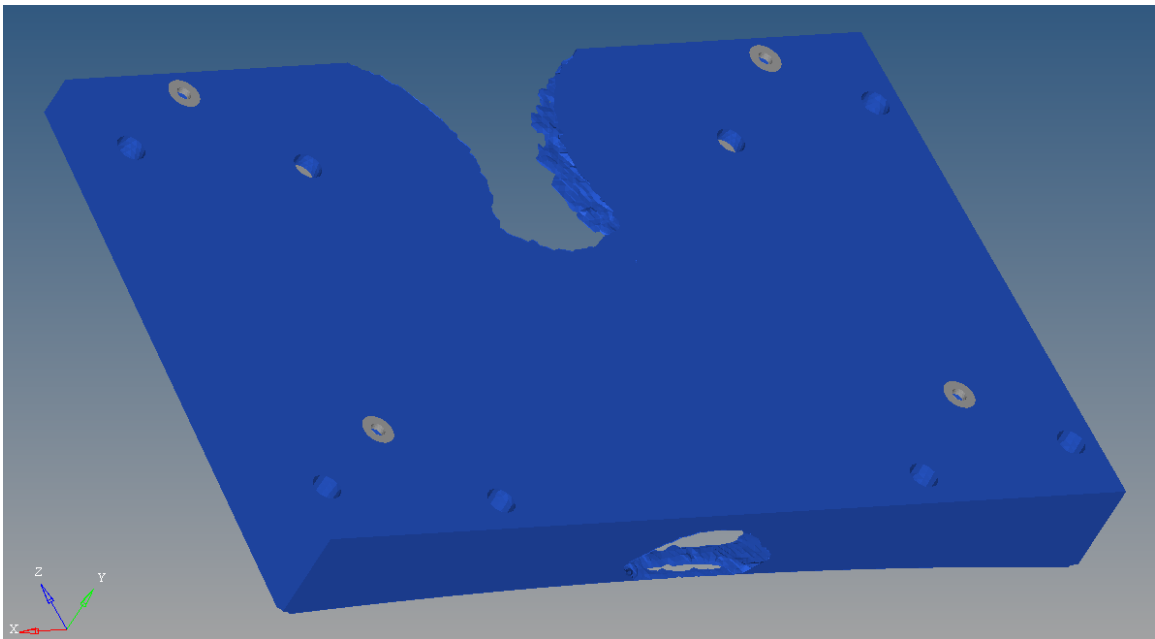
Figure 4-7. Optimized results of elastic box with connections at bolt surfaces
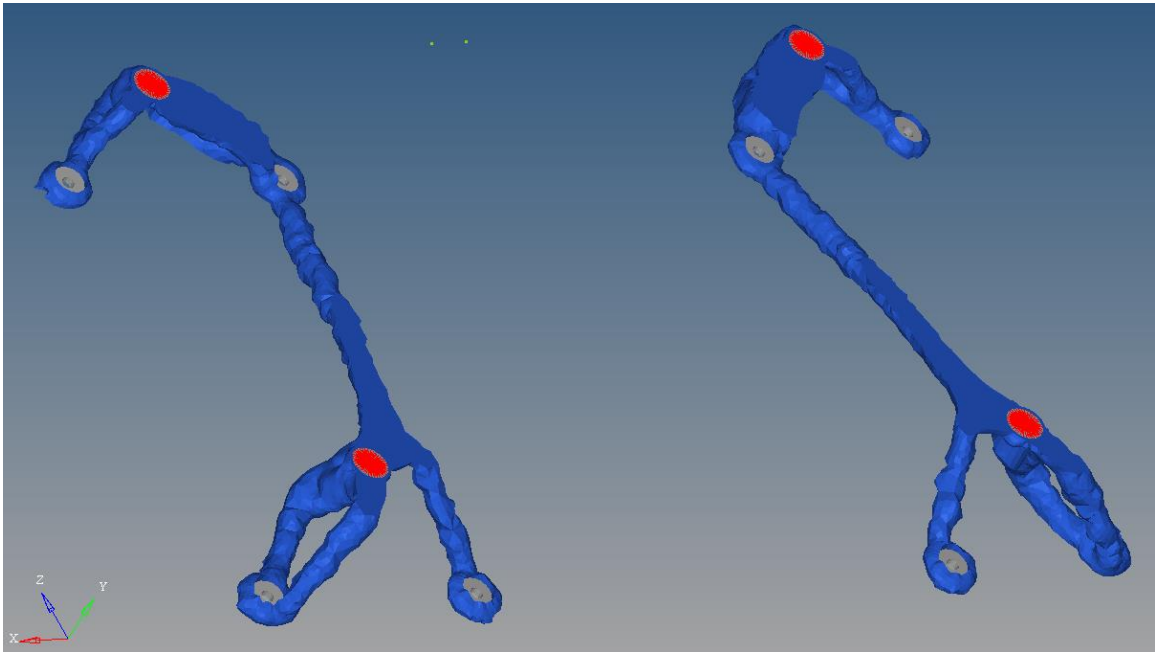
Figure 4-8. Optimized results of elastic box with connections at washer surfaces
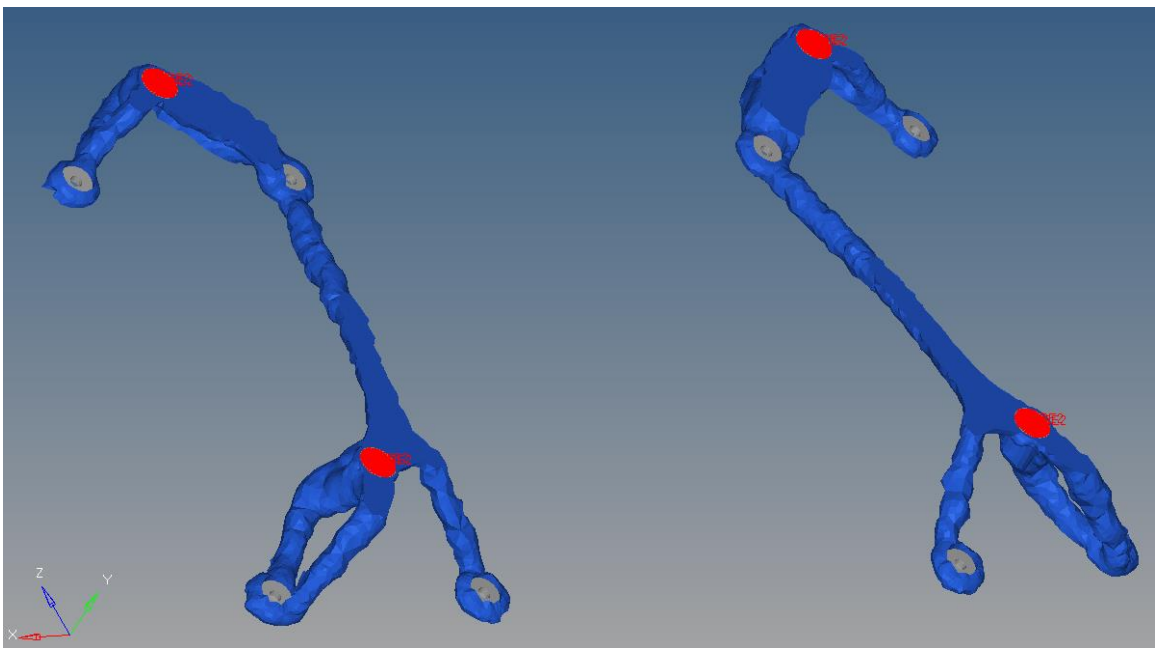
Figure 4-9. Optimized results of elastic box with washer interfaces and spring supports (k = 10^5 lbf/in.)
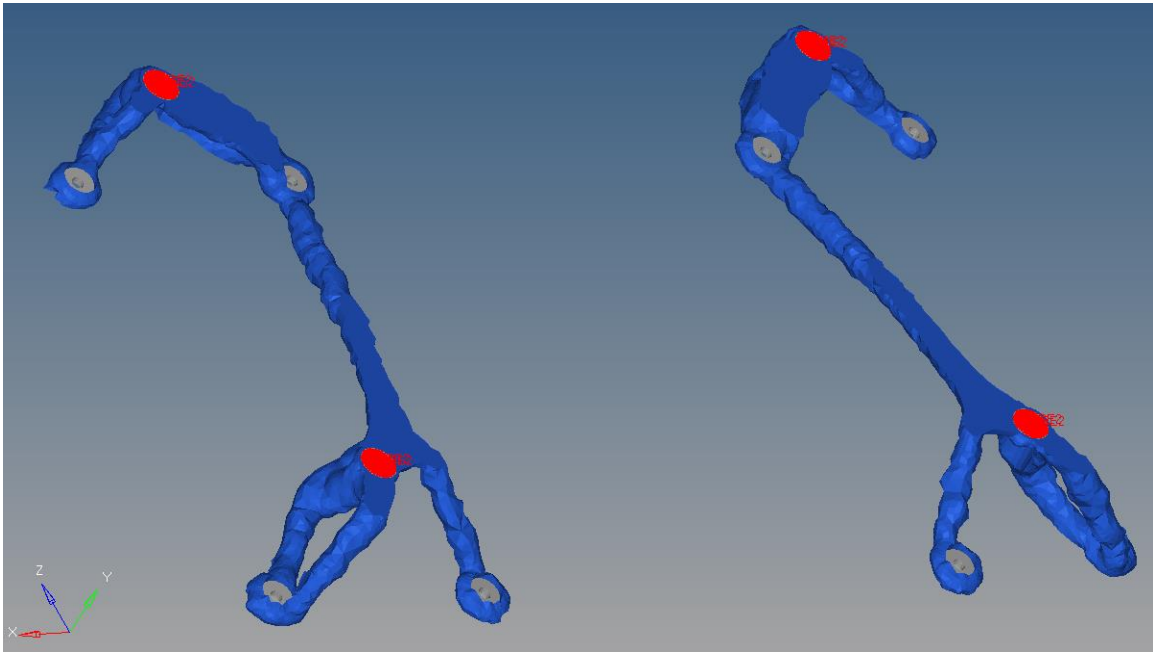
Figure 4-10. Optimized results of elastic box with washer interfaces and spring
supports (k = 10^4 lbf/in.)

All of these results were extracted using OSSmooth at the 0.1 element density threshold

for FEA validation. Each extracted geometry was analyzed to determine its first natural frequency

as well as von Mises stress and displacement contours for each load case. The maximum von

Mises stress and displacement across all cases was recorded for each geometry. The values of

each design's elemental von Mises stresses, nodal displacement, and first natural frequency were

examined. Contour plots of each result's maximum stress and displacement across all load cases

are shown in Figures 4-11 through 4-18.
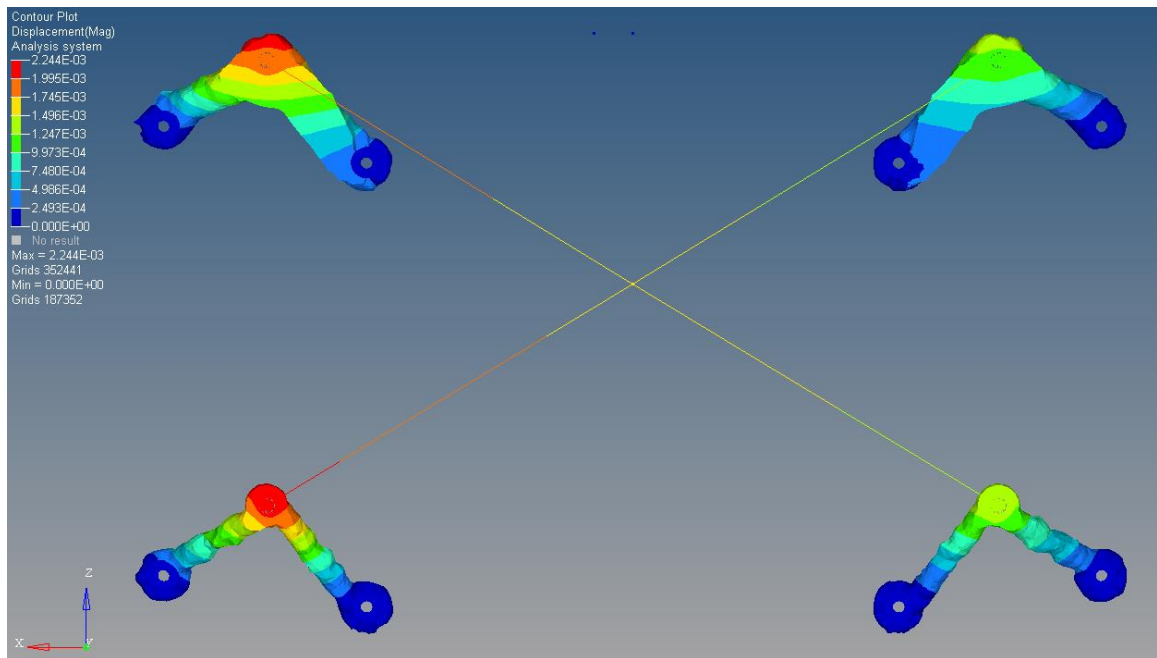
Figure 4-11. Rigid box, bolt interfaces maximum displacement
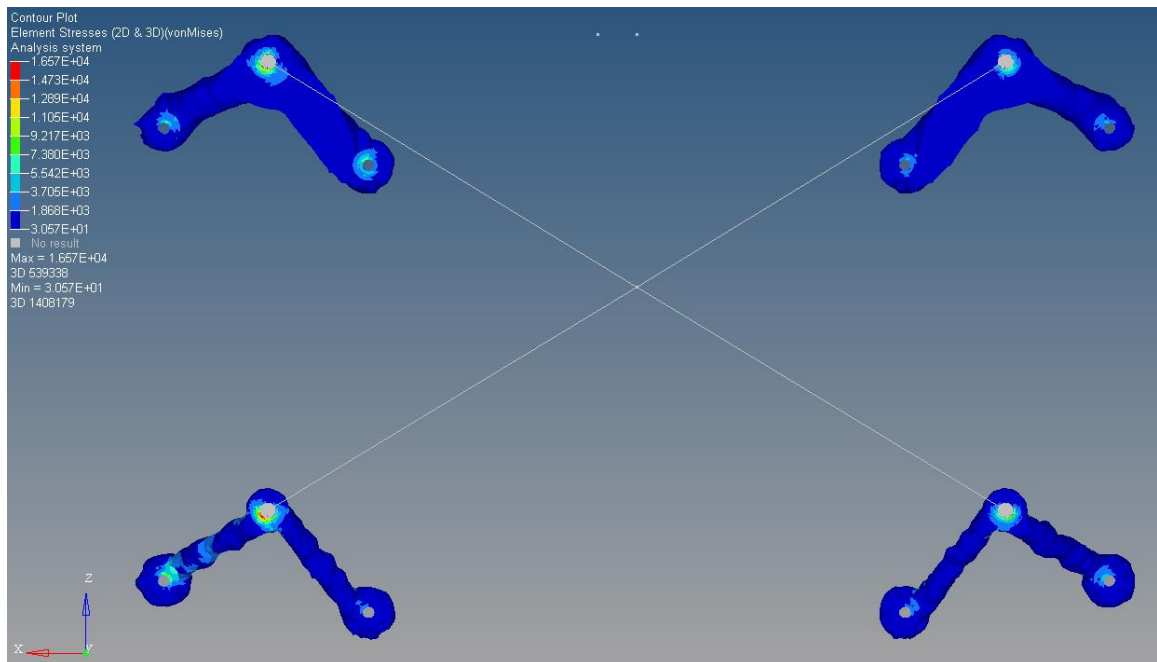
Figure 4-12. Rigid box, bolt interfaces maximum stress
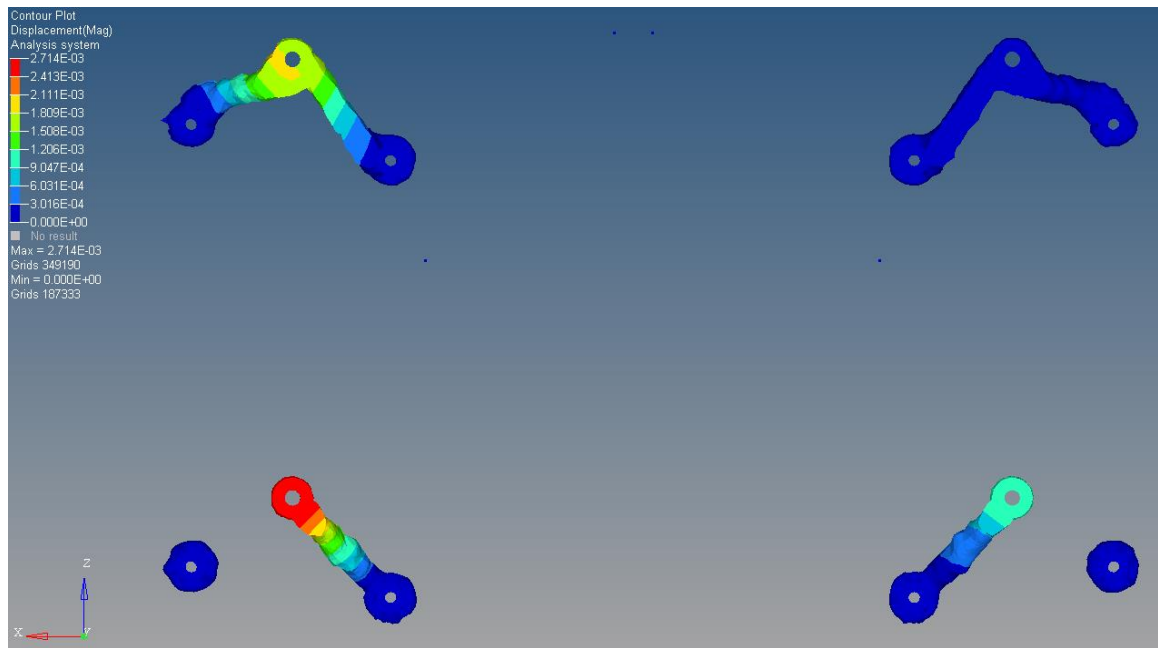
Figure 4-13. Rigid box, washer interfaces maximum displacement
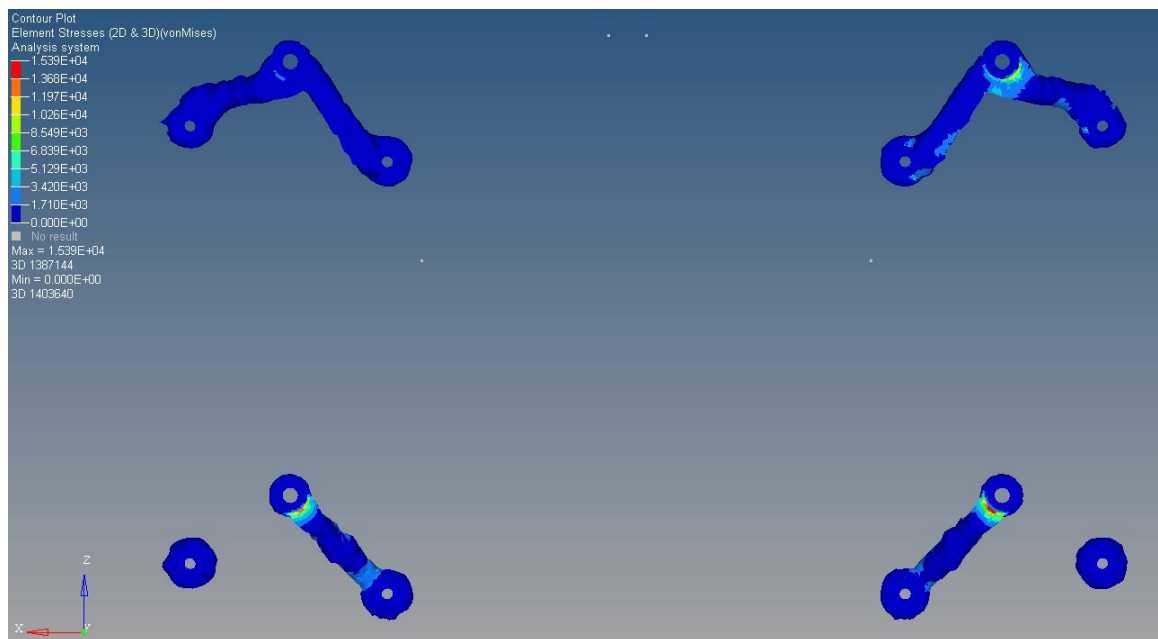
Figure 4-24. Rigid box, washer interfaces maximum stress
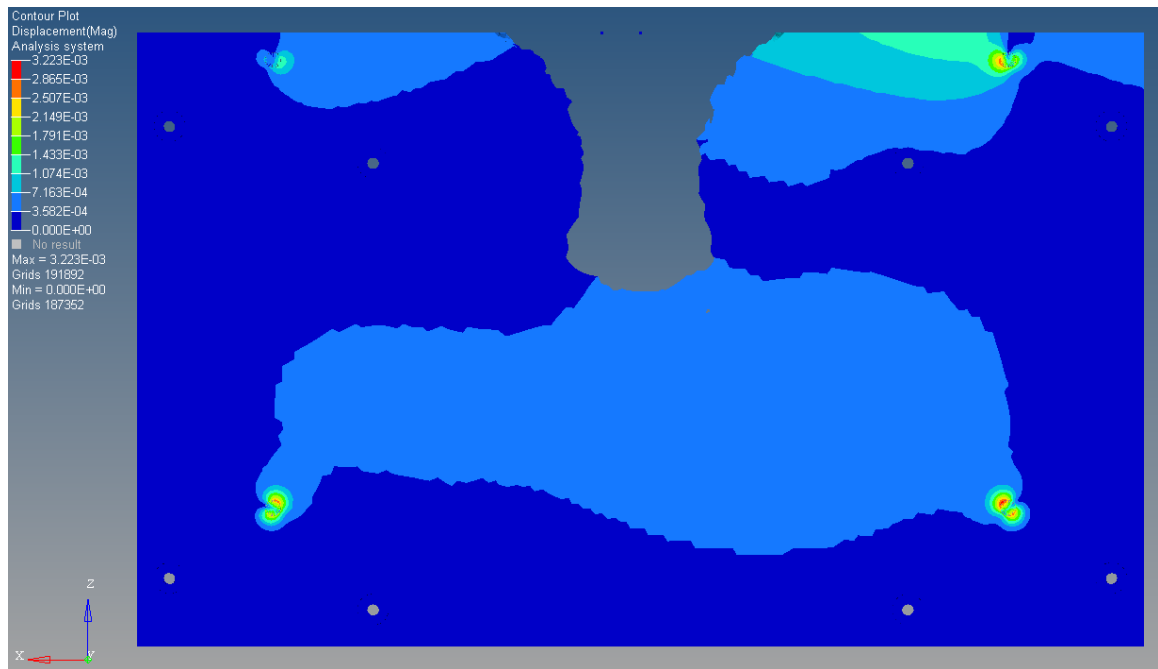
Figure 4-35. Elastic box, bolt interfaces maximum displacement
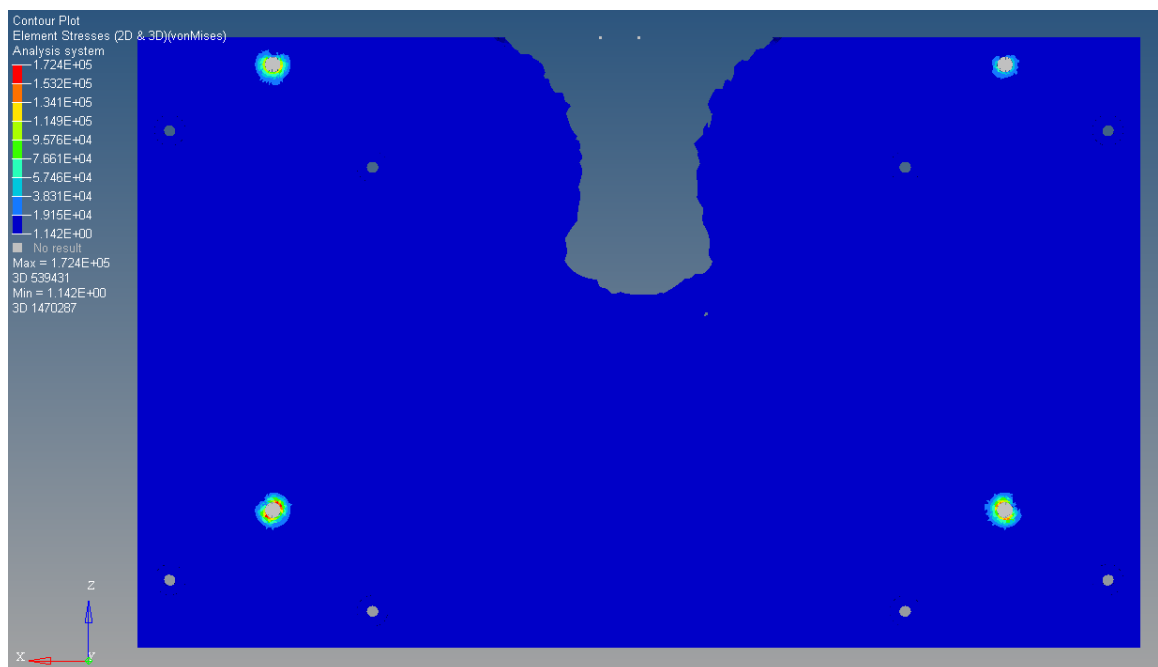
Figure 4-46. Elastic box, bolt interfaces maximum stress
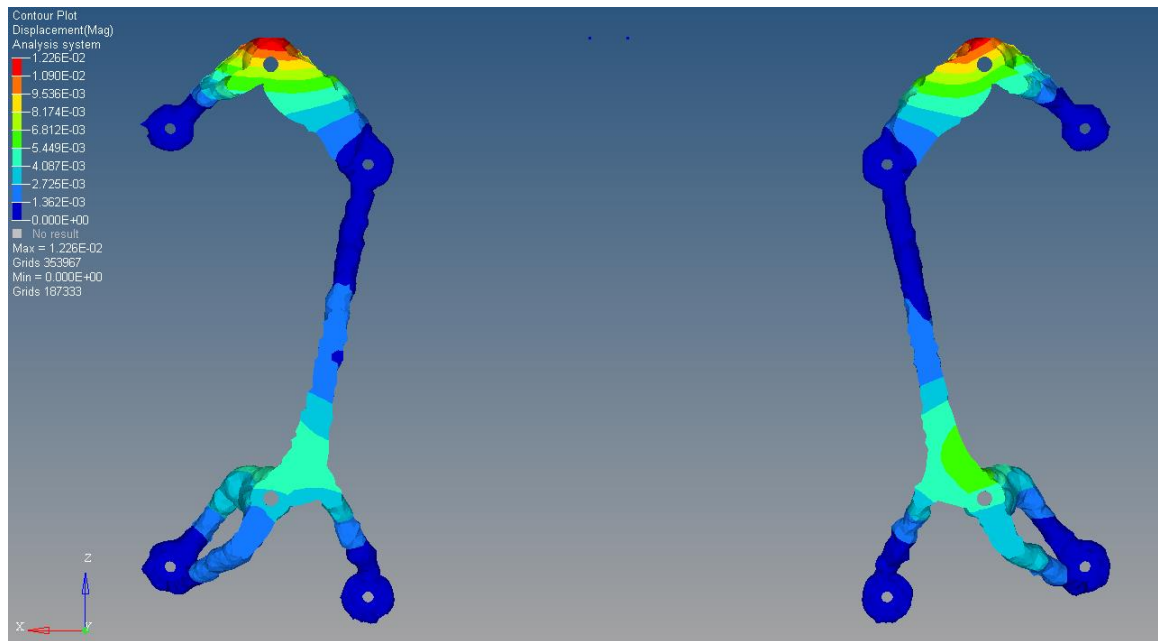
Figure 4-57. Elastic box, washer interfaces maximum displacement
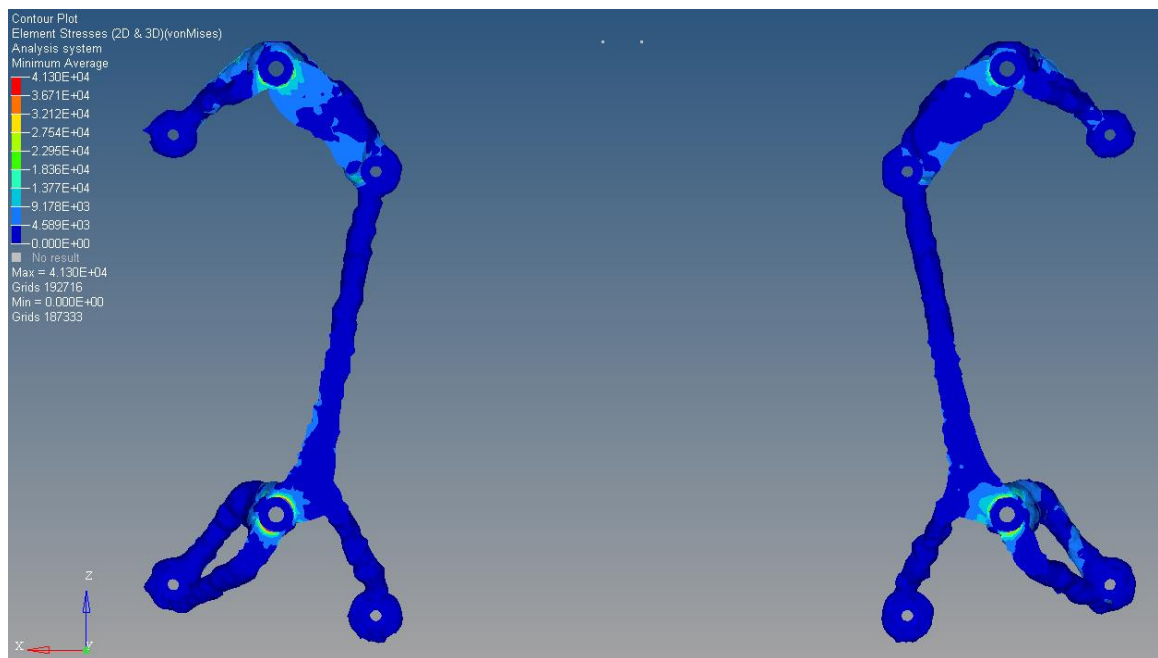
Figure 4-68. Elastic box, washer interfaces maximum stress

Table 4-1 shows a summary of the performance of the extracted results. This information is especially useful when comparing results of similar masses; a design with slightly higher mass but improved performance in terms of mechanical properties could be preferable to a low-mass, poorer-performance result.

Table 4-1. Optimized results mechanical properties

	Mass (lbm)	Max. Displacement (in)	Maximum von Mises Stress (psi)	1st Natural Frequency (Hz)	Number of Separate Pieces
Rigid Box, Bolt interface	1.75	0.0022	16,600	152	4
Rigid Box, Washer interface	1.07	0.0027	15,390	194	4
Elastic Box, Bolt interface	51.4	0.0322	172,000	1090	1
Elastic Box, Washer interface	2.39	0.0123	41,300	991	2

Figures 4-5 through 4-10 show that the interface boundary conditions as well as the model assigned to the box have important impacts on the resulting topology. In the optimizations in which the interfaces are taken as connections along the bolt surface (see Figures 4-5 and 4-7), more material is concentrated around the box interfaces, and in the case where the box is taken as elastic, the optimization ended abruptly because the boundary condition concentrated stress to the extent that it violated the von Mises stress constraint on the optimization (see Figure 4-16). For this reason, the boundary condition of connecting via the bolt contact surface is invalid, and not pursued further. Figures 4-9 and 4-10 show that the spring interface between the conic and the mounting plate described in Section 3.2 has little qualitative effect on the resulting topology. This trend was observed in all cases using spring interfaces. The extra degree of freedom added by the spring is essentially constrained to a low value because of the force constraint on those interfaces and the high stiffness of the conic. In the optimizations in which the box is considered rigid (see

Figures 4-5 and 4-6), the optimization offers only a 4-piece result since the box is essentially being used as a structural member. In the successful case where the box is taken to be elastic (see Figure 4-8), a two-piece result is obtained. This two-piece result is more physically meaningful and useful since the real box has some non-zero elasticity. These optimized results allow the part to function without relying on the structure of the box.

As described in Section 3.3, the optimization was repeated using the washer interfaces and elastic box with Ti-6Al-4V as the part material. The results of this optimization are shown in Figure 4-19:
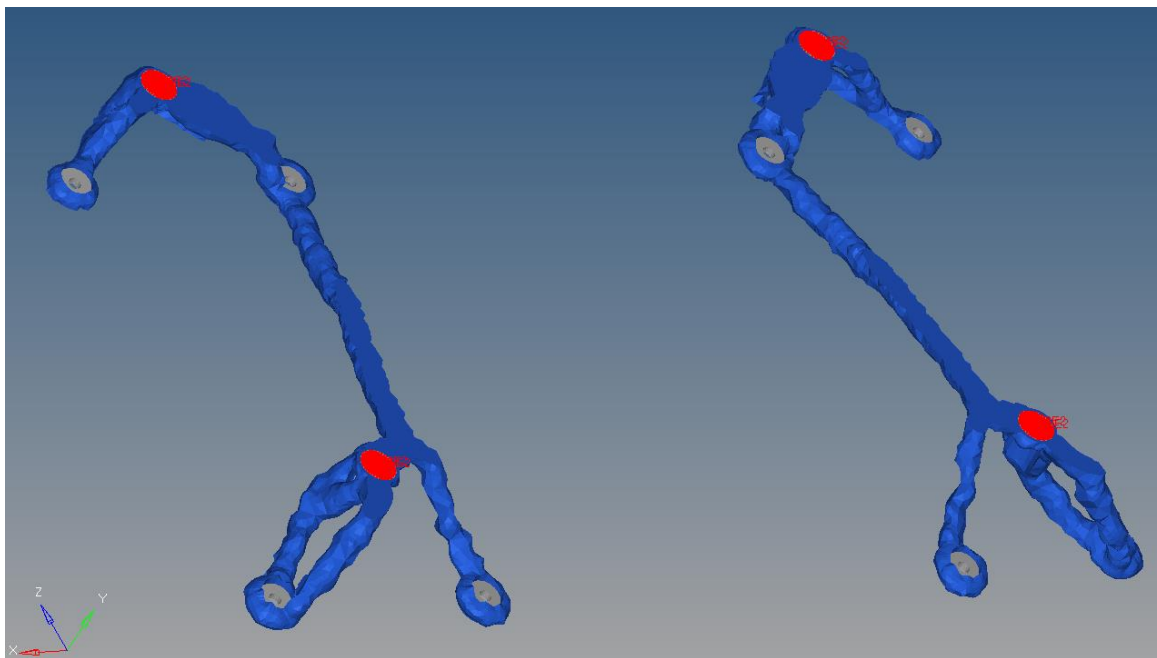
Figure 4-79. Titanium optimization results

The results were extracted at the same 0.1 threshold as the aluminum results, which happened to be the threshold where a continuous structure appeared. Qualitatively the topology is similar to the aluminum results, albeit with thinner members. These results did not represent an improvement over the aluminum results, as the higher density of the titanium led the resulting

part to weigh 2.94 lbm, compared to the 2.39 lbm for the aluminum result. Due to their density difference, for a titanium design to show reduction in mass over an aluminum design, it would need to be less than 63.75% of the volume of the aluminum design. It is possible that, with mesh refinement, finer features with more complex topologies could emerge to allow titanium results to achieve a lower mass than their aluminum counterparts. However, with the computing power available, the aluminum results met the performance criteria at a lower mass. For this reason, the two-piece aluminum solution was chosen for interpretation and prototyping.

The two-piece design was interpreted using SolidWorks and the surfacing method detailed in Section 3.4 to reach the interpreted two-piece design shown in Figure 4-20. This design was analyzed with all loading conditions to ensure that it met all design constraints. The maximum stress and displacement contours are shown in Figures 4-21 and 4-22:
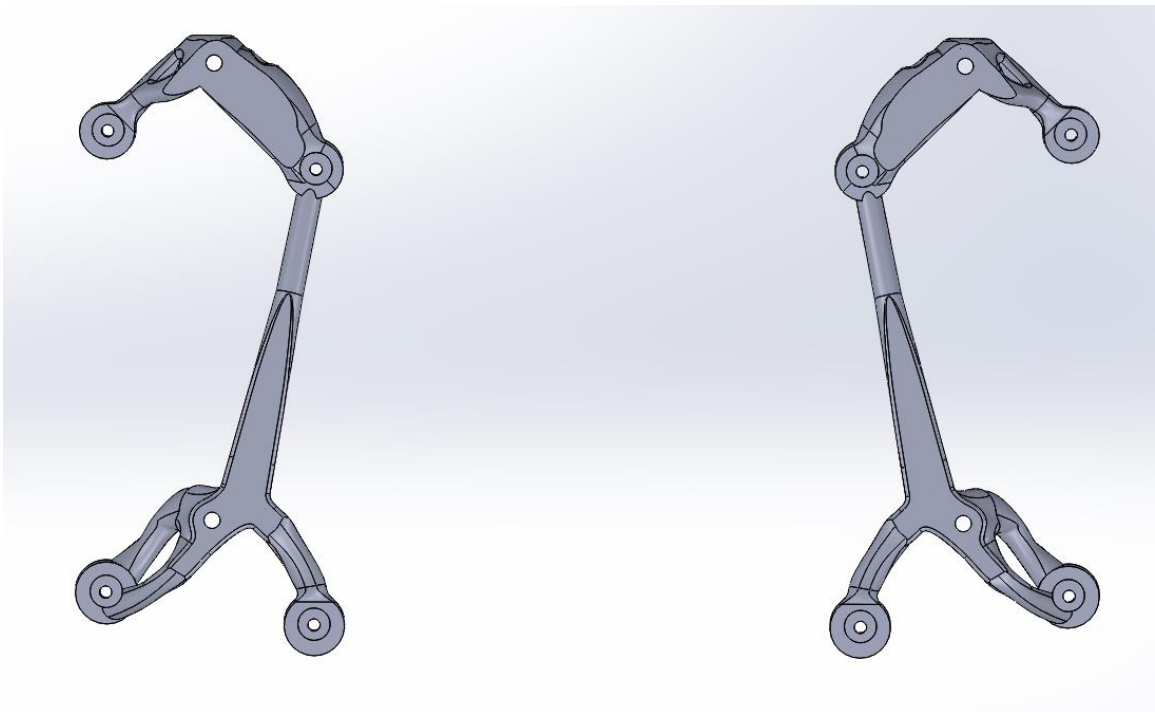
Figure 4-20. Interpreted two-piece design
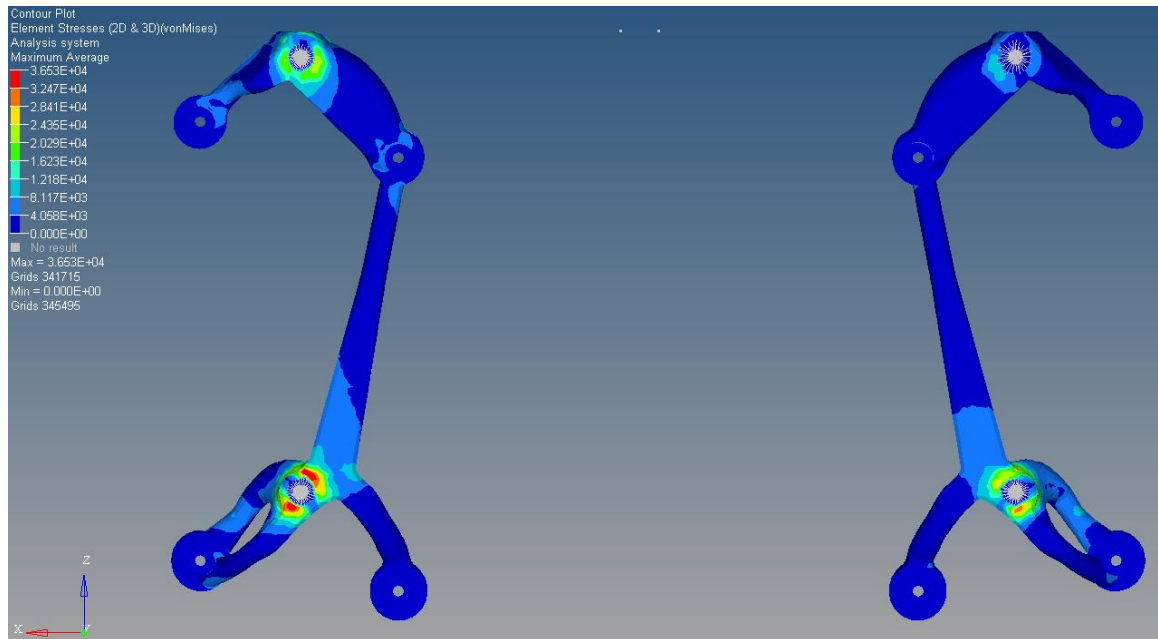
Figure 4-21. Interpreted two-piece design maximum stress
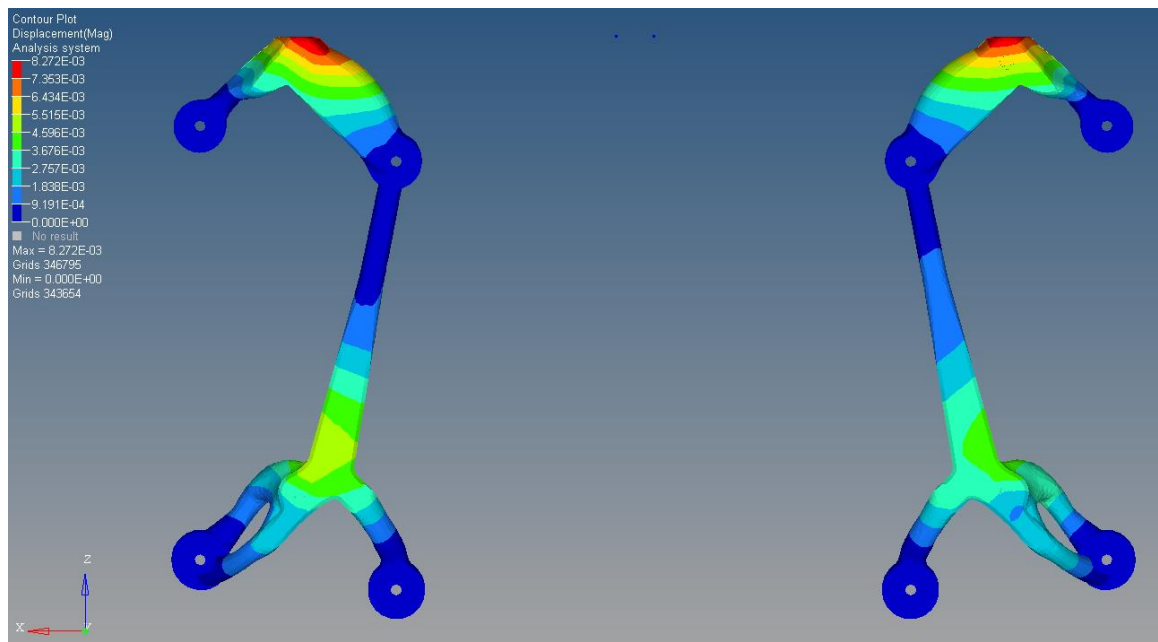
Figure 4-22. Interpreted two-piece design maximum displacement

4.2 Post Processing and Additional Features

As the desired mounting plate design was intended to be one continuous part, the interpreted geometry required the addition of a connecting geometry to join the two symmetrical pieces generated by the optimizer. Reducing the optimized solution to a one-piece design would allow our collaborators to replace the current part in their manufacturing and assembly chain without adding the complexity tracking additional parts. The connecting geometry could also be useful in handling the redesigned mounting plate. This connecting geometry only needed to support loading incurred by handling of the part prior to installation; so, separate loading conditions were developed and applied for design and validation.

Optimization was used to gain insight into the most structurally efficient geometries and positioning. Three load cases were applied to a design space defined as the space between the two mounting plate pieces. The first held the center of the connector static and applied 10lb loads on each side of the mounting plate. The second held one side of the plate static and applied a 20lb downward force to the other side. The third held one side of the plate static, with a twisting load of 160lb·in. applied to the other side. These load cases can be seen in Figure 4-23 through Figure 4-25, respectively.
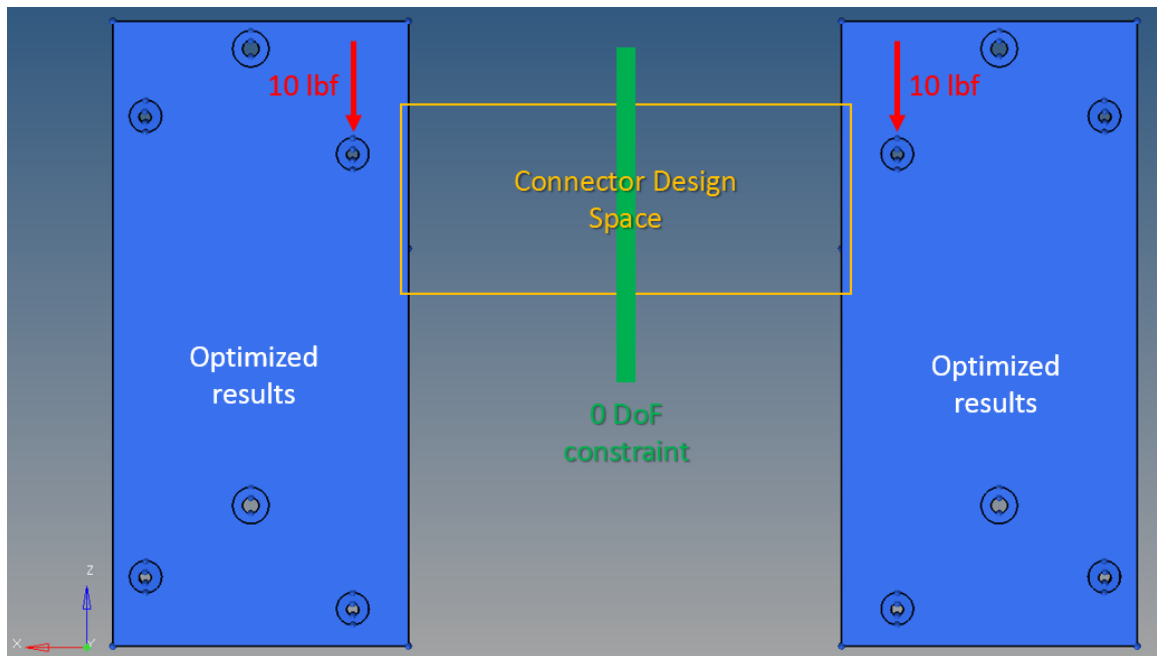
Figure 4-23. Connector optimization and analysis load case 1

Figure 4-24. Connector optimization and analysis load case 2
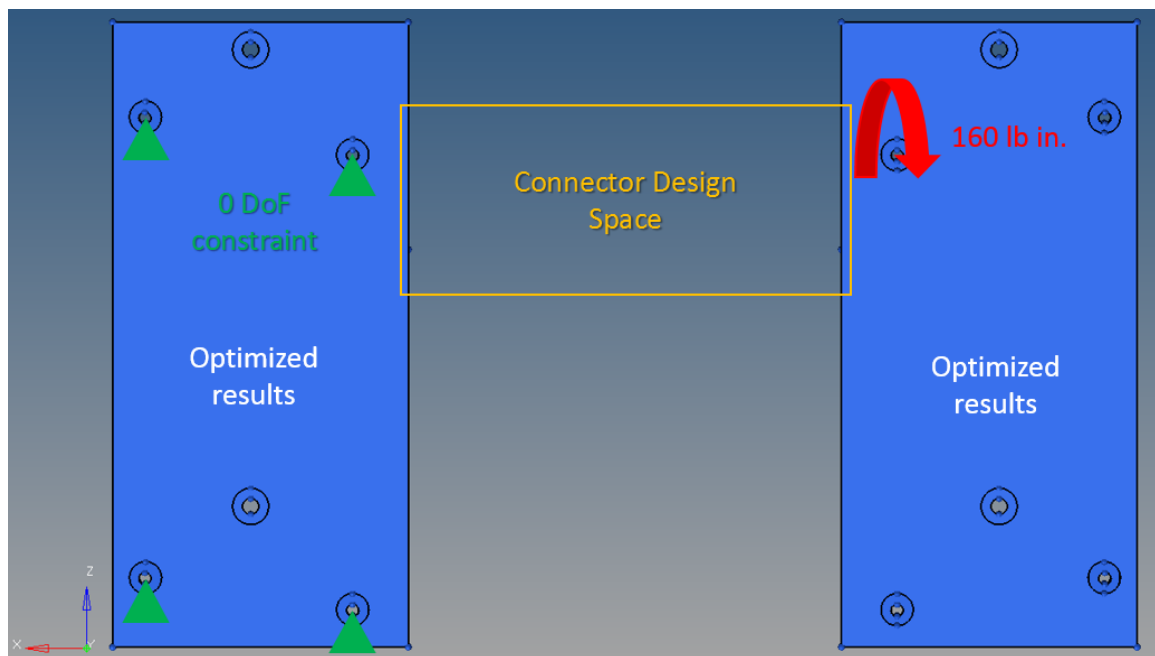
Figure 4-25. Connector optimization and analysis load case 3

The results of the connector optimizations showed members too fine to produce by FDM for prototyping but showed a few important guidelines for designing a low-mass connector. As shown in Figure 4-26, the optimization placed all structural material along the shortest span between the two sides of the mounting plate results, and formed a truss structure to ensure a low compliance while simultaneously lowering mass.
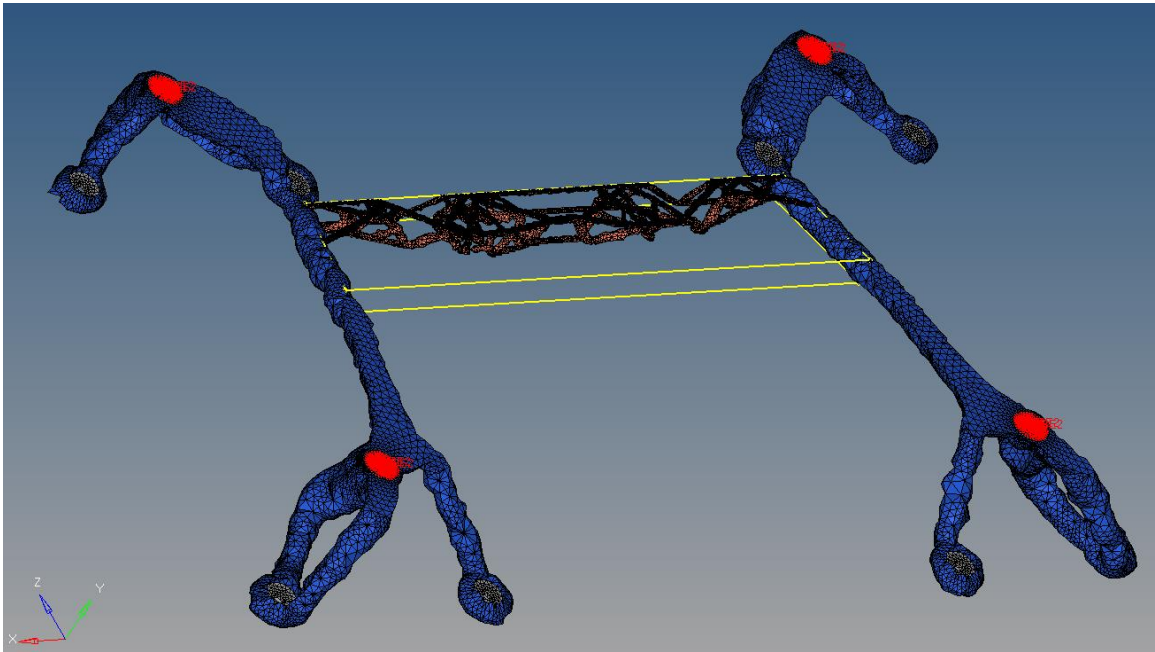
Figure 4-26. Connector optimized results

With these guidelines in mind, four connecting geometries were generated (see Figure 4-27). The first two geometries investigated were a simple rods: (1) one solid and (2) one hollow. The second two geometries were both truss designs with a hexagonal cross-section where the length was comprised of triangular sections. In Truss 1, these triangular sections nested within one another, whereas in Truss 2 all triangle vertices were shared. These connectors were placed at the shortest span between the two interpreted pieces.
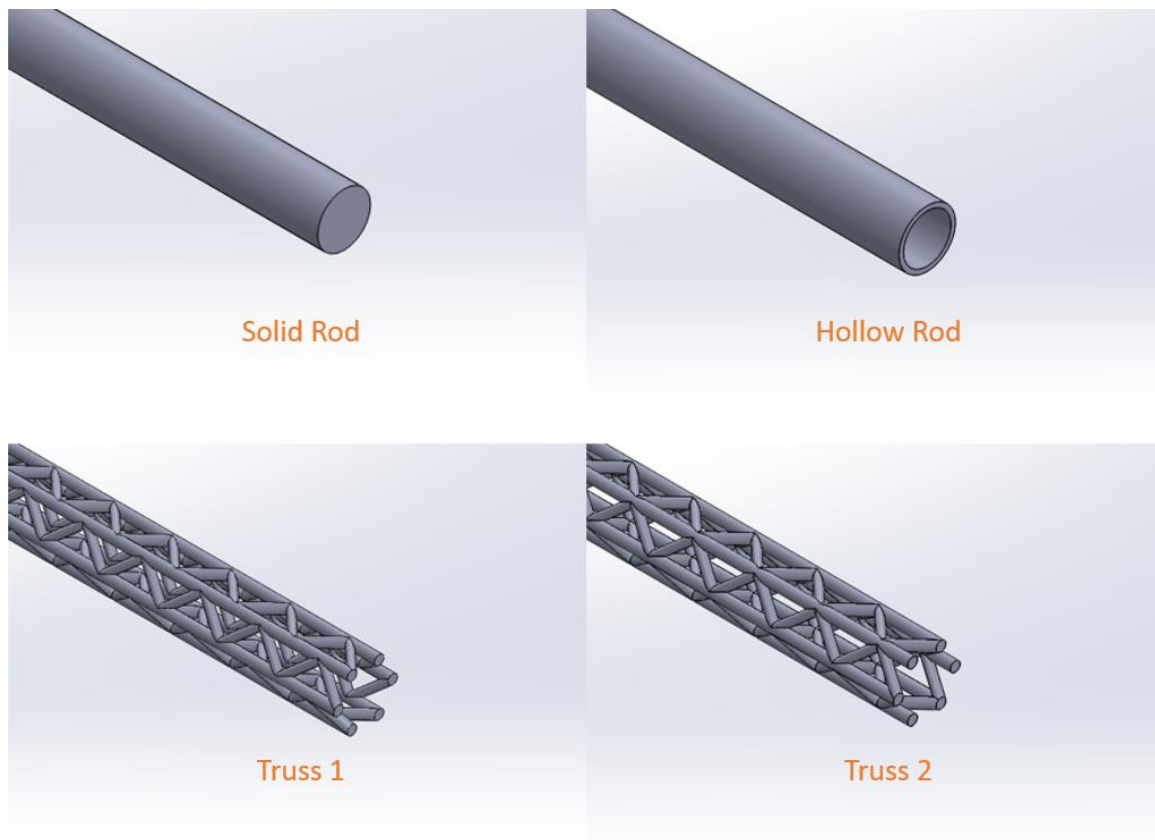
Figure 4-27. Investigated connecting geometries

Each geometry was analyzed with the three aforementioned optimization loading conditions, as well as the original gravitational and modal loading conditions to validate performance in both handling and function. Each geometry was also analyzed over a range of member thicknesses to manually minimize the mass of the design. In both of the cylindrical rods, the connector was analyzed with a starting outer diameter of 0.5in., which was iterated in a decreasing manner by increments of 0.05in. and reanalyzed until failure was achieved. In the hollow rod, the wall thickness was held constant at 0.04in; thick enough to avoid thin wall issues with the available FDM process. In the truss structures, the truss member thickness was varied from 0.2 in. member diameter to 0.04 in. diameter. A summary of the lowest mass for each geometry can be found in Table 4-2.

Table 4-2. Optimized results mechanical properties

	Lowest feasible member thickness (in.)	Part mass with connector (lbm)
Solid Rod	0.40	3.25
Hollow Rod	0.50	3.139
Truss 1	0.016	3.131
Truss 2	0.016	3.130

Truss 2 with a 0.016 in. member thickness was the lowest-mass feasible design that had

no stresses above the yield stress in each of the three loading cases applied and did not lower the

part's natural frequency below the 100Hz constraint. Both of the trusses and the hollow rod

showed similar masses, but the truss structures offer a means to remove solid support material

necessary for printing. The Truss 2 design was selected because it offered a slight mass advantage

over the Truss 1 design. The displacement results of this design's analysis are shown in Figures

4-28 through 4-30, and the one-piece design is shown in Figure 4-31.
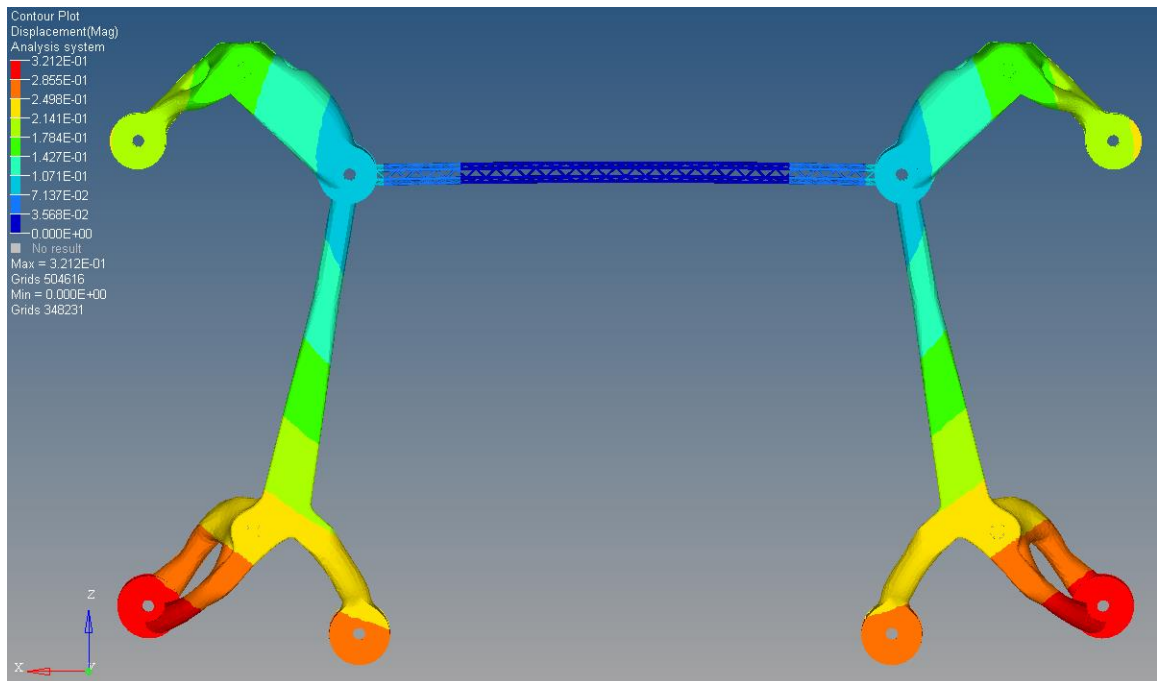
Figure 4-28. Middle bend case displacement
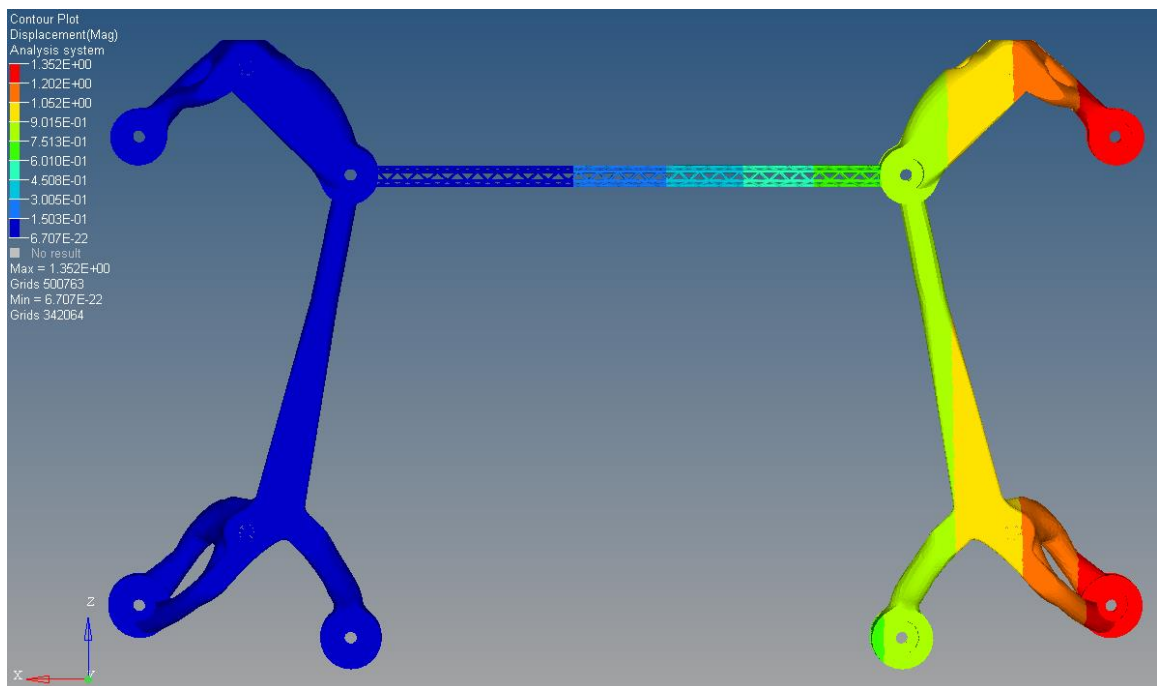
Figure 4-29. Side bend case displacement
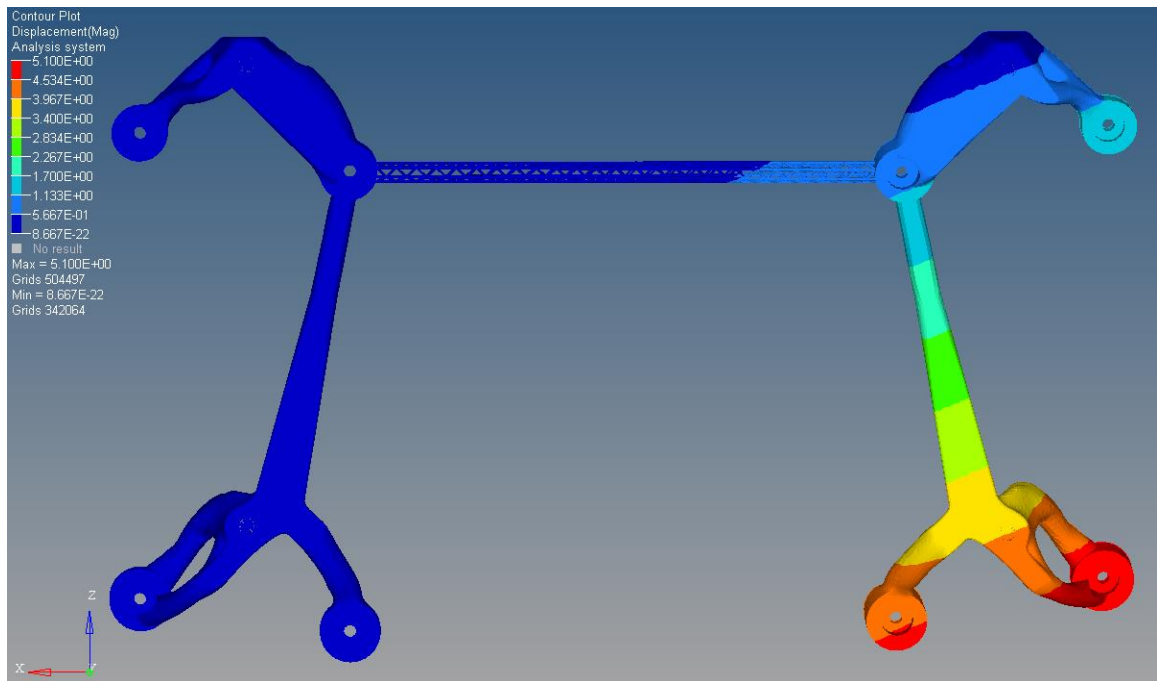
Figure 4-30. Twist case displacement
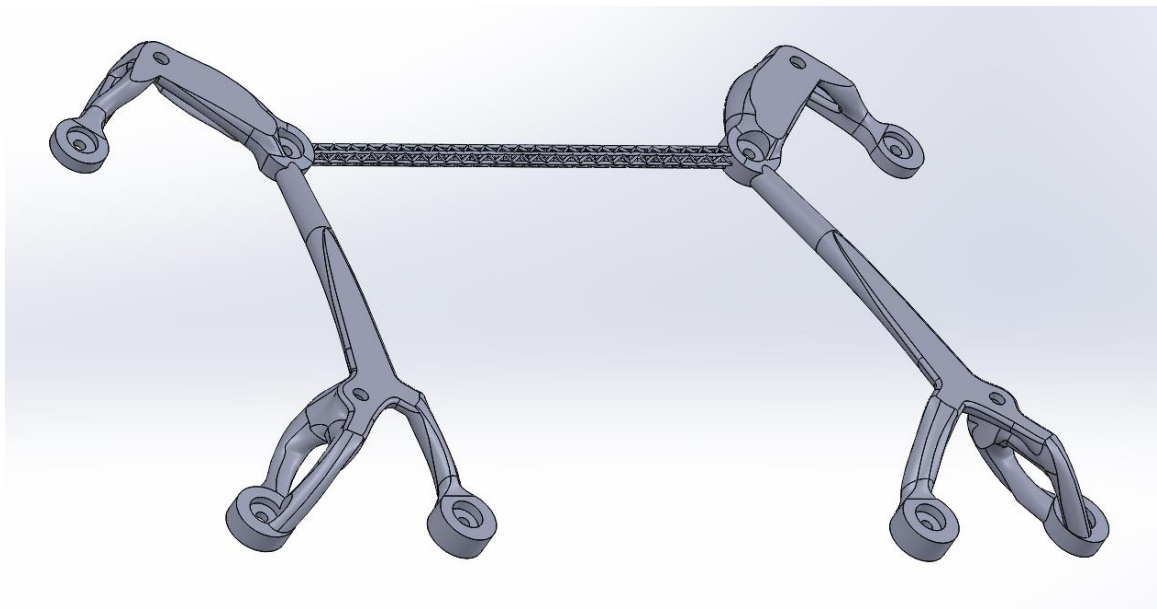
Figure 4-31. Final one-piece design

The design in Figure 4-31 represents a one-piece solution that, when produced, could be installed in place of the current mounting plate with no modification to adjacent part geometry.

This design not only reduces the mass 60.8% from the current design, but it also improves

stiffness, as shown in Table 4-3.

Table 4-3. Optimized results mechanical properties

	Mass (lbm)	Max. Displacement (in)	Maximum von Mises Stress (psi)	1st Natural Frequency (Hz)
Current part	7.99	0.0170	76,200	588
Optimized two-piece result	2.39	0.0123	41,300	991
Interpreted two-piece part	3.06	0.0083	36,500	1440
Interpreted one-piece part	3.13	0.0090	39,500	570

4.3 Prototyping

The three feasible designs shown in Table 4-3 were produced in Ultem 9085 on a Fortus

400mc FDM printer to demonstrate their manufacturability with AM. The supports required for

printing in Ultem require manual removal like those used in DMLS; so, any removal issues would

indicate areas of the part that required modification for eventual production in metal. The one-

piece interpreted part exceeds the build dimensions of the Fortus 400mc FDM process available;

so, the part was divided into three pieces for printing. The connecting geometry was separated

from the two mounting plate sides with a dovetail design to allow rapid assembly and

disassembly for display purposes. The dovetail design is shown in Figure 4-32.

Figure 4-32. Dovetail connection design (credit Corey Dickman)

The optimized results (see Figure 4-33), two-piece interpretation (see Figure 4-34), and final one-piece interpretation (see Figure 2-35) were printed. Due to the imposed symmetry, only one half of the optimized results and the two-piece interpretation were printed. A summary of the amount of material used as well as the machine time to build each part is listed in Table 4-4.

Figure 4-33. Prototyped optimized results (credit Corey Dickman)

Figure 4-34. Prototyped two-part design (credit Corey Dickman)

Figure 4-35. Prototyped one-part design (credit Corey Dickman)

Table 4-4. Prototyping information

	Print time (hours)	Part material (in^3)	Support material (in^3)
Optimized results (one half)	11.5	15.17	5.412
Original part (one half)	23.2	47	0
One-piece part (all 3 pieces)	26.3	61.97	7.895
Two-piece part from box surface (one half)	11.3	15.24	3.301
Two-piece part from conic surface (one half)	11.7	15.29	4.76

It should be noted that the optimized results required the least printing time and used the least amount of material. While this was to be expected since the interpreted geometry was a conservative estimate of the results, the degree to which printing the un-interpreted (i.e., non-

smooth) results saved both time and material confirms the idea that directly manufacturing

topology optimized results could be an effective way to reduce the time of the design process.

With minimal modification to eliminate stress concentrating features that appear due to the coarse

mesh size, the optimized results could be a functional part. Looking to the future, a refined mesh

may discourage the appearance of these stress concentrating features; so, directly printing

optimized results as functional parts within the realm of possibility.

This prototyping phase also exposed the need to consider build direction when

interpreting optimized results or adding features like the connecting geometry. The two sides of

the two-piece interpreted design were printed in two different directions. This led to the side built

starting from the conic surface (see Figure 4-36), requiring significantly more support material

and machine time than the side built starting from the box surface (see Figure 4-37).
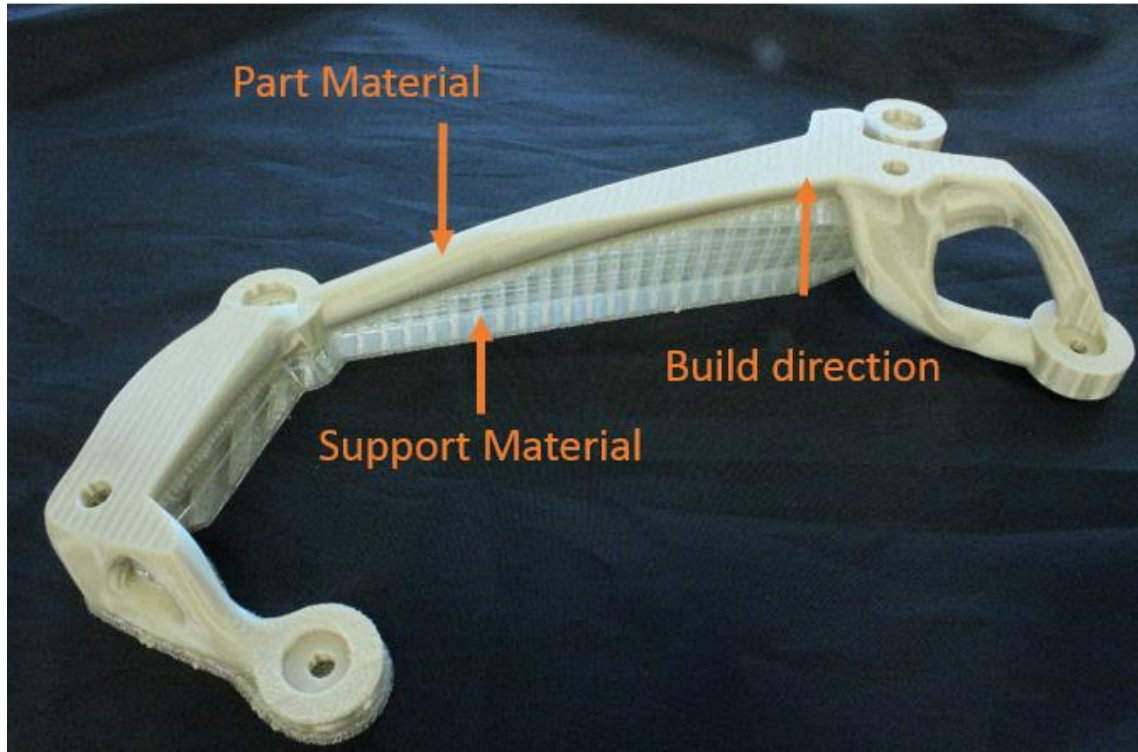
Figure 4-36. Interpreted two-piece design built from conic surface
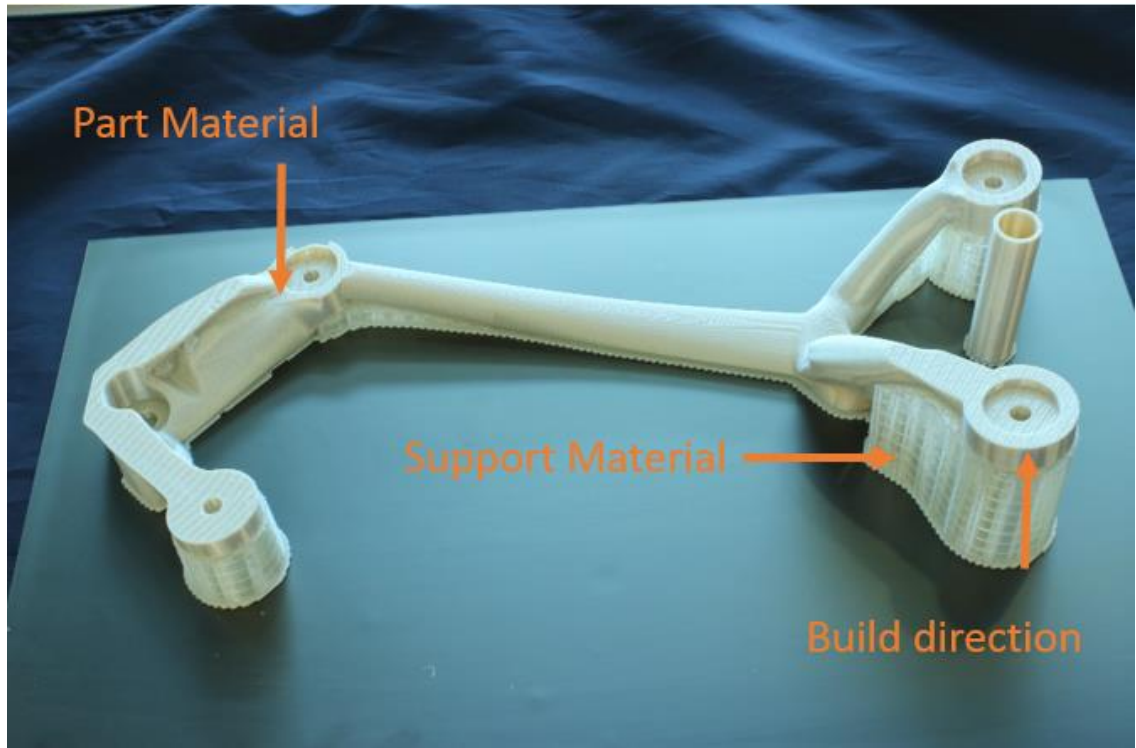
Figure 4-37. Interpreted two-piece design built from box surface

Prototyping the one-piece solution also showed the importance of considering build direction. It was thought that the angles of the members in the connecting truss geometry would allow it to print with minimal support, and that that material could be easily removed. The opposite turned out to be true as some support was needed, and it was time-prohibitive to remove it all (see Figure 4-38). If this part were printed in metal, then removing this support material would be extremely costly, if not impossible, indicating that a geometry tailored to print in the assumed build direction without support would be a better design choice.
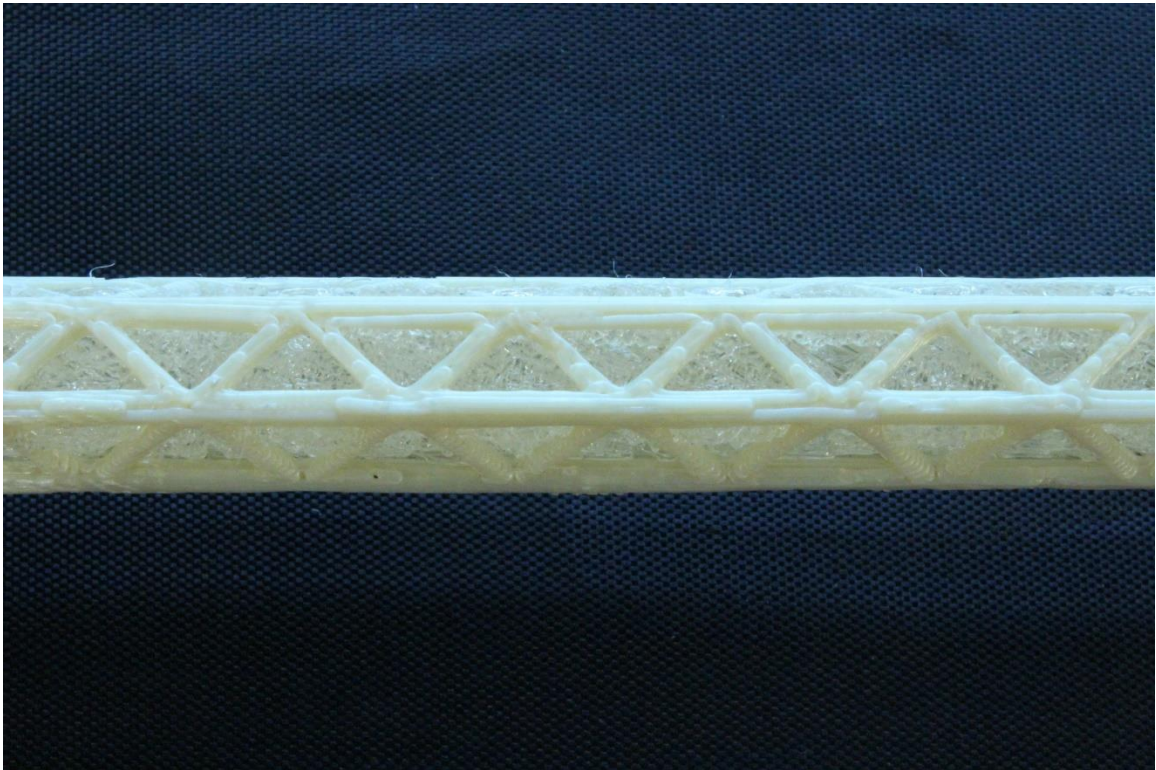
Figure 4-38. Support material within truss structure

4.4 Workflow Ramifications

A major objective of this research was to determine the effect topology optimization could have on design for AM workflow. While topology optimization in its current form can reduce the time in bringing a part from first design to completion, it does not necessarily simplify the workflow yet. The current design for AM workflow has the distinct advantage of having knowledge of the manufacturing process before the first design iteration, as shown in Figure 4-39.
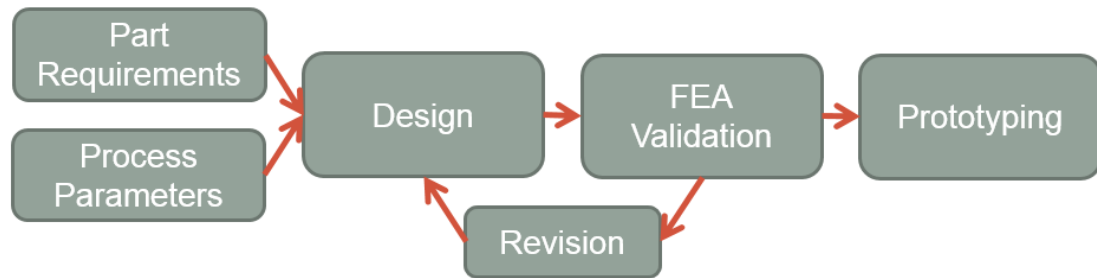
Figure 4-39. Manual design for AM workflow

With the workflow shown in Figure 4-39, every iteration of a part's design should be manufacturable, in theory, with a small amount of support material and additional post-processing, since the designer always keeps the process parameters in mind. However, with current topology optimization software, the machine capabilities and process parameters are not taken into account for the first design iteration; so, design modification is often needed. The current topology optimization for AM workflow is shown in Figure 4-40.
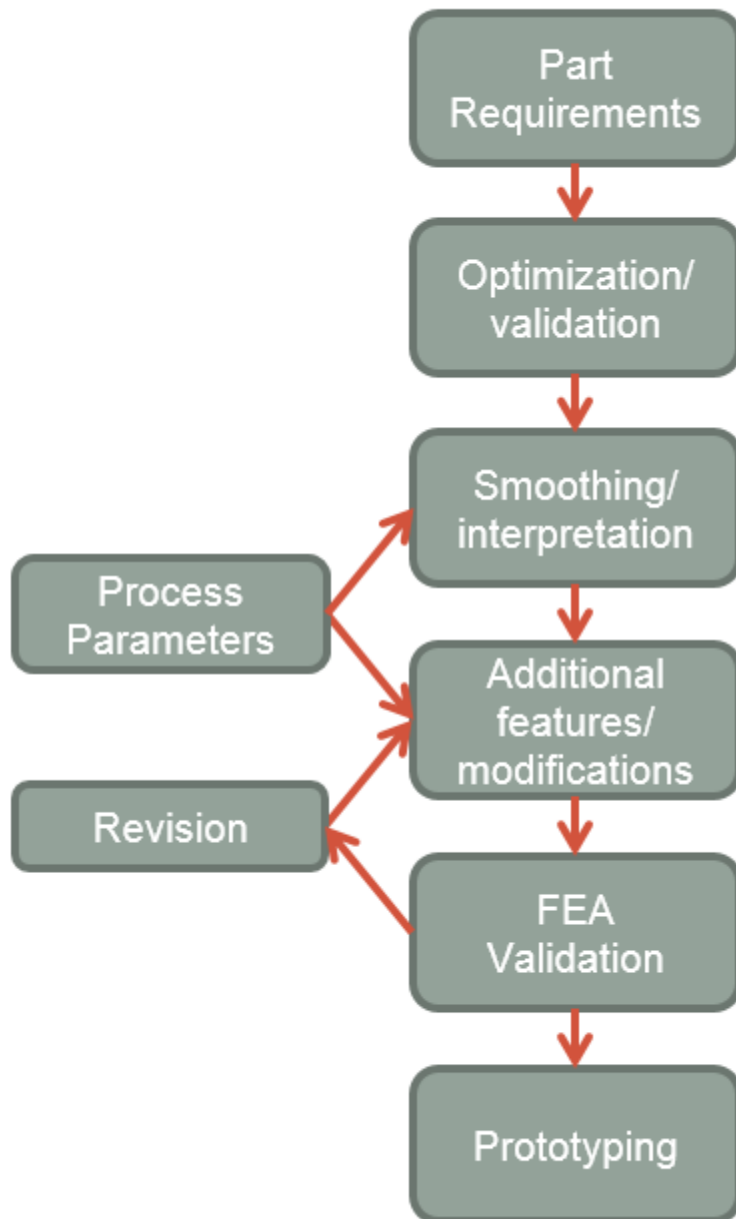
Figure 4-40. AM design flow with topology optimization

It could be argued that in most cases, however, fewer manual design iterations would be

necessary to make optimized results conform to an AM process. The topology optimization

workflow also has the advantage that the first design iteration will be an optimum or near optimum structural efficiency. The manual workflow iterates around design performance, while the optimization workflow iterates around design manufacturability. While manually improving the performance of a design requires numerous iterations to converge on a lightweight design, improving the manufacturability of a design should take fewer iterations once the AM machine capabilities and process parameters are known, and so can be accounted for all at once.

An exciting prospect is what the workflow could look like when constraints for AM are incorporated into the optimization algorithm itself. If constraints to account for build direction, build angle, and distortion due to thermal history could be imposed on the topology optimization algorithm, then the workflow in Figure 4-40 could simplify to the workflow shown in Figure 4-41.
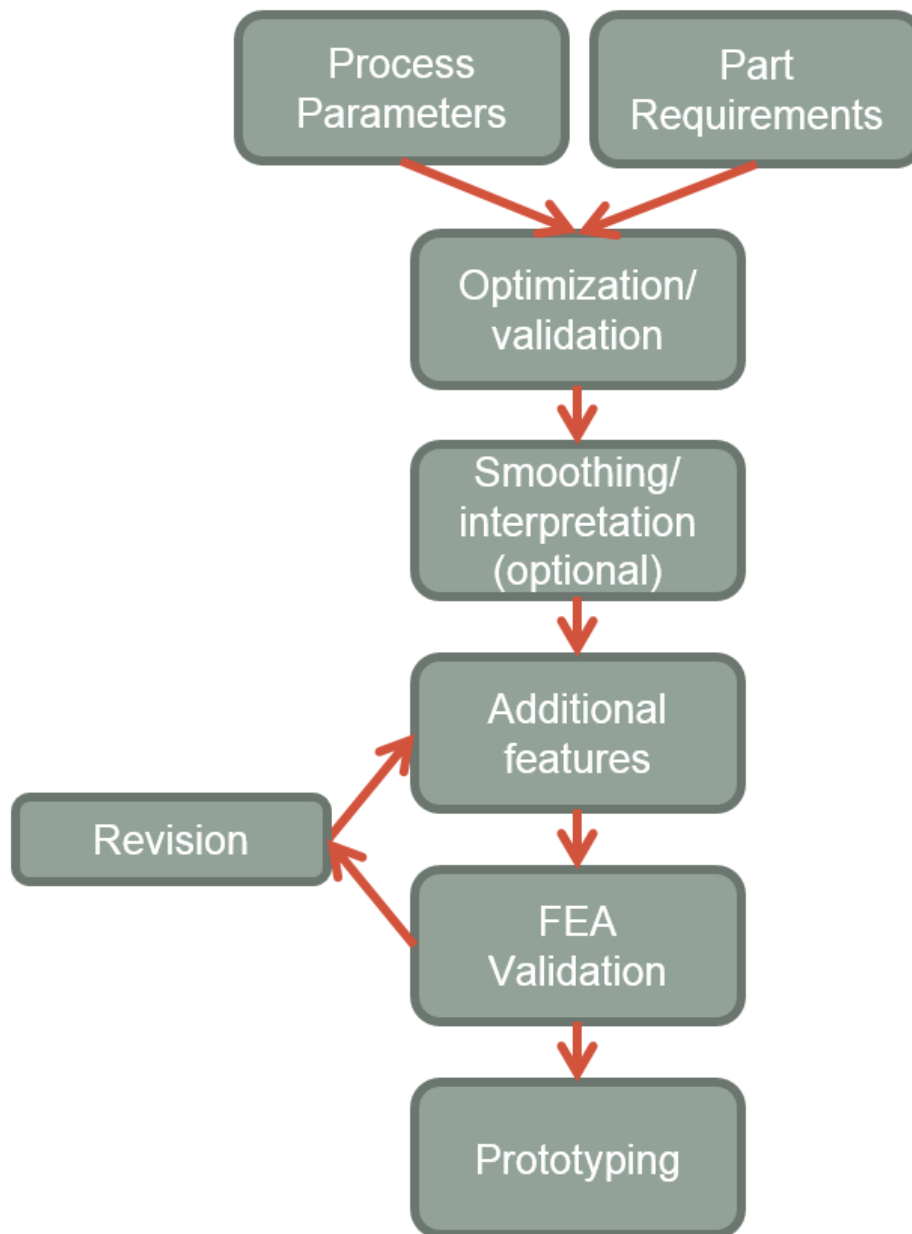
Figure 4-41. AM design flow with optimization

The workflow shown in Figure 4-41 represents a step towards topology design automation for AM, as the designer's part is primarily in adding additional features instead of modifying the entire part for manufacture. This incorporation also cuts down on the need for smoothing or interpretation, as the output results would already be directly manufacturable. With

refinements to the topology optimization algorithm, the designer's effort in iteratively modifying the optimized results for manufacturing could become less and less as the topology optimization technology progresses. Other areas of future work are discussed in the next chapter along with a summary of the thesis and its contributions.

Chapter 5
Conclusions and Future Work

This research has evaluated the current state of topology optimization software, as well as examined the workflow when incorporating topology optimization into design for additive manufacture. Additive manufacturing has been touted as a technology that will enable engineers to easily create complex geometries, allowing optimized designs to be directly translated into physical parts. This research has shown that this ideal workflow is not yet possible with current commercially available topology optimization tools and software.

Through the completion of a software review, it was shown that commercial topology optimization software is fairly standardized in terms of capabilities and methods used. Current software often makes use of the SIMP algorithm for topology optimization, which requires the design engineer to choose an element density threshold to define an output topology. These software packages come with manufacturing constraints that are well-suited to subtractive and formative manufacturing processes, but they do not yet support optimization constraints specifically encountered when using additive manufacturing.

The mounting plate example problem illustrated the various steps required to use this software, interpret the output results, and modify the part for manufacture. The part was modeled and optimized using Altair's OptiStruct, and the effect of different modeling boundary conditions and materials on optimization results was observed. The lowest mass feasible results were then interpreted using SolidWorks, presenting a two-piece solution to the problem. To reduce the solution to a one-piece part, different connecting geometries were investigated and analyzed. The different stages of the design were then prototyped in Ultem 9085 using a Fortus 400mc FDM

process to compare material use, machine time, and manufacturability between the optimized results, the two-piece interpreted design, and the one-piece interpreted design.

Investigating the mounting plate example problem revealed advantages and disadvantages of current topology optimization software. Setting up an optimization problem is straightforward; it is no more complicated than setting up an FEA model, but the choice of boundary conditions is extremely important to achieve physically meaningful results. Boundary conditions like assuming the box in the mounting plate problem is rigid may be acceptable for analysis of completed designs, but when used with optimization, these conditions can lead to infeasible results. For this reason it is useful to investigate how different boundary conditions affect optimized results, while striving to apply those conditions that most accurately reflect real-world loading and geometry.

Another issue that arose during the course of investigating the mounting plate example problem was the issue of computation time. Adding complexity to the optimization model in the form of additional load cases or mesh refinement will always increase computation time and memory requirements. The version of OptiStruct used in this thesis did not support multi-threading; so, optimization became time-intensive. Future versions of commercial topology optimization software will likely support solution on multiple cores, but until then, with complex models, it may prove beneficial to divide the problem manually. Optimization could be performed several times for a single model, with each run only taking into account a few of the load cases. The results could then be manually interpreted and compromised to reach a design that satisfies all load cases.

Prototyping the different designs revealed areas for improvement in the workflow of using topology optimization in design for additive manufacture. The inability of the topology optimization software to take into account support structure requirements meant that manual interpretation had to both include the results as well as account for the AM process capabilities.

This interpretation then had to go through a FEA validation process and manual design iteration, two steps that incorporating topology optimization sought to minimize.

In future work, finer finite element meshes should be investigated in the optimization, as they offer the opportunity to optimize to lower mass outputs than the mesh used in this research. Optimizing the topology with a fine enough mesh could potentially eliminate the need for manual interpretation, as the solver should reduce the appearance of stress risers in the results, leading to a finely tessellated part surface geometry on par with STL interpretations of user-defined smooth surfaces. A finer mesh could also allow finer members to form in the design space, reducing the need for support to dissipate heat and prevent distortion from thermal cycling and gravity in a DMLS process. The downside to using a finer mesh is that computation time will increase.

Future research should also include the incorporation of AM design constraints directly into the topology optimization algorithm. This will not be without difficulty, as the critical constraint of minimum build angle can only be accounted for once a build orientation is determined. This would suggest that this constraint could be pre-specified, be taken into account during post-processing as in [21], or be accounted for with a two-run solution. In a two-run solution, a preliminary optimization could be performed, and the results could be manually or computationally investigated for optimum build orientation. Once this orientation is determined, it could be added as an input to the optimization algorithm and the model could be re-optimized while accounting for minimum build angle to produce resulting geometry that would not require support material for manufacture.

A more complicated constraint to implement would be the prevention or minimization of distortion in the optimization of metal parts made using AM. Current commercial software does offer a maximum member size constraint that can force optimized results to return thinner members, which could reduce distortion during printing, but this may not be ideal for all cases. Instead, with a prescribed build direction, layer thickness, tool path, and thermal parameters of

the AM process, the thermal history of a part may be predicted and accounted for during optimization.

For all of its limitations, topology optimization is still a powerful tool for use in design for additive manufacture. The ability to start the manual portion of the design process with an optimum or near-optimum geometry is a great advantage over purely manual design. Though optimized results currently may require manual interpretation and modification to be producible through AM, they offer engineers a view into the most critical load paths of a structure, reducing the amount of manual design iterations required to reduce the mass of the part. As additive manufacturing becomes more widely used in industry, topology optimization will grow to support constraints for AM processes. As the two technologies become intertwined, the workflow of topology optimization for AM will simplify to the point that someday, the design of structural components could become a fully automated process.

REFERENCES

[1] Carter, W.T., Erno, D.J., Abbott, D.H., Bruck, C.E., Wilson, G.H., Wolfe, J.B., Finkhousen, D.M., Tepper, A., Stevens, R. G., 2014, "The GE Aircraft Engine Bracket Challenge: An Experiment in Crowdsourcing for Mechanical Design Concepts," Solid Freeform Fabrication Symposium, University of Texas at Austin, Austin, Texas, pp. 1402–1411.

[2] Brackett, D., Ashcroft, I., and Hague, R., 2011, "Topology Optimization for Additive Manufacturing," 22nd Annual International Solid Freeform Fabrication Symposium - An Additive Manufacturing Conference, University of Texas at Austin, Austin, Texas, pp. 348–362.

[3] Bendsøe, M. P., 1989, "Optimal Shape Design as a Material Distribution Problem," Structural Optimization, **1**(4), pp. 193–202.

[4] Bendsøe, M. P., and Kikuchi, N., 1988, "Generating Optimal Topologies in Structural Design Using a Homogenization Method," Computer Methods in Applied Mechanics and Engineering, **71**(2), pp. 197–224.

[5] Bendsøe, M. P., and Sigmund, O., 2003, Topology Optimization: Theory, Methods, and Applications, Springer, Berlin, DE.

[6] Bendsøe, M. P., and Sigmund, O., 1999, "Material Interpolation Schemes in Topology Optimization," Archive of Applied Mechanics, **69**(9-10), pp. 635–654.

[7] Rozvany, G. I. N., 2001, "Aims, Scope, Methods, History and Unified Terminology of Computer-Aided Topology Optimization in Structural Mechanics," Structural and Multidisciplinary Optimization, **21**(2), pp. 90–108.

[8] Van Dijk, N. P., Maute, K., Langelaar, M., and Van Keulen, F., 2013, "Level-Set Methods for Structural Topology Optimization: A Review," Structural and Multidisciplinary Optimization, **48**(3), pp. 437–472.

[9] Villanueva, C. H., and Maute, K., 2014, "Density and Level Set-XFEM Schemes for Topology Optimization of 3-D structures," Computational Mechanics, **54**(1), pp. 133–150.

[10] ASTM International, 2013, F2792-12a - Standard Terminology for Additive Manufacturing Technologies, West Conshohocken, PA, United States.

[11] Gibson, I., Rosen, D. W., and Stucker, B., 2009, Additive Manufacturing Technologies: Rapid Prototyping to Direct Digital Manufacturing, Springer Science+Business Media, New York, NY.

[12] Pham, D. ., and Gault, R. ., 1998, "A Comparison of Rapid Prototyping Technologies," International Journal of Machine Tools and Manufacture, **38**(10-11), pp. 1257–1287.

[13]   Khaing, M. W., Fuh, J. Y. H., and Lu, L., 2001, "Direct Metal Laser Sintering for Rapid
         Tooling: Processing and Characterisation of EOS Parts," Journal of Materials Processing
         Technology, **113**(1-3), pp. 269–272.

[14]   Sigmund, O., and Maute, K., 2013, "Topology Optimization Approaches: A Comparative
         Review," Structural and Multidisciplinary Optimization, **48**(6), pp. 1031–1055.

[15]   Dias, M. R., Guedes, J. M., Flanagan, C. L., Hollister, S. J., and Fernandes, P. R., 2014,
         "Optimization of Scaffold Design for Bone Tissue Engineering: A Computational and
         Experimental Study," Medical Engineering and Physics, **36**(4), pp. 448–457.

[16]   Almeida, H. D. A., and da Silva Bártolo, P. J., 2010, "Virtual Topological Optimisation of
         Scaffolds for Rapid Prototyping," Medical Engineering and Physics, **32**(7), pp. 775–782.

[17]   Chahine, G., Smith, P., and Kovacevic, R., 2010, "Application of Topology Optimization
         in Modern Additive Manufacturing Minimal Compliance problem," Solid Freeform
         Fabrication Symposium, University of Texas at Austin, Austin, Texas, pp. 606–618.

[18]   Sepp, J., and Hupfer, A., 2014, "Topology Optimization in Structural Design of a Lp
         Turbine Guide," ASME Turbo Expo 2014: Turbine Technical Conference and Exposition,
         ASME, Düsseldorf, DE, pp. 1–10.

[19]   Rezaie, R., Badrossamay, M., Ghaie, A., and Moosavi, H., 2013, "Topology Optimization
         for Fused Deposition Modeling Process," Procedia CIRP, **6**, pp. 521–526.

[20]   Gaynor, A. T., Meisel, N. a., Williams, C. B., and Guest, J. K., 2014, "Multiple-Material
         Topology Optimization of Compliant Mechanisms Created Via PolyJet Three-
         Dimensional Printing," Journal of Manufacturing Science and Engineering, **136**(6), pp.
         061015–1 – 061015–10.

[21]   Leary, M., Merli, L., Torti, F., Mazur, M., and Brandt, M., 2014, "Optimal Topology for
         Additive Manufacture: A Method for Enabling Additive Manufacture of Support-Free
         Optimal Structures," Materials & Design, **63**, pp. 678–690.

[22]   SolidThinking, 2014, "SolidThinking Inspire" [Online]. Available:
         http://www.solidthinking.com/ProductOverview.aspx?item=Inspire
         Overview&category=Products. [Accessed: 02-Jun-2014].

[23]   Within, 2014, "Within Enhance" [Online]. Available:
         http://www.withinlab.com/software/. [Accessed: 04-Jun-2014].

[24]   Altair Engineering, 2014, "Altair OptiStruct" [Online]. Available:
         http://www.altairhyperworks.com/Product,19,OptiStruct.aspx. [Accessed: 02-Jun-2014].

[25]   Altair Engineering, 2014, "Altair HyperWorks."

Appendix A

Topology Optimization Software Review Results

Software	Company	FEA platform(s)	Shape Optimization	Eigenvalue analysis/optimization	Symmetry Constraints	Draw Constraints	Extrusion	Min/max member dimensions	Repetitive Structures (Lattice Fill)	post processing/smoothing	Training	Computing Requirements	Other features	Pros (from experience)	Cons (from experience)
OptiStruct	Altair Engineering	Hyperworks, NASTRAN	Yes	Yes	Yes	Yes	Yes	Yes	No	Yes	http://training.altairuniversity.com/?q=pt-pricing http://www.altair.com/ProductsSubCategory.aspx?category_id=300&prod_id=30optistruct_support&products optistruct	Windows Vista/7/8.1 64-bit Mac OS X 10.9 OpenGL graphics	Isotropic, Anisotropic, Orthotropic materials non-static analysis Linear buckling analysis Direct and Modal Frequency response analysis Coupled fluid-structure (NVH) analysis Heat transfer analysis Random response analysis Contact analysis	ability to create complex loading cases automatically tracked -extracting optimized geometry takes several steps	Preprocessing time is long -interface is confusing -mix of text and graphics (from older software) -units not automatically tracked
Genesis	Vanderplaats R&D	Genesis, ANSYS	Yes	Yes	Yes	Yes	Yes	Yes	No	Yes	tutorial videos (youtube), workshops https://www.vrand.com/events.html	32 or 64 bit OSOpenGLgraphics	Isotropic, Anisotropic, Orthotropic materials Dynamic normal modes Heat transfer analysis System buckling analysis Random response analysis Contact analysis		
SIMULIA TOSCA STRUCTURE 8.0	FE-Design (Dassault Systems)	Ansys, Abaqus, NASTRAN	Yes	Yes	Yes	Yes	Yes	Yes	No	Yes	Seminars- http://www.fe-design/de/en/events/	Windows Vista 7 32-bit Windows 7/Vista, Server 2008 64-bit OpenGL graphics	Isotropic, Anisotropic, Orthotropic materials Non-linear analysis Heat transfer analysis		
ATOM (Abaqus Unified FEA)	Dassault Systems	Abaqus	Yes	Yes	Yes	Yes	Yes	Yes	No	Yes	http://www.3ds.com/products/simulia/resources/india/resource-center/simulia-files/0b0212y7/nwmx-title/0212/0212dxml-title&field_r=dild&field_n Linux RHEL4, SUSE 11, RHEL5, 6.3 cotrel_industries_ind.at&field_noidered_pr oducts_ind.383	Windows Vista, 7 32-bit Windows 7/Vista, Server 2008 64-bit OpenGL graphics	To be incorporated under Simula suite; uses Tosca solver		
MSC.Nastran	MSC Software	NASTRAN	Yes	Yes	Yes	Yes	Yes	Yes	No	Yes	webinars http://www.mscsoftware.com/resource?ty pe%5B%5Dresources, on_demand_webcast (available with trial request)	Windows 7 32/64-bit, Windows 7/Vista, Server 2008 Windows Server 2008 Windows 864-bit Linux RHEL4, SUSE 11, RHEL5, 6.3	Buckling analysis Nonlinear static/transient, materials Contact analysis Rotordynamics Heat transfer analysis Fatigue Analysis\		
Inspire	Solidthinking (Altair Engineering)	Hyperworks (uses OptiStruct Solver)	No	Yes	Yes	Yes	Yes	Yes	Yes	Yes	tutorial videos, online forums, webinars http://www.solidthinking.com/ProductOver view.aspx?item=inspire%20Overview&category=Produts	4GB RAM (8GB Recommended) 2008 Hard D.x: Space OpenGL graphics card with at least 256 MB of onboard memory	Automatic Meshing Geometry patching/editing	Clear graphical interface intuitive controls -quick and easy geometry editing tools -automatic meshing -low preprocessing time -easy reporting of optimized geometry -automatically tracks units one touch automatic smoothing	Limited optimization goals/constraints -longer computation time (includes meshing)/more optimized geometry computationally expensive
Enhance	Within	integrated	Yes	Yes	Yes	Yes	Yes	Yes	Yes	Yes	Paid training, $159/week http://withinlab.com/contact/	32 or 64 bit OSOpenGLgraphics	Integrated FEA cuts down computation time for lattice elements Library of lattices	Free medical software; does not include optimization, but geometry tools	-No free trial; trial lasts as long as training is paid for
PERMAS-TOPO	Intes	Permas	Yes (separate module)	Yes	Yes	Yes	Yes	Yes	No	No	training in Stuttgart http://www.intes.de/kategorie_support/sch ulung	32 or 64 bit OSOpenGLgraphics	Contact analysis Dynamic mode analysis	Quick customer service for product questions	
FEMtools optimization	Dynamic Design Solutions	NASTRAN, ABAQUS, ANSYS	Yes	Yes	Yes	Yes	Yes	Yes	No	Yes	http://www.femtools.com/courses/index.htm	Windows XP, Vista, 7, 8(32-bit) Windows XP Pro, Vista, 7, 8(64-bit) Mac OS X 10.7+ (Intel based, 64-bit)	Non-linear analysis First and second order checkerboard filters		
OPTISHAPE-TS	Quint	Ansys	Yes	Yes	Yes	Yes	Yes	Yes	No	Yes	http://www.quint.co.jp/eng/tech/index.htm (ANSYS/Linux (64-bit only))	Windows 7/Vista/XP (32 or 64-bit)	30 day trial		Japanese Company; prices on Yen

Educational Tools/Outdated Software

Software	Company	FEA platform(s)	Shape Optimization	Eigenvalue analysis/optimization	Symmetry Constraints	Draw Constraints	Extrusion	Min/max member dimensions	Repetitive Structures (Lattice Fill)	post processing/smoothing	Training	Computing Requirements	Other features	Pros (from experience)	Cons (from experience)
BESO3D	RMIT University	Abaqus	No	No	Not known	Not known	Not known	Not known	Not known	No	intro PDF http://rmit.edu.br/www/Research%20Institute,%20Centres%20and%20Groups%2Fcentres%2Finnovation%20Structures%20and%20Materials%2FSoftware/	Abaqus/Standard (ver. 6.4 or above)	Free one-year license Post-processor to Abaqus		
ParetoWorks	SciArt, LLC.	Integrated (Solidworks)	No	No	Yes	Yes	Not known	Not known	Not known	No	online manual http://www.sciartsoft.com/ParetoWorks.html	Not known			
CATOPTO	Creative Engineering Services	ABAQUS, ANSYS, NASTRAN, OPTISTRUCT, PERMAS and TOSCA	No	Yes	Yes	Not known	Not known	Not known	Not known	No	Not known	Not known			Outdated site/software
topostruct	Sawpan Design	n/a	No	No	Yes	Not known	Not known	Not known	Not known	Yes	PDF instruction http://sawapan.eu/section/vector%2Ftopostruct/download.html	Not known			
ProTop	Center for Advanced Engineering Software and Simulations	standalone	No	No	Yes	Yes	Yes	No	No	No	http://caess.net/site/Software-Tutorials.html	OpenGL graphics Windows 7 64-bit or later Freeware	standalone educational tool for non-engineers to visualize load paths		
SmartDO	FEA-Opt Technology	ansys (available workbench add in)	No	No	Not known	Not known	Not known	Not known	Not known	No	Not known	Not known			
METAXABQ		Abaqus	No	No	Not known	Not known	Not known	Not known	Not known	No	manual: http://www.femas.se/ example/tutorial-only0/topy/	Not known			
ToPy	n/a	standalone (Python)	No	No	Not known	Not known	Not known	Not known	Not known	No	manual: https://code.google.com0/p/topy/	Not known			
TRINITAS	Linkoping University	standalone	No	No	Not known	Not known	Not known	Not known	Not known	No	manual: http://www.solid.iei.liu.se/Offered_services/Trinitas/index.html	Not known			
TopOpt	TopOpt	standalone	No	No	Not known	Not known	Not known	Not known	Not known	No	Tutorials: http://www.topopt.dtu.dk/?q=node/903	Not known			

Appendix A Topology Optimization Software Review Results

Appendix B

OptiStruct Topology Optimization Responses

OptiStruct allows the use of numerous structural responses, calculated in a finite element analysis, or combinations of these responses to be used as objective and constraint functions in a structural optimization.

Responses are defined using DRESP1 bulk data entries. Combinations of responses are defined using either DRESP2 entries, which reference an equation defined by a DEQATN bulk data entry, or DRESP3 entries, which make use of user-defined external routines identified by the LOADLIB I/O option. Responses are either global or subcase (loadstep, load case) related. The character of a response determines whether or not a constraint or objective referencing that particular response needs to be referenced within a subcase.

Subcase Independent

Mass and Volume

Both are global responses that can be defined for the whole structure, for individual properties (components) and materials, or for groups of properties (components) and materials.

It is not recommended to use mass and volume as constraints or objectives in a topography optimization. Neither is very sensitive towards design modifications made in a topography optimization.

In order to constrain the mass or volume for a region containing a number of properties (components), the SUM function can be used to sum the mass or volume of the selected properties (components), otherwise, the constraint is assumed to apply to each individual property (component) within the region. Alternatively, a DRESP2 equation needs to be defined to sum the mass or volume of these properties (components). This can be avoided by having all properties (components) use the same material and applying the mass or volume constraint to that material.

Fraction of Mass and Fraction of Design Volume

Both are global responses with values between 0.0 and 1.0. They describe a fraction of the initial design space in a topology optimization. They can be defined for the whole structure, for individual properties (components) and materials, or for groups of properties (components) and materials.

The difference between the mass fraction and the volume fraction is that the mass fraction includes the non-design mass in the fraction calculation, whereas the volume fraction only considers the design volume.

Formulation for volume fraction:

Volume fraction = (total volume at current iteration – initial non-design volume)/initial design volume

Formulation for mass fraction:

Mass fraction = total mass at current iteration/initial total mass

If, in addition to the topology optimization, a size and shape optimization is performed, the reference value for the volume fraction (the initial design volume) is not altered by size and shape changes. This can, on occasion, lead to negative values for this response. Therefore, if size and shape optimization is involved, it is recommended to use the Volume responses instead of the Volume Fraction response.

These responses can only be applied to topology design domains. OptiStruct will terminate with an error if this is not the case.

Center of Gravity

This is a global response that may be defined for the whole structure, for individual properties (components) and materials, or for groups of properties (components) and materials.

Moments of Inertia

This is a global response that may be defined for the whole structure, for individual properties (components) and materials, or for groups of properties (components) and materials.

Weighted Compliance

The weighted compliance is a method used to consider multiple subcases (loadsteps, load cases) in a classical topology optimization. The response is the weighted sum of the compliance of each individual subcase (loadstep, load case).

$$C_W = \sum W_i C_i = \tfrac{1}{2} \sum W_i u_i^T f_i$$

This is a global response that is defined for the whole structure.

Weighted Reciprocal Eigenvalue (Frequency)

The weighted reciprocal eigenvalue is a method to consider multiple frequencies in a classical topology optimization. The response is the weighted sum of the reciprocal eigenvalues of each individual mode considered in the optimization.

$$f_W = \sum W_i \, l \, \lambda_i \quad with \quad \left[K = \lambda_i M \right] u_i = 0$$

This is done so that increasing the frequencies of the lower modes will have a larger effect on the objective function than increasing the frequencies of the higher modes. If the frequencies of all modes were simply added together, OptiStruct would put more effort into increasing the higher modes than the lower modes. This is a global response that is defined for the whole structure.

Combined Compliance Index

The combined compliance index is a method to consider multiple frequencies and static subcases (loadsteps, load cases) combined in a classical topology optimization. The index is defined as follows:

$$S = \sum W_i C_i + NORM \frac{\sum W_j \, l \, \lambda_j}{\sum W_j}$$

This is a global response that is defined for the whole structure.

The normalization factor, *NORM*, is used for normalizing the contributions of compliances and eigenvalues. A typical structural compliance value is of the order of 1.0e4 to 1.0e6. However, a typical inverse eigenvalue is on the order of 1.0e-5. If *NORM* is not used, the linear static compliance requirements dominate the solution.

The quantity *NORM* is typically computed using the formula:

$$NF = C_{max} \, \lambda_{min}$$

where, C_{max} is the highest compliance value in all subcases (loadsteps, load cases) and λ_{min} is the lowest eigenvalue included in the index.

In a new design problem, you may not have a close estimate for *NORM*. If this happens, OptiStruct automatically computes the *NORM* value based on compliances and eigenvalues computed in the first iteration step.

von Mises Stress in a Topology or Free-Size Optimization

The von Mises stress constraints may be defined for topology and free-size optimization through the STRESS optional continuation line on the DTPL or the DSIZE card. There are a number of restrictions with this constraint:

• The definition of stress constraints is limited to a single von Mises permissible stress. The phenomenon of singular topology is pronounced when different materials with different permissible stresses exist in a structure. Singular topology refers to the problem associated with the conditional nature of stress constraints, i.e. the stress constraint of an element disappears when the element vanishes. This creates another problem in that a huge number of reduced problems exist with solutions that cannot usually be found by a gradient-based optimizer in the full design space.

•Stress constraints for a partial domain of the structure are not allowed because they often create an ill-posed optimization problem since elimination of the partial domain would remove all stress constraints. Consequently, the stress constraint applies to the entire model when active, including both design and non-design regions, and stress constraint settings must be identical for all DSIZE and DTPL cards.

•The capability has built-in intelligence to filter out artificial stress concentrations around point loads and point boundary conditions. Stress concentrations due to boundary geometry are also filtered to some extent as they can be improved more effectively with local shape optimization.

•Due to the large number of elements with active stress constraints, no element stress report is given in the table of retained constraints in the .out file. The iterative history of the stress state of the model can be viewed in HyperView or HyperMesh.

•Stress constraints do not apply to 1-D elements.

•Stress constraints may not be used when enforced displacements are present in the model.

Bead Discreteness Fraction

This is a global response for topography design domains. This response indicates the amount of shape variation for one or more topography design domains. The response varies in the range 0.0 to 1.0 (0.0 < BEADFRAC < 1.0), where 0.0 indicates that no shape variation has occurred, and 1.0 indicates that the entire topography design domain has assumed the maximum allowed shape variation.

Subcase Dependent

Linear Static Analysis
Static Compliance

The compliance C is calculated using the following relationship:

$$C = \tfrac{1}{2} u^T f \quad \text{with} \quad Ku = f$$

or

$$C = \tfrac{1}{2} u^T Ku = \tfrac{1}{2} \int \varepsilon^T \sigma \, dv$$

The compliance is the strain energy of the structure and can be considered a reciprocal measure for the stiffness of the structure. It can be defined for the whole structure, for individual properties (components) and materials, or for groups of properties (components) and materials. The compliance must be assigned to a linear static subcase (loadstep, load case).

In order to constrain the compliance for a region containing a number of properties (components), the SUM function can be used to sum the compliance of the selected properties (components), otherwise, the constraint is assumed to apply to each individual property (component) within the region. Alternatively, a DRESP2 equation needs to be defined to sum the compliance of these properties (components). This can be avoided by having all properties (components) use the same material and applying the compliance constraint to that material.

Static Displacement

Displacements are the result of a linear static analysis. Nodal displacements can be selected as a response. They can be selected as vector components or as absolute measures. They must be assigned to a linear static subcase.

Static Stress of Homogeneous Material

Different stress types can be defined as responses. They are defined for components, properties, or elements. Element stresses are used, and constraint screening is applied. It is also not possible to define static stress constraints in a topology design space (see above). This is a linear static subcase (loadstep, load case) related response.

Static Strain of Homogeneous Material

Different strain types can be defined as responses. They are defined for components, properties, or elements. Element strains are used, and constraint screening is applied. It is also not possible to define strain constraints in a topology design space. This is a linear static subcase (loadstep, load case) related response.

Static Stress of Composite Lay-up

Different composite stress types can be defined as responses. They are defined for PCOMP(G) components or elements, or PLY type properties. Ply level results are used, and constraint screening is applied. It is also not possible to define composite stress constraints in a topology design space. This is a linear static subcase (loadstep, load case) related response.

Static Strain of Composite Lay-up

Different composite strain types can be defined as responses. They are defined for PCOMP(G) components or elements, or PLY type properties. Ply level results are used, and constraint screening is applied. It is also not possible to define composite strain constraints in a topology design space. This is a linear static subcase (loadstep, load case) related response.

Static Failure in a Composite Lay-up

Different composite failure criterion can be defined as responses. They are defined for PCOMP(G) components or elements, or PLY type properties. Ply level results are used, and constraint screening is applied. It is also not possible to define composite failure criterion constraints in a topology design space. This is a linear static subcase (loadstep, load case) related response.

Static Force

Different force types can be defined as responses. They are defined for components, properties, or elements. Constraint screening is applied. It is also not possible to define force constraints in a topology design space. This is a linear static subcase (loadstep, load case) related response.

Single Point Force at a constrained grid point

This response can be defined using the DRESP1 bulk data entry (with RTYPE=SPCFORCE). This response is defined for constrained grid points. Constraint screening is applied to this response. This is a linear static subcase (loadstep, load case) related response.

Grid Point Force

This response can be defined using the DRESP1 bulk data entry (with RTYPE=GPFORCE). This response defines the contribution to a specific grid point force component from a non-rigid element (which is connected to that grid). Constraint screening is applied to this response. If ATTi specify multiple elements, then multiple responses will be generated, where, each response calculates a specified element's contribution to the grid point force component at the specified grid. This is a linear static subcase (loadstep, load case) related response.

Linear Heat Transfer Analysis

Temperature

Temperatures are the result of a heat transfer analysis, and must be assigned to a heat transfer subcase (loadstep, load case). Temperature response cannot be used in composite topology or free-size optimization.

Normal Modes Analysis

Frequency

Natural frequencies are the result of a normal modes analysis, and must be assigned to the normal modes subcase (loadstep, load case). It is recommended to constrain the frequency for several of the lower modes, not just of the first mode.

Mode Shape
Mode shapes are the result of a normal modes analysis. Mode shapes can be selected as a response. They can be selected as vector components or as absolute measures. They must be assigned to a normal modes subcase.

Linear Buckling Analysis

Buckling Factor
The buckling factor is the result of a buckling analysis, and must be assigned to a buckling subcase (loadstep, load case). A typical buckling constraint is a lower bound of 1.0, indicating that the structure is not to buckle with the given static load. It is recommended to constrain the buckling factor for several of the lower modes, not just of the first mode.

Frequency Response Function (FRF Analysis)

Frequency Response Displacement
Displacements are the result of a frequency response analysis. Nodal displacements, i.e. translational, rotational and normal*, can be selected as a response. They can be selected as vector components in real/imaginary or magnitude/phase form. They must be assigned to a frequency response subcase (loadstep, load case).
*The normal at a grid point is calculated based on the normals of the surrounding elements. The normal frequency response displacement at a grid point can be selected as a response and it is the displacement in the normal's direction. The normals are also updated when shape changes occur during shape optimization.

Frequency Response Velocity
Velocities are the result of a frequency response analysis. Nodal velocities, i.e. translational, rotational and normal, can be selected as a response. They can be selected as vector components in real/imaginary or magnitude/phase form. They must be assigned to a frequency response subcase (loadstep, load case).
*The normal at a grid point is calculated based on the normals of the surrounding elements. The normal frequency response velocity at a grid point can be selected as a response and it is the velocity in the normal's direction. The normals are also updated when shape changes occur during shape optimization.

Frequency Response Acceleration
Accelerations are the result of a frequency response analysis. Nodal accelerations, i.e. translational, rotational and normal, can be selected as a response. They can be selected as vector components in real/imaginary or magnitude/phase form. They must be assigned to a frequency response subcase (loadstep, load case).
*The normal at a grid point is calculated based on the normals of the surrounding elements. The normal frequency response acceleration at a grid point can be selected as a response and it is the acceleration in the normal's direction. The normals are also updated when shape changes occur during shape optimization.

Frequency Response Stress
Different stress types can be defined as responses. They are defined for components, properties, or elements. Element stresses are not used in real/imaginary or magnitude/phase form,

and constraint screening is applied. The von Mises stress for solids and shells can also be defined as direct responses. It is not possible to define stress constraints in a topology design space. This is a frequency response subcase (loadstep, load case) related response.

Frequency Response Strain
Different strain types can be defined as responses. They are defined for components, properties, or elements. Element strains are used in real/imaginary or magnitude/phase form, and constraint screening is applied. The von Mises strain for solids and shells can also be defined as direct responses. It is not possible to define strain constraints in a topology design space. This is a frequency response subcase (loadstep, load case) related response.

Frequency Response Force
Different force types can be defined as responses. They are defined for components, properties, or elements in real/imaginary or magnitude/phase form. Constraint screening is applied. It is also not possible to define force constraints in a topology design space. This is a frequency response subcase (loadstep, load case) related response.

Random Response Analysis

PSD and RMS Responses
PSD displacement, PSD velocity, PSD acceleration, PSD acoustic pressure, PSD stress, PSD strain, RMS displacement, RMS velocity, RMS acceleration, RMS acoustic pressure, RMS stress and RMS strain responses are available.

Coupled FRF Analysis on a Fluid-structure Model (Acoustic Analysis)

Acoustic Pressure
Acoustic pressures are the result of a coupled frequency response analysis on a fluid-structure model. This response is available for fluid grids. It must be assigned to a coupled frequency response subcase (loadstep, load case) on a fluid-structure model.

Multi-body Dynamics Analysis

Flexible Body Responses
For Multi-body Dynamics problems, the Mass, Center of gravity, and Moment of Inertia of one or more flexible bodies are available as responses. This is in addition to other usual structural responses.

MBD Displacement
MBD displacements are the result of a multi-body dynamics analysis. They must be assigned to a multi-body dynamics subcase (loadstep, load case).

MBD Velocity
MBD velocities are the result of a multi-body dynamics analysis. They must be assigned to a multi-body dynamics subcase (loadstep, load case).

MBD Acceleration
MBD acceleration are the result of a multi-body dynamics analysis. They must be assigned to a multi-body dynamics subcase (loadstep, load case).

MBD Force
MBD forces are the result of a multi-body dynamics analysis. They must be assigned to a multi-body dynamics subcase (loadstep, load case).

MBD Expression

MBD expression responses are the result of a multi-body dynamics analysis. They are the result of the evaluation of an expression. They must be assigned to a multi-body dynamics subcase (loadstep, load case).

Fatigue

Life/Damage

Life and Damage are results of a fatigue analysis. They must be assigned to a Fatigue subcase.

Dynamic/Nonlinear Analysis

Equivalent Plastic Strain

Equivalent plastic strain can be used as an internal response when a nonlinear response optimization is run using the equivalent static load method. This is made possible through the use of an approximated correlation between linear strain and plastic strain, which are calculated in the inner and outer loops respectively, of the ESL method.

User Responses

Function

A function response is one that uses a mathematical expression to combine design variables, grid point locations, responses, and/or table entries. Whether the function is subcase (loadstep, load case) related or global, is dependent on the response types used in the equation.

External

An external response is one that uses an external user-defined routine to combine design variables, grid point locations, eigenvectors, responses, and/or table entries. Whether the function is subcase (loadstep, load case) related or global is dependent on the response types used in the routine.

Appendix B OptiStruct Topology Optimization Responses